

68-11,222

**KRAMBECK, Frederick J., 1941-
STOCHASTIC MIXING MODELS FOR CHEMICAL
REACTORS.**

**The City University of New York, Ph.D., 1968
Engineering, chemical**

University Microfilms, Inc., Ann Arbor, Michigan

Stochastic Mixing Models

for

Chemical Reactors

by

Frederick J. Krambeck

A dissertation submitted to the
Graduate Faculty in Engineering in Partial
fulfillment of the requirements for the
degree of Doctor of Philosophy, The City
University of New York

1967

This manuscript has been read and accepted for the University Committee in Engineering in satisfaction of the dissertation requirement for the degree of Doctor of Philosophy.

9th January 1968
Date

January 9, 1968
Date

Stanley Katz
Chairman of Examining Committee

[Signature]
Executive Officer

Prof. S. Katz, Chairman

Prof. A. Konheim

Prof. R. Shinnar

Supervisory Committee

The City University of New York

Acknowledgement

The author wishes to thank Professors S. Katz and R. Shinnar, who jointly directed this research, for their many contributions, and Professor A. X. Schmidt, Chairman of the Chemical Engineering Department, for his confidence and encouragement.

The work was supported by AFOSR Grant No. 921-65 (Air Force Office of Scientific Research), and numerical calculations were carried out at the City College Computation Center.

Table of Contents

	<u>Page</u>
I. Introduction	1
II. Formulation of General Model	
A. Nomenclature of Tank Models	8
B. Structure of Mixing Flows	11
III. Treatment of Mixing Model as a Random Walk	
A. Transition Probabilities	16
B. Initial Distribution	17
C. Equations for Probability Distribution	19
D. Contact Time Distribution	21
E. Outlet Age Distribution	28
IV. Probability Structure of Tracer Experiments	
A. Probability Equations	33
B. Inlet Flow Rate vs. Inlet Concentration	34
C. Equations for First Moments	37
D. Equations for Second Moments and Autocorrelations	41
V. Behavior of Model as a Reactor	
A. Probability Equations	48
B. Inlet Flow Rate vs. Inlet Concentration	48
C. Equations for First Moments	49
D. Equations for Second Moments and Autocorrelations	52

VI. Some General Conclusions	61
VII. Single Tank Model	
A. Formulation	66
B. Tracer Experiments	68
C. Moments of Conversion with First Order Reaction	88
D. Probability Distributions for Single Tank with Reaction	97
VIII. Series and Parallel Models	
A. Formulation	118
B. Tracer Experiments	121
C. Moments with First Order Reaction	148
D. Stable Regions in Concentration Space	163
IX. Fluidized Bed Model	
A. Formulation	174
B. Steady Flow Behavior	177
C. Behavior with Fluctuating Flow	187
X. Conclusions	199
References	208
Nomenclature	213

I. Introduction

In fluid systems serving as chemical reactors, the mixing processes that take place have pronounced effects on the reactor performance. Often, these processes involve turbulent motion of the fluid, thus introducing randomly fluctuating behavior into the system. Various approaches have been developed to take the mixing processes into account when describing reactors analytically for design, optimization, control, etc. It is often possible to neglect the detailed structure of the mixing processes and represent the system by some sort of idealized model, such as a perfectly mixed tank, a plug flow reactor, an eddy-diffusion model, or some combination of these connected together [1]. The formulation of such models is accomplished through physical reasoning and, frequently, tracer experiments (see [2], for example.)

When all the flows in the reaction system are steady, certain of these tracer experiments can be interpreted in terms of the probability distribution of residence times experienced by individual particles passing through the system. Thus, in a system with a single inlet and outlet stream, the residence time density function is obtained as the concentration response at the outlet to a unit

impulse of tracer at the inlet. Similarly, the residence time distribution function is the response to a step input of tracer, assuming, of course, that the flow distribution is unaffected by the presence of tracer, so that the tracer output is linearly related to the tracer input. Because it is easily measured and is independent of any assumed model of the process, the residence time distribution serves as a useful characterization of the mixing system. The nature of this distribution can be used to ascertain some of the gross features of the mixing process [3], and it determines the conversion for passive, first order reactions. In other cases it is a useful device for discussing the behavior of the system (see, for example, [4,5]). Danckwerts [6] and Zwietering [7] have developed a method for using the residence time distribution to find bounds on conversion for a large class of reactions. (There are many practical cases where the method fails, however.) Various methods have been proposed to construct models consistent with a given residence time distribution, where the models have some free parameters, to study the types of behavior possible under the constraint of a fixed residence time distribution [8, 9, 10]. Thus the probability

distribution of particle residence times can be applied in various ways to the investigation of reaction behavior.

When the flow patterns in the reactor are not steady, however, the relationship between the results of tracer response experiments and the residence time distribution is not so obvious. In this case the result of a given tracer experiment is a random process, and only the statistics of this process are experimentally accessible. In many systems this randomness in the tracer response is quite apparent [11, 12]. Also, the reaction behavior of such a system will be random, and one is therefore interested in predicting the statistics of the reactor output. One of the results of this thesis is to extend the concept of residence time distributions to systems with randomly fluctuating flows and to see how it is related to the statistics of tracer experiments performed on such systems and the statistics of the systems' reactor performance.

Various approaches have been used to analyze fluctuating systems in more detail. The most fundamental approach makes use of the statistical theory of isotropic turbulence (see [13]). This has been applied to the problem of pure mixing in turbulence [14, 15, 16], and

extended to isothermal, first and second order reactions, albeit in an approximate way [17]. At the present time, however, this approach is of rather limited applicability because of difficulties inherent in the method. Apparently, questions posed within this framework ask for too much information about the fine structure of the turbulence spectrum. It seems that a more coarse-grained approach to turbulent mixing would supply a more tractable theory. What is required is a model somewhere between the extremes of the steady-flow eddy diffusivity models, and the more exact descriptions of the flow processes employed in statistical turbulence theory. Such a model would exhibit the randomly fluctuating behavior so characteristic of turbulent mixing, but retain sufficient simplicity to make its analysis feasible. It would also be useful if the model could incorporate information derived from tracer experiments.

Some beginnings have already been made in this direction. Gibson [18] has developed a stochastic model for turbulent wakes that makes use of the extensive data on velocity fluctuations and tracer diffusion that exists for this specific flow geometry. A Monte-Carlo computation is used to derive the reactant concentration

statistics. A stochastic model for emulsion phase reactions in a well stirred reactor was developed analytically by Curl [19] and solved using Monte-Carlo methods by Spielman and Levenspiel [20]. The model was extended to arbitrary residence time distributions by Kattan and Adler [21]. Monte-Carlo solutions for a plug flow reactor were also presented in [21]. In analyzing this model the emphasis was on the effects of segregation on the mean conversion, rather than on the effects of randomness on the statistics of conversion, but the stochastic effects are clearly present.

In the present study a new type of stochastic mixing model is proposed which is thought to be applicable to a large class of systems, but which retains sufficient analytical structure to allow meaningful conclusions about its properties. The model consists of a network of well mixed tanks, interconnected in some arbitrary way, where the interconnecting flows fluctuate randomly in time. It may be noted that such a model with steady flows can be used to simulate steady mixing processes by taking appropriate arrangements of tanks and allowing their number to increase. Axial diffusion, for example, may be approximated to any degree with a sufficiently large number of

tanks in cascade, with forward and backward flows between each tank. The added feature of randomly fluctuating flows should make it possible to simulate any turbulent mixing process if sufficient numbers of tanks are taken. Of course, such a large number of tanks might be required that there would be no saving in effort over a complete description of the flow process. On the other hand, if conclusions may be drawn about such a model with the number and arrangement of tanks left arbitrary, it is clear that they will apply to a very general class of mixing processes. Also, it may well happen that certain processes allow a representation of this type requiring only a few tanks, in which case many useful predictions can be made with reasonable effort.

One assumption is added to make the analysis possible. This is that the interconnecting flow rates vary in time as discrete-state Markov processes. Such processes are described in detail in Feller [22]. The fact that the states are discrete is not important, since their number is arbitrary. The fact that the process is Markov is an extremely mild restriction because the dimensionality of the state space is arbitrary. This is true because a Markov process is one whose present state determines the

probability structure of its future, independently of its history. But if the meaning of the term "present state" is expanded to include the past of the system, any non-Markov process becomes Markov.

In the analysis that follows, the general model is studied from two different points of view. Attention is first concentrated on the behavior of a single particle traveling through the system. This serves to provide a conceptual framework in which to formulate questions about residence times and other single particle statistics unambiguously. The system is then studied as a mixer, with concentrations in each tank, both with and without chemical reactions. Following this discussion some simple cases of the general model are studied in more detail to provide additional insight into the behavior of such systems.

II. Formulation of General Model

A. Nomenclature of Tank Models

In the most general case the model consists of n stirred tanks arbitrarily connected by interstage flows (see Figure 1), where the volume of the i^{th} tank is v_i , and the volumetric flow rate from the i^{th} tank to the j^{th} is w_{ij} ($i, j=1, 2, \dots, n$). The inlet stream is distributed to the tanks arbitrarily, and the feed rate to the j^{th} tank is denoted w_{0j} . The contribution of the j^{th} tank to the outlet stream is similarly called $w_{j, n+1}$. The amount bypassing the system entirely is $w_{0, n+1}$.

Although the flow rates will be permitted to vary with time, it will be assumed that the volumes, v_i , remain constant. Thus, the total flow entering the j^{th} tank at any instant is equal to the total flow leaving it:

$$\sum_{\substack{i=0 \\ i \neq j}}^n w_{ij} = \sum_{\substack{i=1 \\ i \neq j}}^{n+1} w_{ji} \quad ; \quad j=1, 2, \dots, n \quad (\text{II-1})$$

Also, the total flow entering the system is equal to the total leaving. Denoting this quantity by w ,

$$w = \sum_{j=1}^{n+1} w_{0j} = \sum_{j=0}^n w_{j, n+1} \quad (\text{II-2})$$

It will be convenient to define "diagonal" quantities of

Figure 1: TYPICAL FLOW NETWORK

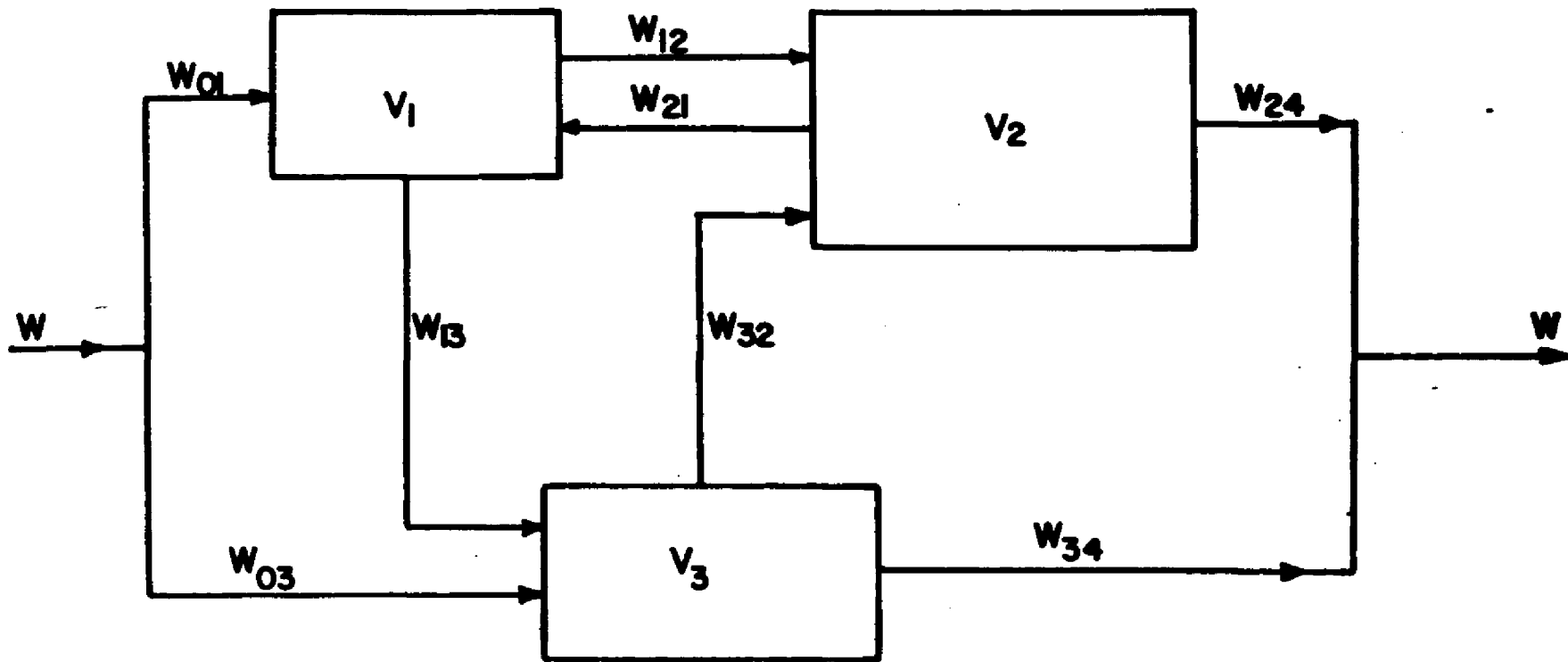


Table 1. Typical Flow Matrix for Figure 1

		Column Index			
		1	2	3	4
Row Index	0	1	0	1	0
	1	[-3]	2	1	0
	2	2	[-3]	0	1
	3	0	1	[-2]	1

the form w_{jj} such that the total inlet flow to the j^{th} tank (equal to the total outlet flow) is the negative of w_{jj} . Thus,

$$w_{jj} = - \sum_{\substack{i=0 \\ i \neq j}}^n w_{ij} = - \sum_{\substack{i=1 \\ i \neq j}}^{n+1} w_{ji} \quad ; \quad j=1,2,\dots,n \quad (\text{II-3})$$

The flow rates w_{ij} so defined fill out a square matrix $(n+1 \text{ by } n+1)$ which has the property (see Table 1):

$$\sum_{i=0}^n w_{ij} = \sum_{k=1}^{n+1} w_{jk} = 0 \quad ; \quad j=1,2,\dots,n \quad (\text{II-4})$$

and where all the elements w_{ij} with $i \neq j$ are non-negative.

B. Structure of Mixing Flows

The random variation of the flow states with time will be assumed to arise from a Markov process with a finite number of states. Each state of the Markov process will correspond to a given matrix of flow rates. Letting α be the index of a flow state, the flow rates corresponding to α are written

$$w_{ij\alpha} \quad ; \quad i = 0, 1, \dots, n \quad ; \quad j = 1, 2, \dots, n+1$$

For every state α

$$\sum_{i=0}^n w_{ij\alpha} = \sum_{k=1}^{n+1} w_{jk\alpha} = 0 \quad ; \quad j=1,2,\dots,n \quad (\text{II-5})$$

$$\sum_{j=1}^{n+1} w_{0j\alpha} = \sum_{i=0}^n w_{i, n+1, \alpha} = w_{\alpha} ; \text{ all } \alpha \quad (\text{II-6})$$

The probability structure of the flows now resides in that of the transitions of the underlying Markov process from one state to another. Denote the probability of a transition from one state α to another, β , in a time τ by $\pi(\alpha \rightarrow \beta; \tau)$. Then the behavior of this function for small τ can be described by

$$\pi(\alpha \rightarrow \beta; \tau) = \lambda_{\alpha\beta} \tau + o(\tau); \quad \alpha \neq \beta \quad (\text{II-7})$$

In this equation $\lambda_{\alpha\beta}$ is an assigned matrix of switching rates and $o(\tau)$ is a function of τ satisfying

$$\lim_{\tau \rightarrow 0} \frac{o(\tau)}{\tau} = 0$$

Since in a time τ the state of the process must either change or remain unchanged, the probability of not changing is

$$\pi(\alpha \rightarrow \alpha; \tau) = 1 - \sum_{\beta \neq \alpha} \lambda_{\alpha\beta} \tau + o(\tau) \quad (\text{II-8})$$

Defining the diagonal quantities $\lambda_{\alpha\alpha}$ so that

$$\lambda_{\alpha\alpha} = - \sum_{\beta \neq \alpha} \lambda_{\alpha\beta} \quad (\text{II-9})$$

the full set of probabilities may be described by the matrix $\lambda_{\alpha\beta}$:

$$\pi(\alpha \rightarrow \beta; \tau) = \delta_{\alpha\beta} + \lambda_{\alpha\beta} \tau + o(\tau) \quad (\text{II-10})$$

where the matrix elements satisfy

$$\sum_{\beta} \lambda_{\alpha\beta} = 0 \quad ; \quad \text{all } \alpha \quad (\text{II-11})$$

and where all the off-diagonal terms are non-negative.

The form of the transition probabilities for small times may be used to derive a differential equation describing the evolution of the probability distribution of states with time by using the defining property of a Markov process: that the probability structure of the future course of such a process depends only on its present state, and is independent of its previous history of states. In particular, the conditional probability of the system being in state β at time $t + \tau$ given that it was in state α at time t is the same as the conditional probability of being in state β at time $t + \tau$ given that it was in state α at time t and that it was in some combination of states at some set of previous times. Any of these conditional probabilities are just equal to $\pi(\alpha \rightarrow \beta; \tau)$. The fact that π is not a function of t makes this a stationary Markov process. Non-stationary Markov processes will be encountered later in connection with random walks and tracer experiments. Let us define $p_{\alpha}(t)$ to be the probability that the process is in state α

at time t , given some initial distribution $p_\alpha(0)$. Then, by the defining property of Markov processes,

$$p_\beta(t + \tau) = \sum_{\alpha} p_\alpha(t) \pi(\alpha \rightarrow \beta; \tau) \quad (\text{II-12})$$

This relationship, called the Chapman-Kolmogorov equation, simply states that the transition probabilities are independent of the past history of the process. Substituting equation (II-10) into equation (II-12) and letting τ go to zero, one finds that

$$\frac{d p_\beta(t)}{d t} = \sum_{\alpha} \lambda_{\alpha\beta} p_\alpha(t) \quad (\text{II-13})$$

Specifying the initial probability distribution, $p_\alpha(0)$, then allows calculation of the entire time history of the process. In what follows it will be assumed that the flow system is quasi-steady, that is, that the probability distribution of flow states becomes stationary and no longer varies with time. It will also be assumed that this distribution is unique, independent of the initial distribution. Denoting the stationary distribution by \bar{p}_α , this requires that the equation

$$\sum_{\alpha} \lambda_{\alpha\beta} \bar{p}_\alpha = 0 \quad (\text{II-14})$$

together with the normalization, $\sum_{\alpha} \bar{p}_\alpha = 1$, have one and only one solution, or, stated another way, that the transpose of the matrix $\lambda_{\alpha\beta}$ have only a single zero eigenvalue. Note that equation (II-11) ensures the existence of at least a single zero eigenvalue, and,

together with the fact that all off-diagonal terms are non-negative, also insures that no eigenvalue can have a positive real part.

III. Treatment of Mixing Model as a Random Walk

A. Transition Probabilities

In order to define such concepts as residence time distribution in an unambiguous way, it is useful to analyze the random passage of a single particle through the mixing system. For this purpose the system consists of the n tanks plus an outlet station, and the state of the particle is just its location index i (ranging from 1 to $n+1$). If the flow state remains unchanged for a small interval τ , the conditional probability of the particle moving from i to j can be taken as

$$\Pr \{i \rightarrow j \mid \alpha \rightarrow \alpha\} = \delta_{ij} + \frac{w_{ij\alpha}}{v_i} \tau + o(\tau) \quad (\text{III-1})$$

In case the flow state does switch, it is assumed that

$$\Pr \{i \rightarrow j \mid \alpha \rightarrow \beta\} = \delta_{ij} + \frac{\bar{w}_{ij}}{v_i} \tau + o(\tau) \quad (\text{III-2})$$

where \bar{w}_{ij} is some bounded quantity. Considering the transition probability $\pi(\alpha, i \rightarrow \beta, j; \tau)$ of changing from state (α, i) to state (β, j) in time τ , where the first index of (α, i) corresponds to the flow state and the second to the particle state, it is seen that

$$\begin{aligned} \pi(\alpha, i \rightarrow \beta, j; \tau) &= \delta_{ij} \delta_{\alpha\beta} + \delta_{\alpha\beta} \frac{w_{ij\alpha}}{v_i} \tau \\ &+ \delta_{ij} \lambda_{\alpha\beta} \tau + o(\tau) \end{aligned} \quad (\text{III-3})$$

It seems reasonable to assume that the composite process with states (α, i) has the Markov property, that is, that the probabilities of changing tanks given by (III-1) or (III-2) will be independent of any previous states of the system. Again the Chapman-Kolmogorov equation may be applied to yield a differential equation describing the evolution of the probability distribution. Defining $p_{\alpha i}(t)$ to be the probability of the system being in state (α, i) at time t , one finds that

$$\frac{d p_{\alpha j}(t)}{d t} = \sum_{i=1}^n \frac{w_{ij\alpha}}{v_i} p_{\alpha i}(t) + \sum_{\alpha} \lambda_{\alpha\beta} p_{\alpha j}(t); \quad (\text{III-4})$$

$$j = 1, 2, \dots, n+1$$

B. Initial Distribution

In this case, however, the stationary distribution is of no particular interest, since the particle will eventually find its way to the outlet with probability one. It is necessary to state explicitly the initial distribution in order to calculate the probability structure of the random walk. If the total flow through the system, w_{α} , is constant ($w_{\alpha} = w$; all α), the initial distribution is given by

$$p_{\alpha j}(0) = \bar{p}_{\beta} \frac{w_{\alpha j\beta}}{w} \quad (\text{III-5})$$

which is to say that the flow state distribution is in its stationary condition, and that the probability

of starting in a certain tank, given the flow state, is proportional to the flow to that tank from the inlet stream. In case the total flow is not constant, some ambiguity arises. One could either assume that at the instant a particle enters, the flow state probabilities have their stationary values, \bar{p}_α , implying that the chance of a particle entering at a certain time is independent of the flow state, or one could assume that the chance of a particle entering at a given instant is proportional to the total flow rate at that instant, so that the initial distribution of flow states, say p_α^0 , is different from \bar{p}_α . In the first case the initial distribution would be given by

$$p_{\rho j}(0) = \bar{p}_\rho \frac{w_{\rho j}}{w_\rho} \quad (\text{III-6})$$

In the second case,

$$p_\alpha^0 = \frac{\bar{p}_\alpha w_\alpha}{\sum_\beta \bar{p}_\beta w_\beta}, \quad (\text{III-7})$$

since the arrival of a particle in a short time given that the flow state is α is proportional to w_α . The initial distribution of the composite process is then

$$p_{\rho j}(0) = p_\rho^0 \frac{w_{\rho j}}{w_\rho} = \bar{p}_\rho \frac{w_{\rho j}}{w} \quad (\text{III-8})$$

Note that if all the w_α are equal, equations (III-6) and (III-8) are identical to equation (III-5). It will be shown later that the initial distribution (III-6)

corresponds to tracer experiments in which the tracer is injected as a pulse at a random time or as a step function in tracer flow rate (constant flow rate of tracer, fluctuating inlet concentration). The initial distribution (III-8) corresponds to tracer experiments in which a constant concentration of tracer is fed regardless of instantaneous total flow rate.

C. Equations for Probability Distribution

At any rate, once the initial distribution is specified by either equation (III-6) or equation (III-8) the complete time history of the probability distribution, $P_{\rho j}(t)$, can be calculated. The cumulative residence time distribution is then given by

$$F(t) = \sum_{\rho} P_{\rho, n+1}(t) \quad (\text{III-9})$$

which is the probability that a particle entering the system at time zero will be in the outlet at time t . The age distribution of a particle in tank j would be given by

$$g_j(t) = \frac{\sum_{\rho} P_{\rho j}(t)}{\int_0^{\infty} \sum_{\rho} P_{\rho j}(t) dt} \quad (\text{III-10})$$

where the probability that a particle has been in the system a time between t_0 and t_1 given that it is in tank j is $\int_{t_0}^{t_1} g_j(\tau) d\tau$.

It is interesting to compute the mean residence time to see how it compares with the value for a steady

system, in which case it would be the total volume divided by the total flow rate. To do this note that

$$1 - F(t) = \sum_p \sum_{j=1}^n P_{pj}(t) \quad (\text{III-11})$$

which simply states that $1-F(t)$ is the probability that a particle which entered at time zero is still in the system at time t . Then θ , the mean residence time, is given by

$$\theta = \int_0^{\infty} [1 - F(t)] dt = \sum_p \sum_{j=1}^n \int_0^{\infty} P_{pj}(t) dt \quad (\text{III-12})$$

Integrating equation (III-4) one finds

$$P_{pj}(\infty) - P_{pj}(0) = \sum_{i=1}^n \frac{w_{ij}p}{v_i} \int_0^{\infty} P_{pi}(t) dt + \sum_{\alpha} \lambda_{\alpha p} \int_0^{\infty} P_{\alpha j}(t) dt \quad ; \quad j = 1, 2, \dots, n \quad (\text{III-13})$$

Defining $\theta_{pj} = \int_0^{\infty} P_{pj}(t) dt$, and noting that $P_{pj}(\infty) = 0$ ($j=1, 2, \dots, n$), this becomes

$$-P_{pj}(0) = \sum_{i=1}^n \frac{w_{ij}p}{v_i} \theta_{pi} + \sum_{\alpha} \lambda_{\alpha p} \theta_{\alpha j} \quad ; \quad j = 1, 2, \dots, n \quad (\text{III-14})$$

If equation (III-14) is solved for the θ_{pj} , the mean residence time can then be calculated:

$$\theta = \sum_p \sum_{j=1}^n \theta_{pj} \quad (\text{III-15})$$

Substituting the initial distribution (III-8) into equation (III-14),

$$-\bar{p}_A \frac{w_{0j}}{w} = \sum_{i=1}^n \frac{w_{ij}}{v_i} \theta_{pi} + \sum_{\alpha} \lambda_{\alpha j} \theta_{\alpha j} ; \quad (\text{III-16})$$

$$j = 1, 2, \dots, n$$

This equation may be solved to yield

$$\theta_{pj} = \frac{\bar{p}_A}{w} v_j \quad (\text{III-17})$$

as can be seen by substitution, and by using equations (II-14) and (II-5).

Substituting (III-17) into (III-15) gives

$$\theta = \frac{\sum_{j=1}^n v_j}{w} \quad (\text{III-18})$$

which states that the mean residence time is just the total volume over the mean total flow. Note, however, that the initial distribution (III-6) does not give this result.

D. Contact Time Distribution

Another important property of the random passage is the contact time distribution of the particle with some part of the system. Such distributions arise, for example, in analyzing the performance of fluidized bed reactors in which the solid is a catalyst. To calculate this distribution, let θ be the instantaneous value of accumulated contact time for a particle in

the system. Then

$$\frac{d\theta}{dt} = \chi_A(\alpha, j) \quad (\text{III-19})$$

gives the variation of θ with clock time, where A is the set of states for which the contact time distribution is desired, and $\chi_A(\alpha, j)$ is equal to one if $(\alpha, j) \in A$ and equal to zero otherwise. The variable θ is then included as a variable of state to define a new Markov process whose states are of the form (α, j, θ) . The transition probability density, defined by

$$\begin{aligned} \pi [(\alpha, i, \theta_1) \rightarrow (\beta, j, \theta) ; \tau] d\theta \\ = \text{Pr} \{ \text{discrete state is } (\beta, j) \text{ and } \theta \\ \text{is in interval } (\theta, \theta + d\theta) \\ \text{at time } t + \tau \text{ given that state} \\ \text{was } (\alpha, i, \theta_1) \text{ at time } t \} \end{aligned} \quad (\text{III-20})$$

is given for small times by

$$\begin{aligned} \pi [(\alpha, i, \theta_1) \rightarrow (\beta, j, \theta) ; \tau] \\ = \pi [(\alpha, i) \rightarrow (\beta, j) ; \tau] \cdot \delta [\theta - \theta_1 - \chi_A(\alpha, i)\tau + o(\tau)] \end{aligned} \quad (\text{III-21})$$

if $(\alpha, i) = (\beta, j)$, and by the same formula with $\chi_A(\alpha, i)$ replaced by $\bar{\chi}_A$ if $(\alpha, i) \neq (\beta, j)$. Expanding the δ -function in a power series, one finds

$$\delta[\theta - \theta_1 - \chi_A(\alpha, i)\tau + o(\tau)] \quad (\text{III-22})$$

$$= \delta(\theta - \theta_1) - \chi_A(\alpha, i)\tau \frac{d}{d\theta}[\delta(\theta - \theta_1)] + o(\tau)$$

Defining the joint probability density $p_{\alpha j}(t, \theta)$ so that the probability that the discrete state is (α, j) and θ is between θ and $\theta + d\theta$ at time t is given by $p_{\alpha j}(t, \theta) d\theta$. The Chapman-Kolmogorov equation then becomes

$$p_{\beta j}(t+\tau, \theta) = \sum_{\alpha} \sum_i \int_0^{\infty} d\theta_1 \cdot \quad (\text{III-23})$$

$$p_{\alpha i}(t, \theta_1) \pi[(\alpha, i, \theta_1) \rightarrow (\beta, j, \theta); \tau]$$

Substituting (III-22) and (III-3) into (III-21) and (III-21) into (III-23), and allowing $\tau \rightarrow 0$, gives

$$\frac{\partial p_{\beta j}(t, \theta)}{\partial t} = -\chi_A(\beta, j) \frac{\partial p_{\beta j}(t, \theta)}{\partial \theta} \quad (\text{III-24})$$

$$+ \sum_{i=1}^n \frac{w_{i\beta}}{v_i} p_{\alpha i}(t, \theta) + \sum_{\alpha} \lambda_{\alpha\beta} p_{\alpha j}(t, \theta);$$

$$j = 1, 2, \dots, n+1$$

In what follows it will be convenient to lump all the exit states $(\alpha, n+1)$ into a single absorbing state α . Then defining

$$p_{\alpha}(t, \theta) = \sum_{\alpha} p_{\alpha, n+1}(t, \theta) \quad (\text{III-25})$$

it is seen that

$$\frac{\partial p_{\alpha}(t, \theta)}{\partial t} = \sum_{\beta} \sum_{i=1}^n \frac{w_{i, n+1, \beta}}{v_i} p_{\beta i}(t, \theta) \quad (\text{III-26})$$

since $\chi_{\alpha}(\beta, n+1) = 0$ and since $\sum_{\beta} \lambda_{\alpha\beta} = 0$ by equation (II-11). Equations (III-24) for $j=1, 2, \dots, n$, and equation (III-26) then describe the contact time distribution completely, once initial conditions are specified. The initial conditions are

$$p_{\beta j}(0, \theta) = \bar{p}_{\beta} \frac{w_{0j, \beta}}{\bar{w}} \delta(\theta) ; j=1, 2, \dots, n \quad (\text{III-27})$$

$$p_{\alpha}(0, \theta) = \sum_{\beta} \bar{p}_{\beta} \frac{w_{0, n+1, \beta}}{\bar{w}} \delta(\theta)$$

Note that initial distribution (III-8) has been assumed, although (III-6) could have been used as well. The desired contact time distribution, in terms of its density function $f(\theta)$, is then given by

$$f(\theta) = \lim_{t \rightarrow \infty} p_{\alpha}(t, \theta) \quad (\text{III-28})$$

Integrating equations (III-24) and (III-26) from zero to infinity,

$$f(\theta) = \sum_{\beta} \bar{p}_{\beta} \frac{w_{0, n+1, \beta}}{\bar{w}} \delta(\theta) \quad (\text{III-29})$$

$$+ \sum_{\beta} \sum_{i=1}^n \frac{w_{i, n+1, \beta}}{v_i} g_{\beta i}(\theta)$$

where the $g_{\beta j}(\theta) = \int_0^{\infty} p_{\beta j}(t, \theta) dt$ satisfy

$$\chi_A(\beta, j) \frac{d g_{\beta j}}{d \theta} = \bar{p}_{\beta} \frac{w_{0j\beta}}{\bar{w}} \delta(\theta) \quad (\text{III-30})$$

$$+ \sum_{i=1}^n \frac{w_{ij\beta}}{v_i} g_{\beta i}(\theta) + \sum_{\alpha} \lambda_{\alpha\beta} g_{\alpha j}(\theta)$$

with initial conditions $\chi_A(\beta, j) g_{\beta j}(0) = 0$.

To eliminate the δ -functions let $F(\theta) = \int_0^{\theta} f(\theta') d\theta'$ and $G_{\beta j}(\theta) = \int_0^{\theta} g_{\beta j}(\theta') d\theta'$. Then

$$F(\theta) = \sum_{\beta} \bar{p}_{\beta} \frac{w_{0j\beta}}{\bar{w}} \theta + \sum_{\beta} \sum_{i=1}^n \frac{w_{ij\beta}}{v_i} G_{\beta i}(\theta) \quad (\text{III-31})$$

and

$$\chi_A(\beta, j) \frac{d G_{\beta j}}{d \theta} = \bar{p}_{\beta} \frac{w_{0j\beta}}{\bar{w}} + \sum_{i=1}^n \frac{w_{ij\beta}}{v_i} G_{\beta i}$$

$$+ \sum_{\alpha} \lambda_{\alpha\beta} G_{\alpha j} \quad ; \quad j = 1, 2, \dots, n \quad (\text{III-32})$$

The initial conditions for the differential equations contained in (III-32) are

$$\chi_A(\beta, j) G_{\beta j}(0) = 0 \quad (\text{III-33})$$

Since for those values of (β, j) which give $\chi_A(\beta, j) = 1$, the function $g_{\beta j}(\theta)$ has its derivative of order $\delta(\theta)$ and is therefore bounded. It might be noted that if the set A consists of all the states in the system (excluding, of course, the outlet states) then equations (III-29) and (III-30) become equivalent to equation

(III-4) with initial conditions (III-8), the equations for the residence time distribution.

The mean contact time can be calculated by a method similar to that for mean residence time. Summing equations (III-30) over β and j , using equations (II-11), (II-6) and (II-5), one finds

$$\delta(\theta) - f(\theta) = \sum_{\beta} \sum_{j=1}^n \chi_A(\beta, j) \frac{dg_{\beta j}}{d\theta} \quad (\text{III-34})$$

Integrating both sides with $\chi_A(\beta, j) g_{\beta j}(0^-) = 0$,

$$1 - F(\theta) = \sum_{\beta} \sum_{j=1}^n \chi_A(\beta, j) g_{\beta j}(\theta) \quad (\text{III-35})$$

Thus, the mean contact time, θ_c , is given by

$$\theta_c = \sum_{\beta} \sum_{j=1}^n \chi_A(\beta, j) \int_0^{\infty} g_{\beta j}(\theta) d\theta \quad (\text{III-36})$$

Integrating equations (III-30) one discovers in a manner similar to equations (III-13) - (III-18) that

$$\theta_c = \frac{1}{\bar{v}} \sum_{j=1}^n \sum_{\beta} \chi_A(\beta, j) \bar{p}_{\beta} v_j \quad (\text{III-37})$$

If the set of contact states, A , consists of certain tanks in the model independently of the flow states, then

$$\chi_A(\beta, j) = \sum_{k \in A} \delta_{jk} \quad (\text{III-38})$$

and (III-37) gives

$$\theta_c = \frac{1}{\bar{\omega}} \sum_{k \in A} \nu_k \quad (\text{III-39})$$

a remarkable result. Again if initial distribution (III-6) is used rather than (III-8) the result is different.

E. Outlet Age Distribution

When discussing the significance of tracer experiments in the next section another statistical property of the random passage will prove useful. This is the distribution of residence times for a particle chosen at a random time from the outlet of the system. This will be called the outlet age distribution. To discuss this situation, it is useful to modify the transition probabilities slightly so as to make all the outlet states, $(\alpha, n+1)$, absorbing. Thus, for $j \neq n+1$, the probabilities will again obey (III-4),

$$\frac{d p_{\beta j}(t)}{dt} = \sum_{i=1}^n \frac{w_{ij}}{v_i} p_{\beta i}(t) + \sum_{\alpha} \lambda_{\alpha \beta} p_{\alpha j}(t) \quad (\text{III-40})$$

$$j = 1, 2, \dots, n$$

but the probabilities for the outlet states will be given by

$$\frac{d p_{\beta, n+1}(t)}{dt} = \sum_{i=1}^n \frac{w_{i, n+1, \beta}}{v_i} p_{\beta i}(t) \quad (\text{III-41})$$

The quantity $p_{\beta, n+1}(t)$ will then be the probability that at time t the particle has left the system and that when it left, the flow was in state β . As $t \rightarrow \infty$, this will just be the probability of the flow state being β at the instant

the particle leaves. Thus, denoting this quantity by p_{β}^e

$$p_{\beta}^e = P_{\beta, n+1}(\infty) \quad (\text{III-42})$$

This may be expressed in terms of the $\theta_{\alpha j}$ defined earlier and given by equation (III-14). Thus

$$p_{\beta}^e = P_{\beta, n+1}(\infty) = P_{\beta, n+1}(0) + \sum_{i=1}^n \frac{w_{i, n+1, \beta}}{v_i} \int_0^{\infty} P_{\beta i}(t) dt \quad (\text{III-43})$$

or

$$p_{\beta}^e = P_{\beta, n+1}(0) + \sum_{i=1}^n \frac{w_{i, n+1, \beta}}{v_i} \theta_{\beta i} \quad (\text{III-44})$$

For the initial distribution (III-8), $\theta_{\beta j}$ is given by (III-17) and

$$P_{\beta, n+1}(0) = \bar{p}_{\beta} \frac{w_{0, n+1, \beta}}{\bar{w}}$$

Thus

$$p_{\beta}^e = \bar{p}_{\beta} \frac{w_{0, n+1, \beta}}{\bar{w}} + \sum_{i=1}^n \bar{p}_{\beta} \frac{w_{i, n+1, \beta}}{\bar{w}} \quad (\text{III-45})$$

which gives

$$p_{\beta}^e = \bar{p}_{\beta} \frac{\bar{w}}{\bar{w}} = \bar{p}_{\beta} \quad (\text{III-46})$$

This result is reasonable, since initial distribution (III-8) corresponds to a particle chosen at random from the entire population, which would imply that the rate of leaving is proportional to the instantaneous total flow, just as is the rate of entering.

For the initial distribution (III-6) the $\Theta_{\beta j}$ depend more on the details of the system, so the p_{β}^e cannot be calculated so simply.

The joint probability $p_{\beta, n+1}(t)$ can be expressed as the product of the probability that the flow state is β when the particle leaves with the conditional probability that the particle has left by time t given that the flow state when it leaves is β . Thus

$$p_{\beta, n+1}(t) = p_{\beta}^e p_{n+1}(t|\beta) \quad (\text{III-47})$$

If now a particle is chosen in the exiting stream at a random time, the distribution of flow states is \bar{p}_{α} rather than p_{α}^e . Thus the joint probability of leaving in flow state α at a time less than t for a particle so chosen is given by $p_{\alpha, n+1}^*(t)$, where

$$p_{\alpha, n+1}^* = \bar{p}_{\alpha} p_{n+1}(t|\alpha) \quad (\text{III-48})$$

This gives

$$p_{\alpha, n+1}^*(t) = \frac{\bar{p}_{\alpha}}{p_{\alpha}^e} p_{\alpha, n+1}(t) \quad (\text{III-49})$$

For initial distribution (III-8), this gives

$$P_{\alpha, n+1}^*(t) = \frac{\bar{w}}{w_{\alpha}} P_{\alpha, n+1}(t) \quad (\text{III-50})$$

The outlet age density under these conditions becomes

$$f_0(t) = \sum_{\alpha} \bar{p}_{\alpha} \frac{w_{0, n+1, \alpha}}{w_{\alpha}} \delta(t) + \bar{w} \sum_{\alpha} \sum_{i=1}^n \frac{w_{i, n+1, \alpha}}{w_{\alpha}} \frac{p_{\alpha i}(t)}{v_i} \quad (\text{III-51})$$

Thus $f_0(t)$ is the density function of residence times for a particle chosen at a random time from the outlet stream, assuming that particles enter in proportion to the instantaneous total flow rate.

It has been seen that, while it is more difficult to calculate, one can also define a residence time distribution for a particle chosen at a random time from the outlet, assuming that particles enter at a rate independent of the instantaneous total flow rate. This quantity, $f_{0\varphi}(t)$, is given by

$$f_{0\varphi}(t) = \sum_{\alpha} \frac{\bar{p}_{\alpha}^2}{P_{\alpha}^e} \frac{w_{0, n+1, \alpha}}{w_{\alpha}} \delta(t) + \sum_{\alpha} \sum_{i=1}^n \frac{\bar{p}_{\alpha}}{P_{\alpha}^e} w_{ij\alpha} \frac{p_{\alpha i}(t)}{v_i} \quad (\text{III-52})$$

when the initial distribution is given by (III-6).

However, the quantity calculated from equation (III-51)

when the initial distribution is (III-6) has no clear probabilistic meaning.

IV. Probability Structure of Tracer Experiments

A. Probability Equations

The method used in the previous section for deriving equation (III-24) may be easily extended to the case where many continuous variable depend on a discrete state Markov process. If the variables $x_j (j=1, 2, \dots, n)$, for example, obey the set of equations

$$\frac{dx_j}{dt} = f_{j\alpha}(x) ; j=1, 2, \dots, n \quad (\text{IV-1})$$

where the subscript α is the flow state of the system, then by a derivation similar to that of the last section we find that the joint probability distribution of the x 's and the flow state satisfies

$$\begin{aligned} \frac{\partial p_\alpha(t, x)}{\partial t} + \sum_{j=1}^n \frac{\partial}{\partial x_j} [f_{j\alpha}(x) p_\alpha(t, x)] \\ = \sum_{\alpha} \lambda_{\alpha\beta} p_\alpha(t, x) \end{aligned} \quad (\text{IV-2})$$

where the probability that the flow state is α and x_1 is between $x_1^{(1)}$ and $x_1^{(2)}$ at time t is given by

$$\int_{x_1^{(1)}}^{x_1^{(2)}} \int_{x_2^{(1)}}^{x_2^{(2)}} \cdots \int_{x_n^{(1)}}^{x_n^{(2)}} p_\alpha(t, x) dx_1 dx_2 \cdots dx_n$$

Letting x_j be the concentration of tracer in the j^{th} tank, the material balance equations become

$$v_j \frac{dx_j}{dt} = \varphi_{\alpha j}(t) + \sum_{\substack{i=1 \\ i \neq j}}^n w_{ij\alpha} x_i \quad (\text{IV-3})$$

$$- \sum_{\substack{k=1 \\ k \neq j}}^{n+1} w_{jk\alpha} x_j \quad ; \quad j = 1, 2, \dots, n$$

where $\varphi_{\alpha j}(t)$ is the rate at which tracer is fed into tank j when the flow state is α . Introducing the pseudo-flows $w_{jj\alpha}$ and using equation (II-5), equation (IV-3) may be rewritten

$$v_j \frac{dx_j}{dt} = \varphi_{\alpha j}(t) + \sum_{i=1}^n w_{ij\alpha} x_i \quad ; \quad j = 1, 2, \dots, n \quad (\text{IV-4})$$

Since this is of the same form as (IV-1), the equations for the probability distribution become

$$\begin{aligned} \frac{\partial P_{\beta}(t, \underline{x})}{\partial t} + \sum_{j=1}^n \frac{\partial}{\partial x_j} \left[\left(\frac{\varphi_{\beta j}(t)}{v_j} + \sum_{i=1}^n \frac{w_{ij\beta}}{v_j} x_i \right) P_{\beta}(t, \underline{x}) \right] \\ = \sum_{\alpha} \lambda_{\alpha\beta} P_{\alpha}(t, \underline{x}) \end{aligned} \quad (\text{IV-5})$$

B. Inlet Flow Rate vs. Inlet Concentration

The inlet flow rates of tracer to the individual tanks may be expressed in terms of the inlet concentration schedule, or in terms of the total feed rate of tracer schedule. Thus, if $x_0(t)$ is the inlet concentration schedule and $\varphi(t)$ is the total tracer feed rate schedule, the two expressions are

$$\varphi_{\alpha j}(t) = w_{oj\alpha} x_o(t) \quad (\text{IV-6})$$

and

$$\varphi_{\alpha j}(t) = \frac{w_{oj\alpha}}{w_\alpha} \varphi(t) \quad (\text{IV-7})$$

It is clear that in a system with fluctuating total throughput, an experiment measuring the response to a step in $x_o(t)$ would be quite different from one measuring the response to a step in $\varphi(t)$. In the first case the tracer inlet concentration would be fixed while the feed rate of tracer would fluctuate in time with the total flow, while in the second case the feed rate of tracer would be fixed and the inlet concentration would fluctuate. Of course, if the total throughput were constant this ambiguity would not arise.

The case of fluctuating total throughput also raises the question of whether to measure outlet concentration or outlet tracer flow rate. Denoting the outlet concentration by z and the outlet tracer flow rate by ψ we see that

$$\psi = w_\alpha z = \sum_{i=1}^n w_{i,n+1,\alpha} x_i + \varphi_{\alpha,n+1} \quad (\text{IV-8})$$

For initial conditions to equation (IV-5), assume that

at the instant the experiment is begun the flow state probabilities have their stationary values, \bar{p}_α . In other words the experiment is begun at a random time independent of the flow state with the system running continuously. Thus

$$p_\alpha(0, \underline{x}) = \bar{p}_\alpha \delta(x_1) \delta(x_2) \dots \delta(x_n) \quad (\text{IV-9})$$

Once the conditions of the tracer experiment are set either through equation (IV-6) or equation (IV-7) the complete probability structure of the process is determined by equation (IV-5) together with the initial conditions (IV-9). The probability structure of γ or z can then be determined by taking appropriate combinations of the x 's, as prescribed by equation (IV-8).

It should be noted that the flow state probabilities, $p_\alpha(t)$, can be obtained from the functions $p_\alpha(t, \underline{x})$ by integration:

$$p_\alpha(t) = \int p_\alpha(t, \underline{x}) d\underline{x} \quad (\text{IV-10})$$

If equation (IV-5) is integrated with respect to \underline{x} over the whole range, the result is

$$\frac{dp_\alpha(t)}{dt} = \sum_{\alpha} \lambda_{\alpha\beta} p_\alpha(t) \quad (\text{IV-11})$$

Similarly, equation (IV-9) gives

$$\rho_{\alpha}(0) = \bar{p}_{\alpha} \quad (\text{IV-12})$$

Equations (IV-11) and (IV-12) require that the $\rho_{\alpha}(t)$ remain constant at their stationary values throughout the process (see equation (II-14)).

C. Equations for First Moments

In order to understand the relationship between the various possible tracer experiments and the probability structure of residence times as studied in the previous section, let us consider the first moments of

$\rho_{\beta}(t, \underline{x})$ defined as follows:

$$\mu_{\beta j}(t) = \int x_j \rho_{\beta}(t, \underline{x}) d\underline{x} = \langle x_j \rangle_{\beta} ; \quad (\text{IV-13})$$

$j = 1, 2, \dots, n$

Multiplying equations (IV-5) and (IV-9) by x_j and integrating, and using equation (IV-10) gives

$$\frac{d\mu_{\beta j}}{dt} = \frac{\bar{p}_{\beta}}{v_j} \varphi_{\beta j}(t) + \sum_{i=1}^n \frac{w_{ij\beta}}{v_j} \mu_{\beta i} \quad (\text{IV-14})$$

$$+ \sum_{\alpha} \lambda_{\alpha\beta} \mu_{\alpha j} ; \quad j = 1, 2, \dots, n$$

and

$$\mu_{\beta j}(0) = 0 \quad (\text{IV-15})$$

The expected outlet concentration response is given by

$$\langle z \rangle = \sum_{\alpha} \sum_{i=1}^n \frac{w_{i,n+1,\alpha}}{w_{\alpha}} \mu_{\alpha i} + \sum_{\alpha} \bar{p}_{\alpha} \frac{\varphi_{\alpha,n+1}}{w_{\alpha}} \quad (\text{IV-16})$$

and the expected outlet tracer flow rate by

$$\langle \psi \rangle = \sum_{\alpha} \sum_{i=1}^n w_{i,n+1,\alpha} \mu_{\alpha i} + \sum_{\alpha} \bar{p}_{\alpha} \varphi_{\alpha,n+1} \quad (\text{IV-17})$$

It is interesting to compare equation (IV-14) with equation (III-4). The systems become equivalent if (IV-18)-(IV-21) are true:

$$p_{\beta j}(t) = v_j \mu_{\beta j}(t) ; \quad j = 1, 2, \dots, n \quad (\text{IV-18})$$

$$p_{\beta j}(0) \delta(t) = \bar{p}_{\beta} \varphi_{\beta j}(t) ; \quad j = 1, 2, \dots, n \quad (\text{IV-19})$$

$$f(t) = \frac{d}{dt} \sum_{\beta} p_{\beta,n+1}(t) = \langle \psi \rangle \quad (\text{IV-20})$$

$$f_0(t) = \frac{d}{dt} \sum_{\beta} p_{\beta,n+1}^*(t) = \bar{w} \langle z \rangle \quad (\text{IV-21})$$

where $f(t)$ is the residence time density function for particles chosen at random from the entire population or

for particles entering the system at a random time, and $f_0(t)$ is the residence time density for particles leaving the system at a random time, provided initial distribution (III-8) applies. The different initial distributions, (III-6) and (III-8), can be matched by supplying the appropriate tracer inputs. Thus, to experimentally determine statistical quantities for initial distribution (III-6), the tracer input must be

$$\varphi_{\theta j}(t) = \frac{w_{0j}}{w_p} \delta(t) \quad (\text{IV-22})$$

which can be achieved by an impulse in tracer feed rate:

$$\varphi(t) = \delta(t) \quad (\text{IV-23})$$

To determine statistical quantities for initial distribution (III-8), the input is

$$\varphi_{\theta j}(t) = \frac{w_{0j}}{\bar{w}} \delta(t) \quad (\text{IV-24})$$

which can be achieved with an impulse in inlet concentration:

$$x_0(t) = \frac{1}{\bar{w}} \delta(t) \quad (\text{IV-25})$$

The difference between an impulse in tracer flow rate and an impulse in tracer concentration is that the amount injected for an impulse in flow rate is the same for each

realization, while for an impulse in concentration, the amount injected is proportional to the instantaneous total flow rate.

Since the system of equations (IV-14) is linear in the μ_{aj} and also in either $\varphi(t)$ or $x_0(t)$, whichever is used to describe the tracer input, the expected response to arbitrary inputs are given by the convolutions:

$$\begin{aligned} \langle \psi(t) \rangle &= \int_0^t \langle \psi_x(t-\tau) \rangle x_0(\tau) d\tau \\ \langle \psi(t) \rangle &= \int_0^t \langle \psi_\varphi(t-\tau) \rangle \varphi(\tau) d\tau \quad (\text{IV-26}) \\ \langle z(t) \rangle &= \int_0^t \langle z_x(t-\tau) \rangle x_0(\tau) d\tau \\ \langle z(t) \rangle &= \int_0^t \langle z_\varphi(t-\tau) \rangle \varphi(\tau) d\tau \end{aligned}$$

where $\psi_x(t)$ is the response in flow rate to an impulse in concentration, $\psi_\varphi(t)$ is the response in flow rate to an impulse in flow rate, $z_x(t)$ is the concentration response to an impulse in concentration, and $z_\varphi(t)$ is the concentration response to an impulse in tracer flow rate. The various residence time densities are given by

$$f_x(t) = \frac{1}{\bar{v}} \langle \psi_x(t) \rangle$$

$$f_\varphi(t) = \langle \psi_\varphi(t) \rangle$$

$$f_0(t) = \langle z_x(t) \rangle$$

where $f_x(t)$ is the residence time density of a particle chosen at random from the entire population, $f_\varphi(t)$ is that of a particle chosen at a random time at the inlet of the system, and $f_o(t)$ is that of a particle chosen at a random time at the outlet of the system. Because of (IV-26) it is clear that the responses to a step input is just the integral of the corresponding impulse response. Thus, the distribution functions corresponding to f_x , f_φ , and f_o are just the expected step responses. The impulse response $\langle z_\varphi(t) \rangle$, however, is difficult to interpret as a probability distribution.

D. Equations for Second Moments and Autocorrelations

If tracer experiments are to be used to determine a model's suitability for a given system or to calculate various parameters in the model, one can use, in addition to the mean response just discussed, further tracer response statistics for comparison with the model.

Defining second moments of $p_\theta(t, x)$ by

$$S_{\theta jk}(t) = \langle x_j x_k \rangle_\theta = \int x_j x_k P_\theta(t, x) dx \quad ; \quad (\text{IV-27})$$

$$j, k = 1, 2, \dots, n$$

one can derive in a manner similar to that used in deriving equation (IV-14) the result

$$\begin{aligned} \frac{d s_{\rho i k}}{d t} = & \left[\frac{\varphi_{\rho j}(t)}{v_j} \mu_{\rho k} + \frac{\varphi_{\rho k}(t)}{v_k} \mu_{\rho j} \right] \\ & + \sum_{i=1}^n \left(\frac{w_{i j \rho}}{v_j} s_{\rho i k} + \frac{w_{i k \rho}}{v_k} s_{\rho i j} \right) \quad (\text{IV-28}) \\ & + \sum_{\alpha} \lambda_{\alpha \rho} s_{\alpha j k} \quad ; \quad j, k = 1, 2, \dots, n \end{aligned}$$

$$s_{\rho j k}(0) = 0 \quad ; \quad j, k = 1, 2, \dots, n \quad (\text{IV-29})$$

with the $\mu_{\rho j}(t)$ calculated from equation (IV-5).

The mean-square outlet tracer flow rate is then given by

$$\begin{aligned} \langle \psi^2 \rangle = & \sum_{\alpha} \bar{p}_{\alpha} \varphi_{\alpha, n+1}^2 + \sum_{\alpha} 2 \varphi_{\alpha, n+1} \sum_{i=1}^n w_{i, n+1, \alpha} \mu_{\alpha i} \\ & + \sum_{\alpha} \sum_{j=1}^n \sum_{i=1}^n w_{i, n+1, \alpha} w_{j, n+1, \alpha} s_{\alpha i j} \quad (\text{IV-30}) \end{aligned}$$

Similarly, the mean-square outlet concentration is given by

$$\begin{aligned} \langle z^2 \rangle = & \sum_{\alpha} \bar{p}_{\alpha} \left(\frac{\varphi_{\alpha, n+1}}{w_{\alpha}} \right)^2 + \sum_{\alpha} 2 \frac{\varphi_{\alpha, n+1}}{w_{\alpha}} \sum_{i=1}^n \frac{w_{i, n+1, \alpha}}{w_{\alpha}} \mu_{\alpha i} \\ & + \sum_{\alpha} \sum_{j=1}^n \sum_{i=1}^n \frac{w_{i, n+1, \alpha}}{w_{\alpha}} \frac{w_{j, n+1, \alpha}}{w_{\alpha}} s_{\alpha i j} \quad (\text{IV-31}) \end{aligned}$$

The corresponding variances can also be calculated:

$$\sigma_{\psi}^2(t) = \langle \psi^2 \rangle - \langle \psi \rangle^2 \quad (\text{IV-32})$$

$$\sigma_z^2 = \langle z^2 \rangle - \langle z \rangle^2 \quad (\text{IV-33})$$

Another useful statistical measure would be the autocorrelation function of the output, although for a non-stationary process one does not have much insight into the meaning of this quantity. Thus $\rho_z(\tau)$ may be defined either as

$$\rho_z(\tau) = \frac{\langle \psi(t) \psi(t+\tau) \rangle - \langle \psi(t) \rangle \langle \psi(t+\tau) \rangle}{\sigma_\psi(t) \sigma_\psi(t+\tau)} \quad (\text{IV-34})$$

or as

$$\rho_z(\tau) = \frac{\langle z(t) z(t+\tau) \rangle - \langle z(t) \rangle \langle z(t+\tau) \rangle}{\sigma_z(t) \sigma_z(t+\tau)} \quad (\text{IV-35})$$

For a stationary process this would just be the ordinary autocorrelation function and would be independent of t .

To calculate this function for the model, note that

$$\psi(t) = \varphi_{\alpha, n+1}(t) + \sum_{j=1}^n w_{j, n+1, \alpha} x_j(t) \quad (\text{IV-36})$$

and

$$\psi(t+\tau) = \varphi_{\beta, n+1}(t+\tau) + \sum_{j=1}^n w_{j, n+1, \beta} x_j(t+\tau) \quad (\text{IV-37})$$

where α is the flow state at time t and β is that at time $t+\tau$. Then

$$\langle \psi(t) \psi(t+\tau) \rangle = \sum_{\alpha} \sum_{\beta} \int d\underline{x} \int d\underline{y} \cdot (\varphi_{\alpha, n+1}(t) + \sum_{j=1}^n w_{j, n+1, \alpha} x_j) \quad (\text{IV-38})$$

$$\cdot (\varphi_{\beta, n+1}(t+\tau) + \sum_{j=1}^n w_{j, n+1, \beta} y_j) p_{\alpha}(t, \underline{x}) \pi_{\tau}(\alpha, \underline{x} \rightarrow \beta, \underline{y}; \tau)$$

where $\pi_{\tau}(\alpha, \underline{x} \rightarrow \beta, \underline{y}; \tau)$ is the transition probability density of the non-stationary tracer response behavior. It is defined so that $\pi_{\tau}(\alpha, \underline{x} \rightarrow \beta, \underline{y}; \tau) d\underline{y}$ is the probability of being in flow state β and in the region $(\underline{y}, \underline{y}+d\underline{y})$ at time $t+\tau$ given that the system was in state (α, \underline{x}) at time t . Since the probability $p_{\alpha}(t, \underline{x})$ obeys equation (IV-5) for arbitrary starting conditions, it must be that $\pi_{\tau}(\alpha, \underline{x} \rightarrow \beta, \underline{y}; \tau)$ also obeys it in the following sense:

$$\begin{aligned} & \frac{\partial}{\partial \tau} \pi_{\tau}(\alpha, \underline{x} \rightarrow \beta, \underline{y}; \tau) \\ & + \sum_{j=1}^n \frac{\partial}{\partial y_j} \left[\left(\frac{v_{\beta j}(t+\tau)}{v_j} + \sum_{i=1}^n \frac{w_{i j \beta}}{v_j} y_i \right) \pi_{\tau}(\alpha, \underline{x} \rightarrow \beta, \underline{y}; \tau) \right] \quad (\text{IV-39}) \\ & = \sum_{\gamma} \lambda_{\gamma \beta} \pi_{\tau}(\alpha, \underline{x} \rightarrow \gamma, \underline{y}; \tau) \end{aligned}$$

with initial conditions

$$\pi_{\tau}(\alpha, \underline{x} \rightarrow \beta, \underline{y}; 0) = \delta_{\alpha \beta} \delta(\underline{y} - \underline{x}) \quad (\text{IV-40})$$

Equation (IV-38) may be rearranged to give

$$\begin{aligned} \langle \psi(t) \psi(t+\tau) \rangle &= \sum_{\rho} \varphi_{\rho, n+1}(t+\tau) r_{\rho} \\ &+ \sum_{\rho} \sum_{j=1}^n w_{j, n+1, \rho} q_{\rho j} \end{aligned} \quad (\text{IV-41})$$

where

$$\begin{aligned} r_{\rho} &= \sum_{\alpha} \int d\alpha \int d\beta [\varphi_{\alpha, n+1}(t) + \sum_{j=1}^n w_{j, n+1, \alpha} x_j] \\ &\cdot p_{\alpha}(t, \alpha) \pi_{\tau}(\alpha, \alpha \rightarrow \rho, \beta; \tau) \end{aligned} \quad (\text{IV-42})$$

and

$$\begin{aligned} q_{\rho j} &= \sum_{\alpha} \int d\alpha \int d\beta [\varphi_{\alpha, n+1}(t) + \sum_{k=1}^n w_{k, n+1, \alpha} x_k] y_j \\ &\cdot p_{\alpha}(t, \alpha) \pi_{\tau}(\alpha, \alpha \rightarrow \rho, \beta; \tau) \end{aligned} \quad (\text{IV-43})$$

Differentiating (IV-42) with respect to τ and using (IV-39) and (IV-40), it is found that

$$\frac{dr_{\rho}}{d\tau} = \sum_{\alpha} \lambda_{\alpha\rho} r_{\alpha} \quad (\text{IV-44})$$

with initial conditions,

$$\tau = 0:$$

$$r_{\rho} = \bar{p}_{\rho} \varphi_{\rho, n+1}(t) + \sum_{j=1}^n w_{j, n+1, \rho} \mu_{\rho j}(t) \quad (\text{IV-45})$$

Similarly, $q_{\rho j}$ is found to satisfy

$$\frac{dq_{\beta j}}{d\tau} = \frac{\varphi_{\beta j}(t+\tau)}{\nu_j} \sum_{\alpha} \sum_{j=1}^n \pi(\alpha \rightarrow \beta; \tau) w_{j, n+1, \alpha} \quad (\text{IV-46})$$

$$\mu_{\beta j}(t) + \sum_{i=1}^n \frac{w_{i i \beta}}{\nu_j} q_{\beta i} + \sum_{\alpha} \lambda_{\alpha \beta} q_{\alpha j}$$

with initial conditions

$$\tau = 0: \quad q_{\beta j} = \varphi_{\beta, n+1}(t) \mu_{\beta j}(t) + \sum_{k=1}^n w_{k, n+1, \beta} s_{\beta j k} \quad (\text{IV-47})$$

The flow state transition probabilities $\pi(\alpha \rightarrow \beta; \tau)$ in equation (IV-46) are determined by

$$\frac{d}{d\tau} \pi(\alpha \rightarrow \beta; \tau) = \sum_{\gamma} \lambda_{\gamma \beta} \pi(\alpha \rightarrow \gamma; \tau) \quad (\text{IV-48})$$

with

$$\pi(\alpha \rightarrow \beta; 0) = \delta_{\alpha \beta} \quad (\text{IV-49})$$

To find $\rho_t(\tau)$, then, one must solve equation (IV-48) for the $\pi(\alpha \rightarrow \beta; \tau)$, equation (IV-14) for the $\mu_{\beta j}(t)$, equation (IV-27) for the $s_{\beta j k}(t)$, equation (IV-44) for the $r_{\beta}(\tau)$, equation (IV-46) for the $q_{\beta j}(\tau)$, substitute in equation (IV-41) for $\langle \psi(t) \psi(t+\tau) \rangle$, and, finally, use equation (IV-34) to determine $\rho_t(\tau)$. Similar equations can be derived for $\langle \mathbf{z}(t) \mathbf{z}(t+\tau) \rangle$

Comparing equation (IV-44) with equation (II-13), one notes that the two differ only in the initial conditions. Similarly, equation (IV-46) differs from equation

(IV-14) only in the initial conditions and the non-homogeneous terms.

The methods given above can be extended to calculate many other statistical measures of the tracer response. Such calculations could be used for deciding upon the applicability of a given model for a given physical system or for fixing the values of parameters in the model by comparison with experimentally determined tracer response statistics.

V. Behavior of Model as a Reactor

A. Probability Equations

It is clear from equation (IV-2) that quite general processes occurring in the model under the influence of the random disturbances can be treated. For brevity, however, this section will deal only with the case of a single isothermal chemical reaction. Some other situations will be studied for specific examples of the model later.

In the presence of reaction equation (IV-4) becomes

$$v_j \frac{dx_j}{dt} = \varphi_{aj}(t) + \sum_{i=1}^n w_{ij} x_i - v_j R(x_j) \quad (V-1)$$

where x_j is now the concentration of reactant in tank j , and $R(x)$ is the reaction rate expression. Applying (IV-2), it is found that the joint probability distribution of reactant concentration and flow state is given by

$$\frac{\partial p_\beta(t, \mathbf{x})}{\partial t} + \sum_{j=1}^n \frac{\partial}{\partial x_j} \left[\left\{ \frac{\varphi_{aj}}{v_j} + \sum_{i=1}^n \frac{w_{ij}}{v_j} x_i - R(x_j) \right\} \cdot p_\beta(t, \mathbf{x}) \right] = \sum_{\alpha} \lambda_{\alpha\beta} p_\alpha(t, \mathbf{x}) \quad (V-2)$$

B. Inlet Flow Rate vs. Inlet Concentration

In considering the model as a reactor, one is primarily concerned with its stationary behavior, that which prevails at some large time after startup. Such a stationary distribution will exist only if φ_{aj} is

independent of t . Again, two possibilities occur, depending on whether one feeds reactant at a constant rate or at constant concentration. Thus either

$$\varphi_{\alpha j} = w_{0j\alpha} x_0 \quad (V-3)$$

or

$$\varphi_{\alpha j} = \frac{w_{0j\alpha}}{w_{\alpha}} \varphi \quad (V-4)$$

where x_0 is the constant inlet concentration and φ is the constant reactant feed rate. Defining $\bar{p}_{\alpha}(z) = p_{\alpha}(\infty, z)$,

$$\begin{aligned} \sum_{j=1}^n \frac{\partial}{\partial x_j} \left[\left\{ \frac{\varphi_{\beta j}}{v_j} + \sum_{i=1}^n \frac{w_{ij\beta}}{v_j} x_i - R(x_j) \right\} \bar{p}_{\beta}(z) \right] \\ = \sum_{\alpha} \lambda_{\alpha\beta} \bar{p}_{\alpha}(z) \end{aligned} \quad (V-5)$$

The outlet reactant concentration and reactant flow rate will again be given by equation (IV-8).

C. Equations for First Moments

To compare the reactor behavior to the tracer response behavior, define

$$m_{\beta j} = \langle x_j \rangle_{\beta} = \int x_j \bar{p}_{\beta}(z) dz \quad (V-6)$$

Then, from equation (V-5),

transform variable k , and with

$$m_{pj} = \hat{\mu}_{pj} = \int_0^{\infty} e^{-kt} \mu_{pj}(t) dt \quad (V-11)$$

Thus, the moments of reactant concentration, m_{pj} , for a system with first order reaction and with feed distribution φ_{pj} are just the Laplace transforms of the moments of tracer concentration, $\mu_{pj}(t)$, with tracer feed rate $\varphi_{pj} \delta(t)$. Since the expected outlet concentration and the expected outlet flow rate of tracer and reactant are given by the same linear combination of the respective individual moments, and since the Laplace transform operation is linear, the expected outlet concentration in the reaction case will be the Laplace transform of the expected outlet concentration for the corresponding tracer experiment, and the expected outlet reactant flow rate will be the Laplace transform of the expected outlet tracer flow rate. The tracer input that corresponds to the constant inlet concentration reactor case,

$$\varphi_{pj}(t) = w_{oj} x_o \delta(t), \quad (V-12)$$

as comparison with equation (IV-6) shows, is an impulse in tracer inlet concentration of height x_o . Similarly, the tracer input corresponding to the constant reactant feed rate case is

$$\varphi_{\theta j}(t) = \frac{w_{\theta j}}{w_p} \varphi \delta(t) \quad (V-13)$$

which is seen to be an impulse in tracer feed rate of height φ on comparison with equation (IV-7). Since $f_x(t)$ and $f_\varphi(t)$ are the expected responses in outlet tracer flow rate for an impulse in inlet tracer concentration (of height $\frac{1}{w}$) and a unit impulse in inlet tracer flow rate, respectively, it is seen that, for a reactor with constant inlet reactant concentration x_0 ,

$$\frac{\langle \psi \rangle}{\bar{w} x_0} = \int_0^{\infty} e^{-kt} f_x(t) dt \quad (V-14)$$

and for one with a constant inlet reactant flow rate ,

$$\frac{\langle \psi \rangle}{\varphi} = \int_0^{\infty} e^{-kt} f_\varphi(t) dt \quad (V-15)$$

Similarly, one can express the expected outlet concentration of reactant as the Laplace transform of the expected outlet tracer concentration for the appropriate tracer input. The terms on the left of equation (V-14) and (V-15) are both seen to be the expected fraction of reactant which leaves unconverted.

The results above can be applied to systems with a number of first order reactions occurring simultaneously by expressing the concentration as linear combinations of independent components. The conversion of each of the independent components can then be calculated from equation (V-14) or (V-15). The independent components, as explained by

Prater and Wei [13,14], are just eigenvectors of the reaction rate constant matrix. Thus, suppose the rate of reaction of species i is given by

$$r_i = \sum_j k_{ji} x_j \quad (\text{V-16})$$

Then, by diagonalizing,

$$r_i' = k_i' x_i' \quad (\text{V-17})$$

where x_i' is the contribution of the i^{th} eigenvector of k_{ij} to the concentration, and k_i' is the i^{th} eigenvalue.

If the reaction system contains a region where reaction takes place, with the rest of the reactor being inert, the contact time distribution for the active region replaces the residence time distribution in (V-14) or (V-15) above. To see this consider the Laplace transform of equation (III-30):

$$\begin{aligned} \chi_A(\beta, j) k \hat{g}_{\beta j} &= \bar{P}_\beta \frac{w_{\beta j}}{w} + \sum_{i=1}^n \frac{w_{i\beta}}{v_i} \hat{g}_{\beta i} \\ &+ \sum_{\alpha} \lambda_{\alpha\beta} \hat{g}_{\alpha j} \quad ; \quad j = 1, 2, \dots, n \end{aligned} \quad (\text{V-18})$$

Comparison of (V-18) with (V-10) shows that $m_{\beta j} = \frac{\hat{g}_{\beta j}}{v_j}$ when $k m_{\beta j}$ is set to zero for $j \neq A$. Comparison of (V-9) with (III-29) then finishes the proof.

D. Equations for Second Moments and Autocorrelations

Second moments are calculated from equation (V-4) in a similar manner to first moments. Thus one finds

$$\begin{aligned} \langle R(x_j) \rangle_{\beta} &= \bar{p}_{\beta} \frac{\varphi_{\beta j}}{v_j} + \sum_{i=1}^n \frac{w_{ij\beta}}{v_j} m_{\beta i} \\ &+ \sum_{\alpha} \lambda_{\alpha\beta} m_{\alpha j} \quad ; j=1,2,\dots,n \end{aligned} \quad (\text{V-7})$$

The expected outlet concentration will then be given by

$$\langle Z \rangle = \sum_{\alpha} \sum_{i=1}^n \frac{w_{i,n+1,\alpha}}{w_{\alpha}} m_{\alpha i} + \sum_{\alpha} \bar{p}_{\alpha} \frac{\varphi_{\alpha,n+1}}{w_{\alpha}} \quad (\text{V-8})$$

which corresponds to equation (IV-16) for tracer experiments. Similarly, the expected outlet flow rate of reactant will be given by

$$\langle \psi \rangle = \sum_{\alpha} \sum_{i=1}^n w_{i,n+1,\alpha} m_{\alpha i} + \sum_{\alpha} \bar{p}_{\alpha} \varphi_{\alpha,n+1} \quad (\text{V-9})$$

The set of equations (V-7) will determine the $m_{\alpha i}$ completely only if $R(x_i)$ is a linear function of x_i . Thus, let $R(x_i) = kx_i$. Then one obtains

$$\begin{aligned} k m_{\beta j} &= \bar{p}_{\beta} \frac{\varphi_{\beta j}}{v_j} + \sum_{i=1}^n \frac{w_{ij\beta}}{v_j} m_{\beta i} \\ &+ \sum_{\alpha} \lambda_{\alpha\beta} m_{\alpha j} \quad ; j=1,2,\dots,n \end{aligned} \quad (\text{V-10})$$

which is a set of algebraic equations sufficient to determine the $m_{\beta j}$. Comparing equation (V-10) with equation (IV-14) it is seen that replacement of $\varphi_{\beta j}(t)$ in (IV-14) with $\varphi_{\beta j} \delta(t)$, where $\varphi_{\beta j}$ is constant, makes (V-10) the Laplace transform of (IV-14) with

$$\begin{aligned}
\langle x_j R(x_k) \rangle_\rho + \langle x_k R(x_j) \rangle &= \left\{ \frac{\varphi_{aj}}{\nu_j} m_{\rho k} + \frac{\varphi_{ak}}{\nu_k} m_{\rho j} \right\} \\
&\quad (V-19) \\
&+ \sum_{i=1}^n \left\{ \frac{w_{ij\beta}}{\nu_j} \langle x_i x_j \rangle_\beta + \frac{w_{ik\beta}}{\nu_k} \langle x_i x_k \rangle_\beta \right\} \\
&+ \sum_{\alpha} \lambda_{\alpha\beta} \langle x_j x_k \rangle_\alpha
\end{aligned}$$

Again, for first order reactions, $R(x_k) = kx_k$. Letting $s'_{\rho jk} = \langle x_j x_k \rangle_\rho$, this gives

$$\begin{aligned}
2 k s'_{\rho jk} &= \left\{ \frac{\varphi_{aj}}{\nu_j} m_{\rho k} + \frac{\varphi_{ak}}{\nu_k} m_{\rho j} \right\} \\
&\quad (V-20) \\
&+ \sum_{i=1}^n \left\{ \frac{w_{ij\beta}}{\nu_j} s'_{\rho ij} + \frac{w_{ik\beta}}{\nu_k} s'_{\rho ik} \right\} \\
&+ \sum_{\alpha} \lambda_{\alpha\beta} s'_{\alpha jk}
\end{aligned}$$

This may be compared to the Laplace transform of equation (IV-28):

$$\begin{aligned}
k \hat{s}_{\rho jk} &= \frac{[\widehat{\varphi_{aj}(t)} \mu_{\rho k}(t)]}{\nu_j} + \frac{[\widehat{\varphi_{ak}(t)} \mu_{\rho j}(t)]}{\nu_k} \\
&+ \sum_{i=1}^n \left\{ \frac{w_{ij\beta}}{\nu_j} \hat{s}_{\rho ij} + \frac{w_{ik\beta}}{\nu_k} \hat{s}_{\rho ik} \right\} \\
&+ \sum_{\alpha} \lambda_{\alpha\beta} \hat{s}_{\alpha jk}
\end{aligned} \quad (V-21)$$

For the impulse inputs (IV-21) or (IV-23), equation (V-21) is different from (V-20), for in this case

$$\varphi_{\rho j}(t) = \varphi_{\rho j} \cdot \delta(t) \quad \text{and} \quad \varphi_{\rho j}(t) \mu_{\rho k}(t) = \frac{\bar{P}_a}{V_k} \frac{\varphi_{\rho j} \varphi_{\rho k}}{2} \cdot \delta(t).$$

However, if $\mu_{\rho j}(t)$ is taken for the impulse response and $\varphi_{\rho j}(t)$ is taken as the step input, $\varphi_{\rho j}(t) = \varphi_{\rho j} =$ constant, equations (V-21) and (V-20) become identical, with

$$\begin{aligned} k' &= 2k \\ \hat{S}_{\rho j k} &= S'_{\rho j k} \\ \hat{\mu}_{\rho j} &= m_{\rho j} \end{aligned} \tag{V-22}$$

In this situation, equation (V-21) does not describe any realizable experiment with a single tracer, so it must be concluded that tracer response measurements of the type described cannot be used to predict the variance in conversion for first order reactions.

Actually equation (V-21) can describe an experiment performed with two tracers, one of which is injected as a pulse and the other of which is injected as a step. The expected product of the two concentrations will then be described by (V-21) with $\varphi_{\rho j}(t) = \varphi_{\rho j}$ and with $\mu_{\rho j}$ equal to expected impulse response. The mean-square unconverted fraction with first order reaction will then be the Laplace transform of the expected product of the two outlet flow rates, with the Laplace transform variable replaced by $2k$.

The calculation of the autocorrelation function of outlet concentration or reactant flow rate for the first order reaction case is entirely analogous to that for tracer experiments. However, in this case $\rho_+(t)$ is no longer dependent on t because the process is stationary. Again, experiments with two tracers are required to predict the autocorrelation function with a reaction from tracer experiments.

The expression for $\langle \psi(t)\psi(t+\tau) \rangle$ corresponding to equation (IV-41) becomes, for the first order reaction case,

$$\langle \psi(t)\psi(t+\tau) \rangle = \sum_{\beta} \varphi_{\beta, n+1} r_{\beta} + \sum_{\beta} \sum_j W_{j, n+1, \beta} q_{\beta j} \quad (V-23)$$

where r_{β} satisfies

$$\frac{dr_{\beta}}{d\tau} = \sum_{\alpha} \lambda_{\alpha\beta} r_{\alpha} \quad (V-24)$$

$$\tau=0: r_{\beta} = \bar{p}_{\beta} \varphi_{\beta, n+1} + \sum_{j=1}^n W_{j, n+1, \beta} m_{\beta j}$$

and $q_{\beta j}$ satisfies

$$\begin{aligned} k q_{\beta j} + \frac{dq_{\beta j}}{d\tau} &= \frac{\varphi_{\beta j}}{v_j} \sum_{\alpha} \sum_{j=1}^n \pi(\alpha \rightarrow \beta; \tau) W_{j, n+1, \alpha} m_{\alpha j} \\ &+ \sum_{i=1}^n \frac{W_{ij\beta}}{v_j} q_{i\beta} + \sum_{\alpha} \lambda_{\alpha\beta} q_{\alpha j} \quad (V-25) \end{aligned}$$

$$\tau=0: q_{\beta j} = \varphi_{\beta, n+1} m_{\beta j} + \sum_{k=1}^n W_{k, n+1, \beta} S'_{\beta j k}$$

VI. Some General Conclusions

In the course of describing the general model mathematically, some interesting conclusions have emerged. Since the number and configuration of the tanks, the number of flow states, and the flow state transition matrix have remained arbitrary so far, one would expect that such conclusions would have a rather general validity.

One of these involves the relationship between the probability structure of particle residence times in the system and the statistics of tracer response experiments. It was found that the expected response of the model to a step input in tracer concentration, $F_x(t)$, is just the distribution function of residence times for one initial probability distribution, and that for a step input in tracer feed rate, $F_v(t)$, is the distribution function of residence times for another initial distribution. The corresponding mean impulse responses, $f_x(t)$, and $f_v(t)$, are equal to the respective density functions. The two types of distribution become identical where the total flow rate through the system remains constant. In both cases it is the outlet tracer flow rate rather than the outlet tracer concentration that must be measured.

The experimental conditions corresponding to $f_x(t)$ would be hard to realize in practice, since it would require that the instantaneous flow rate at the (random) instant of injection be known and used as a weighting factor in

averaging together the experimental realizations. If this is not done, the result will be $f_{\varphi}(t)$ instead. Note that if the total flow rate at the instant of injection is known, the same set of experiments could be used to calculate $f_x(t)$ or $f_{\varphi}(t)$, where as the corresponding step experiments would have to be carried out differently for the two cases.

Another interesting conclusion is that the mean residence time calculated from $f_x(t)$ is equal to the total volume of the system divided by the mean total flow rate, while that calculated from $f_{\varphi}(t)$ is not. Thus, if tracer experiments are used to find the volume of a flow system, as is done in determining the volume of the circulatory system for medical diagnosis, it is $f_x(t)$ that must be determined (or $F_x(t)$).

It was noted, in addition, that the mean contact time with a given region of the system of a particle traveling through the system assuming the same initial distribution as for $f_x(t)$, is equal to the volume of the region divided by the mean total flow through the system. Again, for the initial distribution corresponding to $f_{\varphi}(t)$, this is not the case.

The two distributions can be described intuitively by giving the corresponding populations of particles. For $f_x(t)$, the particle is chosen at random from the whole mass of particles that eventually travel through

the system, while for $f(t)$ the entrance time is chosen at random and the particle is started in the system at that instant.

The relationship between the tracer response statistics and the mean conversion for a first order reaction occurring in the model was also investigated. It was found that the mean value of the fraction of reactant unconverted is given by the Laplace transform of $f_x(t)$ when the reactor is run at constant inlet concentration of reactant, and by that of $f_\varphi(t)$ when run at constant inlet flow rate of reactant. Also, if the reaction is limited to a certain region of the reactor, the mean fraction unconverted is given by the Laplace transform of the contact time distribution with that region, where the initial distribution used in calculating the contact time distribution is the one appropriate to $f_x(t)$ for constant concentration input, and to $f_\varphi(t)$ for constant reactant flow rate.

The mean outlet concentration for a first order reaction (rather than the mean outlet reactant flow rate) can be calculated from the expected concentration response of the corresponding tracer experiment, $\langle \bar{x}(t) \rangle$ in the same way, although such functions cannot be interpreted as residence time distributions.

The results for a single first order reaction may be extended to complex first order systems by means of

a transformation suggested by Prater and Wei [23,24].

Finally, it should be noted that the results above also apply to any non-stochastic system with time-varying flow rates, since a variable following a fixed function of time is trivially a Markov process.

VI. Some General Conclusions

In the course of describing the general model mathematically, some interesting conclusions have emerged. Since the number and configuration of the tanks, the number of the flow states, and the flow state transition matrix have remained arbitrary so far, one would expect that such conclusions would have a rather general validity.

One of these involves the relationship between the probability structure of particle residence times in the system and the statistics of tracer response experiments. Four impulse response experiments were discussed, ψ_x , ψ_φ , Ξ_x , Ξ_φ , which are the tracer flow rate responses to impulse in concentration and tracer flow rate respectively, and the concentration response to concentration and flow rate respectively. When the total flow rate through the system is constant, all four expected responses are identical. In general, however, three of these can be given a probabilistic interpretation. Thus

$$\begin{aligned} f_x(t) &= \frac{1}{\bar{w}} \langle \psi_x(t) \rangle \\ f_\varphi(t) &= \langle \psi_\varphi(t) \rangle \\ f_o(t) &= \langle \Xi_x(t) \rangle \end{aligned} \tag{VI-1}$$

where $f_x(t)$, $f_\varphi(t)$ and $f_o(t)$ are residence time density

functions for different populations of particles. The function $f_x(t)$ is the density for the entire population of particles that pass through the system. This is the "true" residence time distribution for the system. It has the property that its mean value is equal to the total volume of the system divided by the average total flow rate, while the other distributions do not, in general, have this property. The function $f_p(t)$ is the residence time density of a particle injected into the system at a random time, and $f_o(t)$ is the residence time density of a particle taken from the outlet stream at a random time. In general, all three functions are different. However, $f_p(t)$ and $f_o(t)$ are rather closely related. At the point $t=0$, for example, the functions are equal ($f_p(0)=f_o(0)$).

The density functions can be evaluated from impulse experiments, as described in (VI-1), or from the corresponding step experiments. In the case of step experiments the expected response will just be the distribution function for the corresponding density function. When conventional experimental techniques are used, however, not all the responses are as convenient to determine. It is usual to measure tracer outlet concentration directly. Determination of tracer outlet flow rate thus requires simultaneous

knowledge of the total outlet flow rate. Also, it is more convenient to inject pulses of constant amount which correspond to pulses in inlet tracer flow rate, than to vary the amounts in proportion to the instantaneous total inlet flow rate, which would correspond to pulse in inlet concentration. Of course, since the expected response of the system depends linearly on the input, the response to a concentration impulse can be determined by injecting equal pulses but multiplying the output by the total flow rate at the instant of injection before averaging the realizations together. Again, this would require knowledge of the total flow rate. The twostep inputs, constant tracer inlet concentration and constant inlet tracer flow rate, can both be achieved without measuring flow rate. Thus, if total flow rate is measured along with outlet concentration, all the responses, both impulse and step, can be measured, but if total flow rate is not measured, only the impulse response $\langle \bar{x}_\varphi(t) \rangle$ and the step responses corresponding to $\langle \bar{x}_\varphi(t) \rangle$ and $\langle \bar{x}_x(t) \rangle$ can be found. It has been shown that $\langle \bar{x}_\varphi(t) \rangle$ is hard to interpret in any probabilistic sense, while $\langle \bar{x}_x(t) \rangle$ gives the residence time density for a special class of particles, those chosen at random times from the outlet stream. The true residence

time density, $f_x(t) = \langle \psi_x(t) \rangle$, could not be determined by such experiments. This is of some interest when tracer experiments are used to determine the volume of the system, as is done in medical diagnosis. Only the density $f_x(t)$ has the mean value given by total volume divided by mean flow rate.

It was also noted that the mean contact time of a particle with a given region of the system, considering the entire population of particles, is equal to the volume of the region divided by the total flow through the system. For other populations this is not true.

The relationship between the tracer response statistics and mean conversion for a first order reaction occurring in the model was also investigated. It was found that the expected outlet flow rate of unconverted reactant when the reactant enters at constant concentration is the Laplace transform of $f_x(t) = \frac{1}{\bar{v}} \langle \psi_x(t) \rangle$. Similarly, when reactant enters at constant flow rate, the outlet flow rate of unconverted reactant is the Laplace transform of $f_\phi(t) = \langle \psi_\phi(t) \rangle$. The outlet concentration of unconverted reactant for constant inlet concentration of reactant is the Laplace transform of $f_o(t) = \langle z_x(t) \rangle$. Finally, the expected outlet concentration of reactant for constant inlet flow

rate of reactant is the Laplace transform of $\langle \bar{x} \varphi(t) \rangle$

When the reaction occurs only in some zone of the entire system, the unconverted fraction is given by the Laplace transform of the contact time distribution. This is not easily obtained from tracer response statistics, however.

The results for a single first order reaction may be extended to complex first order systems by a method suggested by Wei and Prater [23,24].

VII. Single Tank Model

A. Formulation

In order to study the properties of stochastic models in more detail, some simple examples will be analyzed by the methods described. The simplest that comes to mind consists of a single tank with a fluctuating flow rate. Also for simplicity, the number of flow states will be taken as two.

For the case of two flow states, because of condition (II-11), the transition matrix $\lambda_{\alpha\beta}$ can be expressed in terms of two parameters, λ_1 , and λ_2 . Thus letting the matrix element λ_{12} equal the parameter λ_1 , and, similarly, $\lambda_{21} = \lambda_2$, the diagonal terms become $\lambda_{11} = -\lambda_1$, and $\lambda_{22} = -\lambda_2$. The probability distribution then satisfies

$$\frac{dp_1}{dt} = -\lambda_1 p_1 + \lambda_2 p_2 \quad (\text{VII-1})$$

$$\frac{dp_2}{dt} = \lambda_1 p_1 - \lambda_2 p_2$$

corresponding to equation (II-13). If the initial values of p_1 and p_2 are p_1^0 and p_2^0 , with $p_1^0 + p_2^0 = 1$, the solution to (VII-1) becomes

$$p_1 = \bar{p}_1 + (p_1^0 - \bar{p}_1) e^{-(\lambda_1 + \lambda_2)t} \quad (\text{VII-2})$$

$$p_2 = \bar{p}_2 + (p_2^0 - \bar{p}_2) e^{-(\lambda_1 + \lambda_2)t}$$

where \bar{p}_1 and \bar{p}_2 are the stationary probabilities, given by

$$\bar{p}_1 = \frac{\lambda_2}{\lambda_1 + \lambda_2}, \quad \bar{p}_2 = \frac{\lambda_1}{\lambda_1 + \lambda_2} \quad (\text{VII-3})$$

Equation (VII-2) can be used to find the transition probabilities, $\pi(\alpha \rightarrow \beta; \tau)$, by choosing the proper initial distributions. Thus, $\pi(1 \rightarrow 2; \tau)$ is just $p_2(\tau)$ with the initial distribution $p_1^0=1, p_2^0=0$. Thus,

$$\begin{aligned} \pi(1 \rightarrow 2; \tau) &= \bar{p}_2 [1 - e^{-(\lambda_1 + \lambda_2)\tau}] \\ \pi(1 \rightarrow 1; \tau) &= \bar{p}_1 + \bar{p}_2 e^{-(\lambda_1 + \lambda_2)\tau} \\ \pi(2 \rightarrow 1; \tau) &= \bar{p}_1 [1 - e^{-(\lambda_1 + \lambda_2)\tau}] \\ \pi(2 \rightarrow 2; \tau) &= \bar{p}_2 + \bar{p}_1 e^{-(\lambda_1 + \lambda_2)\tau} \end{aligned} \quad (\text{VII-4})$$

The transition probabilities given by (VII-4) define the probability structure of the flow states completely.

It will be useful to compute some statistics of the stationary flow state distribution. If the two values of flow rate are w_1 and w_2 ,

$$\bar{w} = \bar{p}_1 w_1 + \bar{p}_2 w_2 \quad (\text{VII-5})$$

$$\sigma_w^2 = \bar{p}_1 \bar{p}_2 (w_1 - w_2)^2 \quad (\text{VII-6})$$

where w is the mean flow rate and σ_w^2 is the variance of the flow rate. The autocorrelation function of the

flow rate may be calculated from the transition probabilities (VII-4):

$$\begin{aligned} \langle w(t)w(t+\tau) \rangle &= w_1^2 \bar{p}_1 \pi(1 \rightarrow 1; \tau) \\ &+ w_1 w_2 \bar{p}_1 \pi(1 \rightarrow 2; \tau) + w_1 w_2 \bar{p}_2 \pi(2 \rightarrow 1; \tau) \\ &+ w_2^2 \bar{p}_2 \pi(2 \rightarrow 2; \tau) \end{aligned} \quad (\text{VII-7})$$

$$\rho(\tau) = \frac{\langle w(t)w(t+\tau) \rangle - \langle w(t) \rangle^2}{\sigma_w^2} \quad (\text{VII-8})$$

Substituting (VII-4), (VII-5), (VII-6) and (VII-7) into (VII-8) gives

$$\rho(\tau) = e^{-(\lambda_1 + \lambda_2)\tau} \quad (\text{VII-9})$$

Actually (VII-9) applies only if $\tau \geq 0$. Since the process is stationary, $\rho(-\tau) = \rho(\tau)$ can be used to find ρ for negative τ . This is equivalent to replacing τ by $|\tau|$ in equation (VII-9).

B. Tracer Experiments

With the probability structure of the flow states established, let us next investigate the tracer response of the single tank model. For a single tank, the tracer material balance, equation (IV-4) becomes

$$v \frac{dx}{dt} = \varphi_\alpha(t) - w_\alpha x \quad (\text{VII-10})$$

The probability density, $p_{\alpha}(t, x)$, then satisfies

$$\begin{aligned} \frac{\partial p_1(t, x)}{\partial t} + \frac{\partial}{\partial x} \left[\left(\frac{\varphi_1(t)}{v} - \frac{w_1}{v} x \right) p_1(t, x) \right] \\ = -\lambda_1 p_1(t, x) + \lambda_2 p_2(t, x) \end{aligned} \quad (\text{VII-11})$$

$$\begin{aligned} \frac{\partial p_2(t, x)}{\partial t} + \frac{\partial}{\partial x} \left[\left(\frac{\varphi_2(t)}{v} - \frac{w_2}{v} x \right) p_2(t, x) \right] \\ = \lambda_1 p_1(t, x) - \lambda_2 p_2(t, x) \end{aligned}$$

with initial conditions

$$p_1(0, x) = \bar{p}_1 \delta(x), \quad p_2(0, x) = \bar{p}_2 \delta(x) \quad (\text{VII-12})$$

Rather than solving equation (VII-11) directly for the probability density, the tracer response will be characterized by its moments. Corresponding to equation (IV-14) for the first moments, one finds for a single tank

$$\frac{d\mu_1}{dt} = \frac{\bar{R}}{v} \varphi_1(t) - \left(\frac{w_1}{v} + \lambda_1 \right) \mu_1 + \lambda_2 \mu_2 \quad (\text{VII-13})$$

$$\frac{d\mu_2}{dt} = \frac{\bar{R}}{v} \varphi_2(t) + \lambda_1 \mu_1 - \left(\frac{w_2}{v} + \lambda_2 \right) \mu_2$$

with $\mu_1(0) = \mu_2(0) = 0$. Recall that $\mu_1(t) = \int x p_1(t, x) dx = \langle x \rangle_1$, according to definition (IV-13). The expected outlet concentration, which is equal to the concentration in the tank, is then given by

$$\langle x \rangle = \mu_1 + \mu_2 \quad (\text{VII-14})$$

and the expected outlet tracer flow rate by

$$\langle \psi \rangle = w_1 \mu_1 + w_2 \mu_2 \quad (\text{VII-15})$$

The two types of impulse inputs discussed in section IV are different for the single tank model because the total flow rate through the system fluctuates. For an impulse in tracer concentration, $\varphi_1(t)$ and $\varphi_2(t)$ are given by

$$\varphi_1(t) = w_1 \delta(t) \quad (\text{VII-16})$$

$$\varphi_2(t) = w_2 \delta(t)$$

For an impulse in tracer flow rate, these become

$$\varphi_1(t) = \varphi_2(t) = \delta(t) \quad (\text{VII-17})$$

The expected response to these inputs are, using the symbols $\langle \psi_x(t) \rangle$, $\langle \psi_\varphi(t) \rangle$, $\langle z_x(t) \rangle$, $\langle z_\varphi(t) \rangle$ as previously defined (see equation (IV-26)),

$$f_x(t) = \frac{1}{\bar{w}} \langle \psi_x(t) \rangle = \frac{\bar{p}_1 w_1^2 + \bar{p}_2 w_2^2}{\bar{w} v} \frac{b_1 e^{b_1 t} - b_2 e^{b_2 t}}{b_1 - b_2} \quad (\text{VII-18})$$

$$- \left\{ \frac{\bar{p}_1 w_1^2 + \bar{p}_2 w_2^2}{v^2 \bar{w}} + \frac{(w_1 - w_2)^2 \bar{p}_1 \lambda}{v \bar{w}} \right\} \frac{e^{b_1 t} - e^{b_2 t}}{b_1 - b_2}$$

$$f_\varphi(t) = \langle \psi_\varphi(t) \rangle = \frac{\bar{w}}{v} \frac{b_1 e^{b_1 t} - b_2 e^{b_2 t}}{b_1 - b_2} \quad (\text{VII-19})$$

$$- \frac{\bar{p}_1 w_1^2 + \bar{p}_2 w_2^2}{v^2} \frac{e^{b_1 t} - e^{b_2 t}}{b_1 - b_2}$$

$$f_o(t) = \langle z_x(t) \rangle = \frac{\bar{w}}{v} \frac{b_1 e^{b_1 t} - b_2 e^{b_2 t}}{b_1 - b_2} \quad (\text{VII-20})$$

$$- \frac{\bar{p}_1 w_1^2 + \bar{p}_2 w_2^2}{v^2} \frac{e^{b_1 t} - e^{b_2 t}}{b_1 - b_2}$$

$$\bar{w} \langle z_{\varphi}(t) \rangle = \frac{\bar{w}}{v} \frac{b_1 e^{b_2 t} - b_2 e^{b_1 t}}{b_1 - b_2} - \left(\frac{\bar{w}}{v} \right)^2 \frac{e^{b_1 t} - e^{b_2 t}}{b_1 - b_2} \quad (\text{VII-21})$$

where b_1 and b_2 are the two roots of

$$b^2 + \left[\frac{w_1}{v} + \frac{w_2}{v} + \lambda_1 + \lambda_2 \right] b + \frac{w_1 w_2}{v^2} + (\lambda_1 + \lambda_2) \frac{\bar{w}}{v} = 0 \quad (\text{VII-22})$$

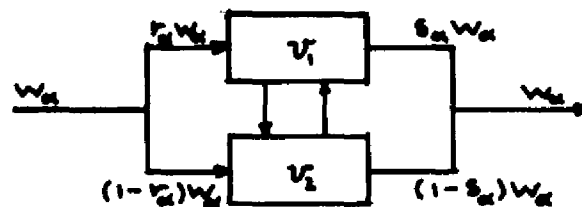
The function $f_x(t)$ is the true residence time distribution, that is the one for the entire population of particles.

As indicated, it is given by the expected response in tracer flow rate to an impulse in tracer concentration.

The function $f_{\varphi}(t)$ is the residence time distribution for a particle chosen at a random time in the inlet stream and $f_o(t)$ that for a particle chosen at a random time in the outlet stream. The concentration response to an impulse in tracer flow rate, $\langle z_{\varphi}(t) \rangle$, has been multiplied by \bar{w} to make its dimensions consistent with those of the other responses.

Comparison of equation (VII-19) with (VII-20) shows that for the single tank model, the density functions $f_{\varphi}(t)$ and $f_o(t)$ are identical, which means that particles chosen at a random time in the inlet stream have the same residence time distribution as particles chosen at a random time in the outlet stream. The fact that this is true for the single tank model might lead one to suspect that a similar

result would be true in general. In fact it is not hard to show, using equations (IV-16) and (IV-17), that the two functions have the same initial value. However, although the functions are closely related and are equal in certain simple cases, they are not equal in general. In the network shown below, for example, they are different, provided $r \neq s$:



One would expect the two functions to be different in general because the two populations are not the same. At the inlet, one chooses particles entering in one flow state or another with a certain probability. At the exit, particles leaving in one flow state entered in various flow states, so that the population changes. Apparently, in the single tank case there is a cancellation of effects that causes the second population to have the same residence time distribution on the first.

The mean residence time calculated from $f_x(t)$, equation (VII-18), is just equal to $\frac{V}{\bar{w}}$, as explained earlier. The mean residence time calculated from $f_\varphi(t)$ or $f_0(t)$, equation (VII-19) or (VII-20), is given by

$$\theta_{\varphi} = \frac{v}{\bar{w}} \left[1 + \frac{\bar{\beta}_1 \bar{\beta}_2 (w_1 - w_2)^2}{v \bar{w} (\lambda_1 + \lambda_2) + w_1 w_2} \right] \quad (\text{VII-23})$$

which can differ appreciably from $\frac{v}{\bar{w}}$. Values of θ_{φ} calculated from equation (VII-23) are always greater than $\frac{v}{\bar{w}}$. This occurs because a particle injected at a random time is more likely to start when the flow rate is low than an average particle is, and low flow rates cause larger residence times. Similarly a particle injected at a random time is less likely than an average particle to begin when the flow rate is high.

The expected response in tracer concentration to an impulse in tracer flow rate given by equation (VII-21), is difficult to interpret as a residence time distribution. In fact its integral from zero to infinity is equal to $\frac{\bar{w} \theta_{\varphi}}{v}$ where θ_{φ} is given by equation (VII-23), rather than being equal to one.

In the limit of large switching rates, as $(\lambda_1 + \lambda_2) \rightarrow \infty$, it can be seen that $\theta_{\varphi} \rightarrow \frac{v}{\bar{w}}$. In fact, in this limit, all four responses, equations (VII-18)-(VII-21), become identical and approach the impulse response of a steady flow system with flow rate \bar{w} and volume v . This is clear from equation (VII-22), which shows that as $(\lambda_1 + \lambda_2) \rightarrow \infty$, the roots b_1 and b_2 become

$$b_1 = -\frac{v}{\bar{w}}, \quad b_2 = -(\lambda_1 + \lambda_2) \quad (\text{VII-24})$$

The contribution of b_2 to the solution decays almost immediately, so the remainder of the curve is just

$$f(t) = \frac{v}{\bar{w}} e^{-\frac{\bar{w}}{v} t} \quad (\text{VII-25})$$

The constant $\frac{\bar{w}}{v}$ appears in front because the integral of $f_x(t)$ or $f_\varphi(t)$ is one for any parameter values, and that of $\bar{w} \langle z_\varphi(t) \rangle$ approaches one as $(\lambda_1 + \lambda_2) \rightarrow \infty$. Thus, as the switching rate becomes large, the expected behavior of the system becomes the same as the behavior of a steady system.

One recalls that the expected response to an arbitrary input can be calculated from the four expected impulse responses:

Thus

$$\langle \psi(t) \rangle = \int_0^t \langle \psi_x(t-\tau) \rangle x_0(\tau) d\tau \quad (\text{VII-26})$$

$$\langle \psi(t) \rangle = \int_0^t \langle \psi_\varphi(t-\tau) \rangle \varphi(\tau) d\tau \quad (\text{VII-27})$$

$$\langle z(t) \rangle = \int_0^t \langle z_x(t-\tau) \rangle x_0(\tau) d\tau \quad (\text{VII-28})$$

$$\langle z(t) \rangle = \int_0^t \langle z_\varphi(t-\tau) \rangle \varphi(\tau) d\tau \quad (\text{VII-29})$$

Then the distribution function $F_x(t)$ corresponding to $f_x(t)$ is just the expected response in outlet tracer flow rate to a step change in inlet tracer concentration. Similarly $F_\varphi(t)$ is the expected response in outlet tracer flow rate to a step change in inlet tracer flow rate, and $F_o(t)$ is the expected response in outlet tracer concentration to a step change in inlet tracer concentration. Of course, for the single tank, $F_o(t) = F_\varphi(t)$. Equation (VII-29) shows that when tracer is fed at a constant rate φ , the expected outlet concentration after a large time has elapsed is given by

$$\langle z(\infty) \rangle = \varphi \int_0^{\infty} \langle z_\varphi(t) \rangle dt \quad (\text{VII-30})$$

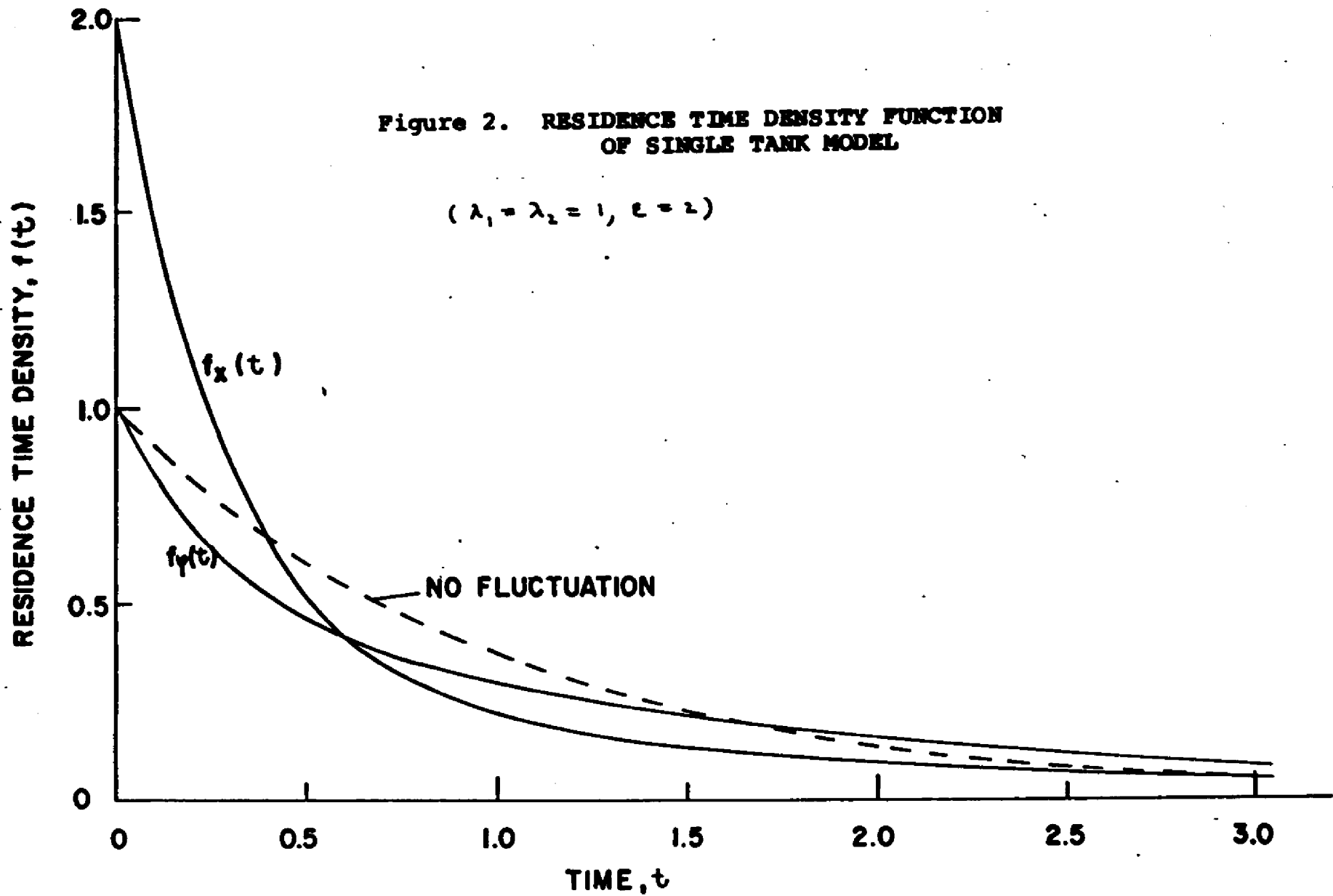
Then, from equation (VII-21),

$$\langle z(\infty) \rangle = \frac{\varphi \theta_\varphi}{V} \quad (\text{VII-31})$$

where θ_φ is given by equation (VII-23).

Curves of f_x and f_φ for some typical values of the parameter are shown in Figure 2. In this plot, $v=w=1$. Actually, this is equivalent to introducing dimensionless time and flow rates, t' , w'_1 and w'_2 given by

$$t' = \frac{\bar{w} t}{V}, \quad w'_1 = \frac{w_1}{\bar{w}}, \quad w'_2 = \frac{w_2}{\bar{w}} \quad (\text{VII-32})$$



The quantity ε , defined as $w_1 - w_2$, has been taken as 2 and $\lambda_1 = \lambda_2 = 1$. Note that this requires that $w_1 = 0$, $w_2 = 2$, and $\bar{p}_1 = \bar{p}_2 = \frac{1}{2}$. The impulse response of a steady system with flow \bar{w} is shown for comparison.

It is seen that the intercept of $f_x(t)$ is 2.0, while that of $f_\varphi(t)$ is 1.0. This fact can be understood in terms of the tracer experiments corresponding to the two curves. In the tracer experiment corresponding to $f_\varphi(t)$, the same amount of tracer is injected for each realization, regardless of the initial flow state. Thus, the initial concentration for the given parameter values is equal to 1.0 for each realization. The initial outlet flow rate of tracer is then equal to either 2.0 or 0.0, each with probability $\frac{1}{2}$, so the expected initial value is 1.0. In the tracer experiment corresponding to $f_x(t)$, the amount of tracer injected for a given realization is proportional to the flow rate at the instant of injection. Thus, in this case, the initial concentration of tracer will be either 2.0 or 0.0, each with probability $\frac{1}{2}$. If the initial concentration is 2.0, corresponding to $w = 2.0$, the initial outlet flow rate of tracer will be 4.0. Thus, the initial outlet flow rate of tracer is either 4.0 or 0.0, each with probability $\frac{1}{2}$, so the expected initial value

is 2.0. For the values of the parameters chosen in this case, the mean residence time calculated from $f_x(t)$ is 1.0, while that calculated from $f_\psi(t)$ is 1.5, which is significantly different.

A useful device for evaluating residence time distributions is to express them in terms of the escape intensity, $h(t)$, as defined by Shinnar and Naor [3]:

$$h(t) = \frac{f(t)}{\int_t^{\infty} f(s) ds} = \frac{f(t)}{1 - F(t)} \quad (\text{VII-33})$$

where $f(t)$ is the residence time density function and $F(t)$ is the corresponding distribution function. The quantity $h(t)$ has the significance of the rate at which particles which have been in the system a time t will escape from the system. This is plotted in Figure 3 for the two density functions of Figure 2. In the graph, $h_x(t)$ corresponds to $f_x(t)$ and $h_\psi(t)$ corresponds to $f_\psi(t)$. The two functions have the same interpretation, except that they refer to the two different populations of particles.

In a steady system, when the curve of $h_x(t)$ decreases over some range, it is an indication that the flow pattern exhibits bypassing or stagnancy, since the tendency of a particle to leave the system is higher when it has been in the system a short time than it is at longer times.

Figure 3

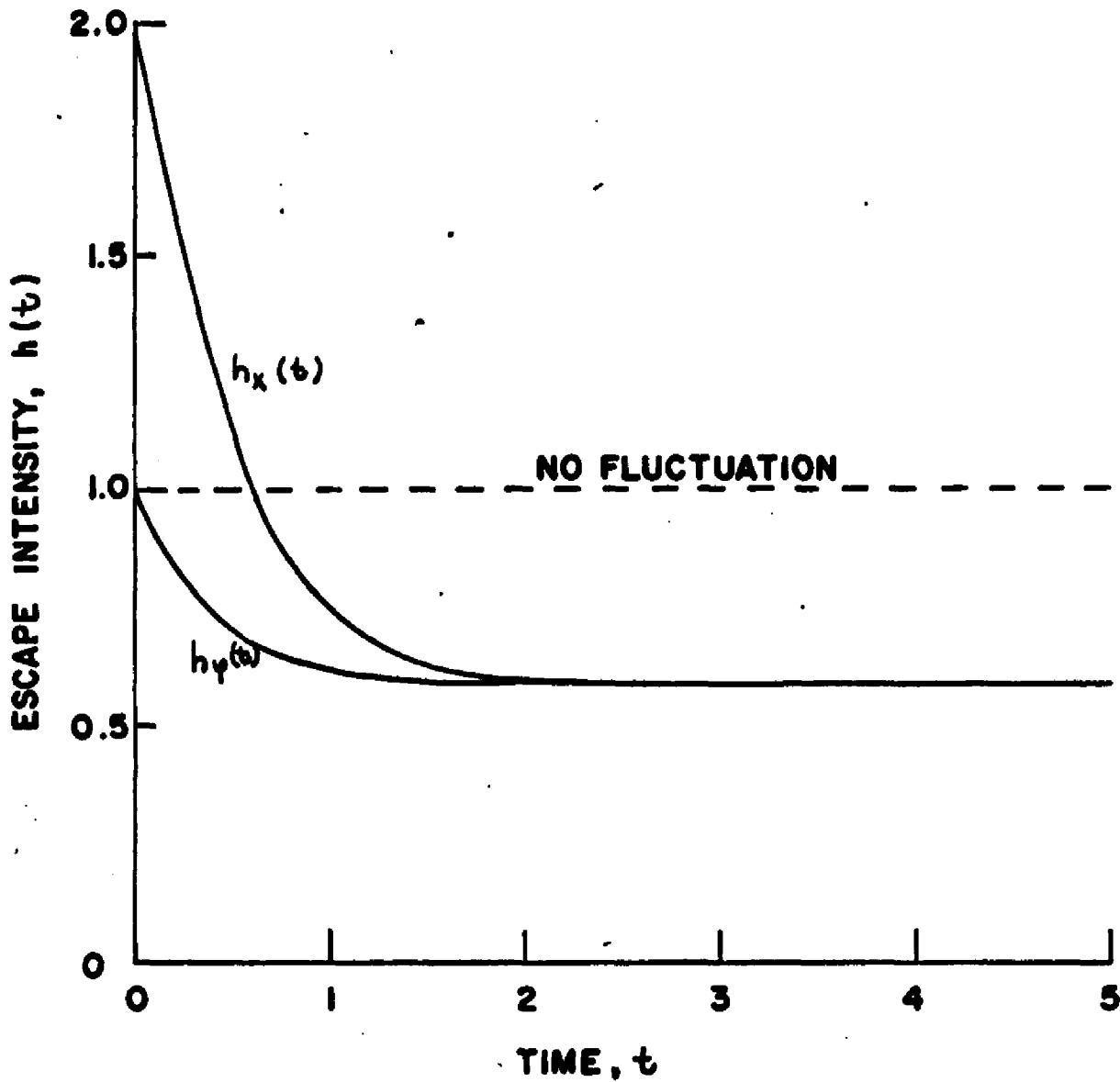


Figure 3. ESCAPE INTENSITY OF SINGLE TANK MODEL

$$(\lambda_1 = \lambda_2 = 1, \epsilon = 2)$$

It is shown in Figure 3 that this effect is present in $h_x(t)$, the intensity corresponding to $f_x(t)$, and in $h_\varphi(t)$, the intensity corresponding to $f_\varphi(t)$, both. The effect is much more noticeable in $h_x(t)$, however. Thus the effect of the fluctuating flow rate is similar to that of bypassing.

Second moments of the tracer response can also be calculated, as indicated in equation (IV-28). In this case, taking second moments in equation (VII-11) yields

$$\frac{ds_1}{dt} = 2 \frac{\varphi_1(t)}{V} \mu_1(t) - \left(2 \frac{w_1}{V} + \lambda_1 \right) S_1 + \lambda_2 S_2 \quad (\text{VII-34})$$

$$\frac{ds_2}{dt} = 2 \frac{\varphi_2(t)}{V} \mu_2(t) + \lambda_1 S_1 - \left(2 \frac{w_2}{V} + \lambda_2 \right) S_2$$

$$t = 0 : s_1 = s_2 = 0$$

where $s_i = \langle x^2 \rangle_i = \int x^2 p_i(t, x) dx$. Then

$$\langle \psi^2 \rangle = w_1^2 S_1 + w_2^2 S_2 \quad (\text{VII-35})$$

$$\langle z^2 \rangle = S_1 + S_2 \quad (\text{VII-36})$$

The variables $\mu_1(t)$ and $\mu_2(t)$ in equation (VII-34) must be determined from equation (VII-13). Note that, taken as a group, equations (VII-34) and (VII-13) together form a nonlinear system, although the independence of (VII-13) permits them to be reduced to two linear systems that can be solved sequentially. This nonlinearity makes it impossible to express the mean-square output for an arbitrary

input as a convolution with the mean-square impulse response. Thus it is not clear how the knowledge of the mean-square impulse response can be used to calculate the mean-square step response. This fact is true in general and is not restricted to the single tank model.

By the procedure explained, the following mean-square impulse responses are obtained:

$$\begin{aligned} \langle \psi_x^2 \rangle &= \frac{\bar{p}_1 w_1^4 + \bar{p}_2 w_2^4}{v^2 \bar{w}^2} \frac{b_1 e^{b_1 t} - b_2 e^{b_2 t}}{b_1 - b_2} \\ &\quad - \frac{\bar{p}_1 \bar{p}_2 (\lambda_1 + \lambda_2) (w_1^2 - w_2^2)^2 + \frac{2}{v} (\bar{p}_1 w_1^5 + \bar{p}_2 w_2^5)}{v^2 \bar{w}^2} \frac{e^{b_1 t} - e^{b_2 t}}{b_1 - b_2} \end{aligned} \quad (\text{VII-37})$$

$$\begin{aligned} \langle \psi_\varphi^2 \rangle &= \frac{\bar{p}_1 w_1^2 + \bar{p}_2 w_2^2}{v^2} \frac{b_1 e^{b_1 t} - b_2 e^{b_2 t}}{b_1 - b_2} \\ &\quad - \frac{2}{v^3} (\bar{p}_1 w_1^3 + \bar{p}_2 w_2^3) \frac{e^{b_1 t} - e^{b_2 t}}{b_1 - b_2} \end{aligned} \quad (\text{VII-38})$$

$$\begin{aligned} \langle Z_x^2 \rangle &= \frac{\bar{p}_1 w_1^2 + \bar{p}_2 w_2^2}{v^2} \frac{b_1 e^{b_1 t} - b_2 e^{b_2 t}}{b_1 - b_2} \\ &\quad - \frac{2}{v^3} (\bar{p}_1 w_1^3 + \bar{p}_2 w_2^3) \frac{e^{b_1 t} - e^{b_2 t}}{b_1 - b_2} \end{aligned} \quad (\text{VII-39})$$

$$\langle Z_\varphi^2 \rangle = \frac{\bar{w}^2}{v^2} \frac{b_1 e^{b_1 t} - b_2 e^{b_2 t}}{b_1 - b_2} - 2 \frac{\bar{w}^3}{v^3} \frac{e^{b_1 t} - e^{b_2 t}}{b_1 - b_2} \quad (\text{VII-40})$$

In all of the above, b_1 and b_2 are the roots of

$$b^2 + (\lambda_1 + \lambda_2 + 2\frac{w_1}{v} + 2\frac{w_2}{v})b + 4\frac{w_1 w_2}{v^2} + 2(\lambda_1 + \lambda_2)\frac{w}{v} = 0 \quad (\text{VII-41})$$

Note that $\langle z_x^2 \rangle = \langle \psi_\psi^2 \rangle$, again by coincidence. This shows a fortuitous balancing between the corresponding variances within each realization and between realizations.

The variances of the various quantities can be calculated from

$$\sigma_x^2 = \langle x^2 \rangle - \langle x \rangle^2 \quad (\text{VII-42})$$

where σ_x is the standard deviation of some quantity x .

The results for $\sigma(t)$ for the values of the parameter used in Figures 2 and 3 are shown in Figure 4. It is seen that the variability of ψ_x is appreciably greater than that of ψ_ψ , so that it would require more experimental runs to estimate $f_x(t) = \frac{1}{\omega} \langle \psi_x \rangle$ with a given accuracy than $f_\psi(t) = \langle \psi_\psi \rangle$. This is seen more clearly in Figure 5, which gives the coefficients of variation, $\sigma(t)/\mu(t)$, of the various impulse responses. The variability of outlet concentration for a given input is less than that of outlet tracer flow rate because the outlet tracer flow rate takes a jump whenever the total flow rate changes.

The values of $\frac{\sigma}{\mu}$ for the various responses increase without bound with increasing time, so that estimation of the impulse response at large times after injection becomes

Figure 4. STANDARD DEVIATION OF IMPULSE RESPONSE
OF SINGLE TANK MODEL

$$(\lambda_1 = \lambda_2 = 1, \varepsilon = 2)$$

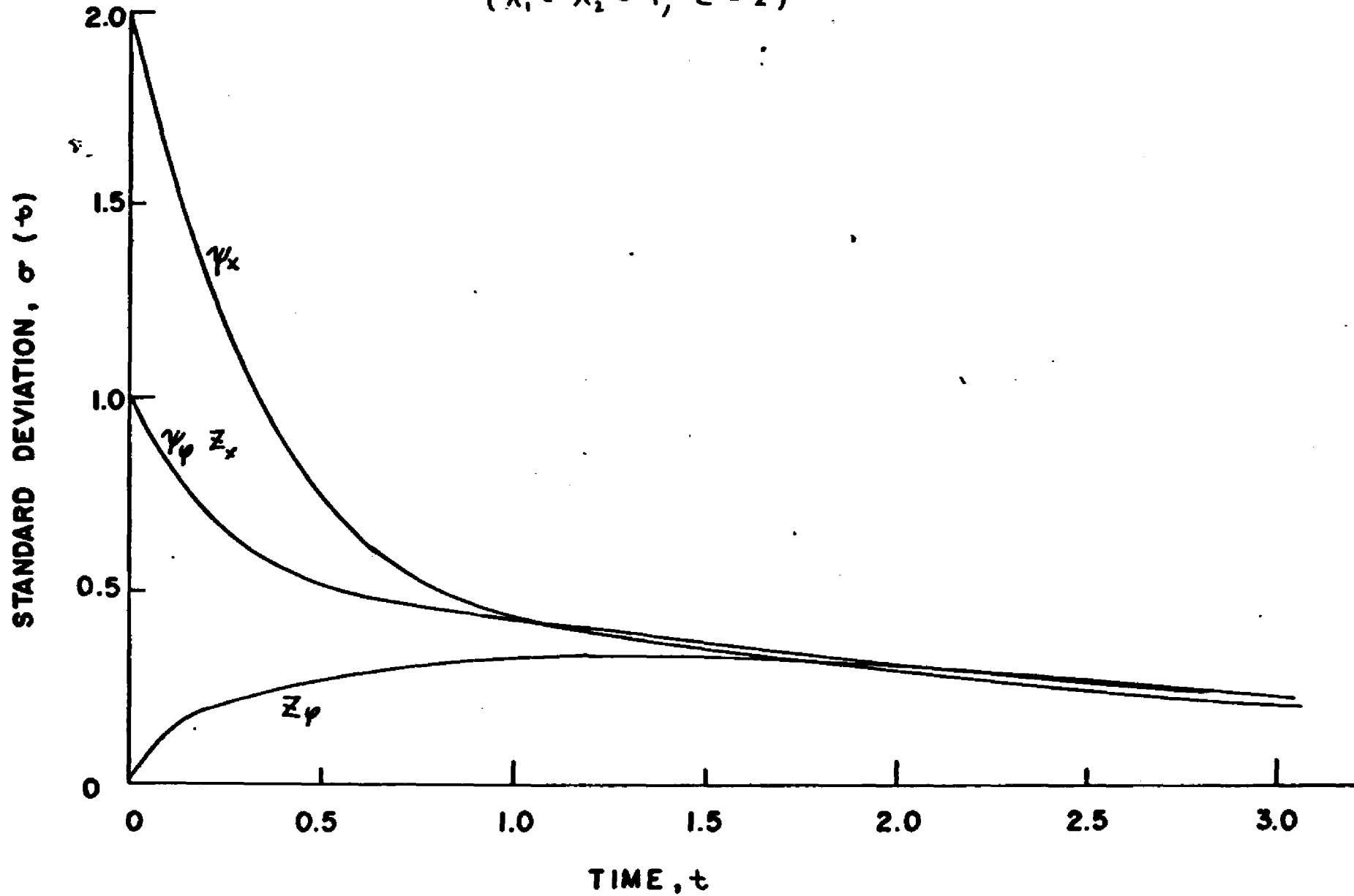
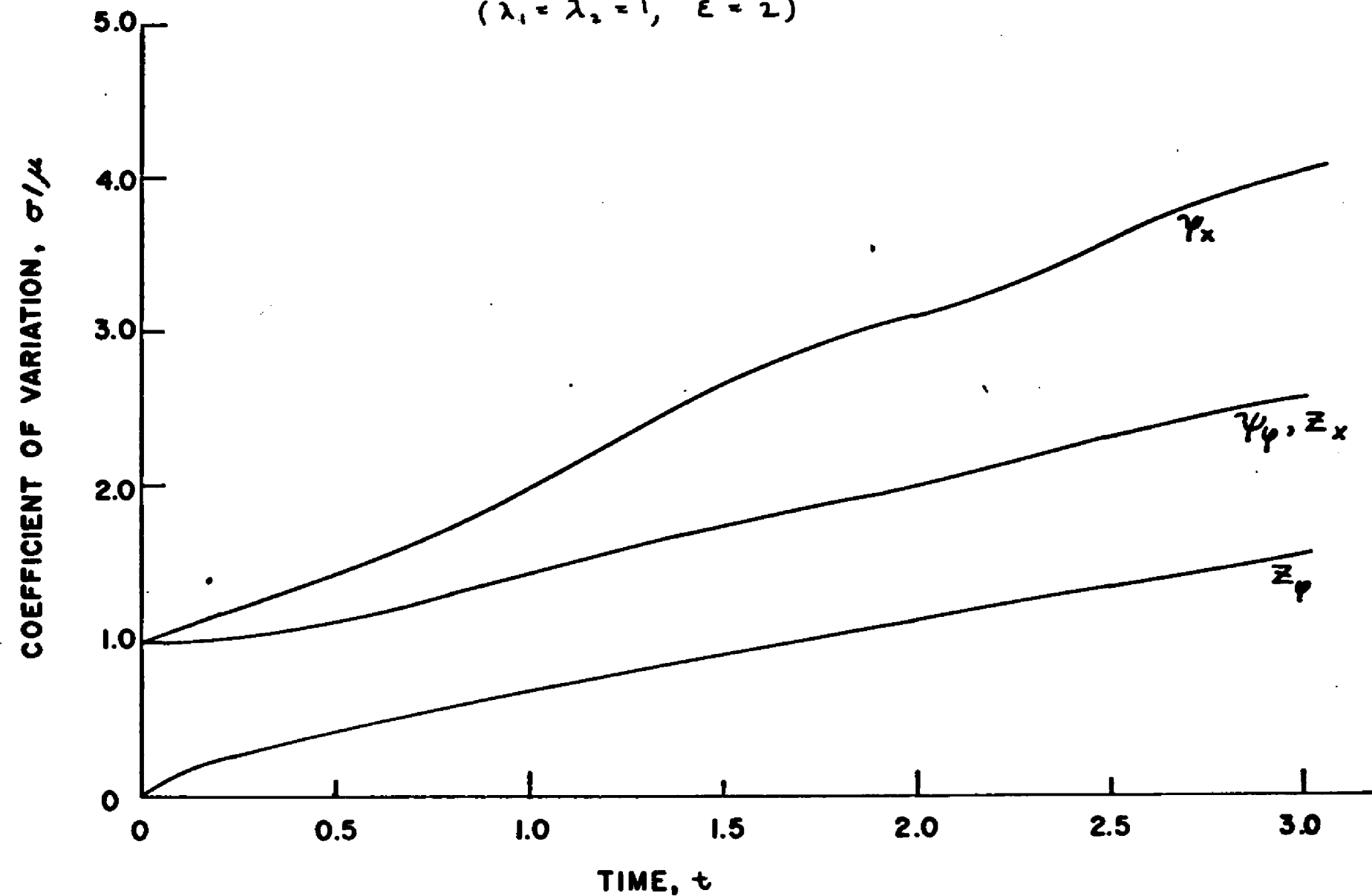


Figure 5. COEFFICIENT OF VARIATION OF IMPULSE RESPONSE
OF SINGLE TANK MODEL

$$(\lambda_1 = \lambda_2 = 1, \quad E = 2)$$



very unreliable. In the limit of large switching rates, $(\lambda_1 + \lambda_2) \rightarrow \infty$, it is found that, for ψ_x ,

$$\frac{\sigma}{\mu} \rightarrow \sqrt{[\bar{p}_1 \left(\frac{w_1}{w}\right)^2 + \bar{p}_2 \left(\frac{w_2}{w}\right)^2] - 1} \quad (\text{VII-43})$$

for ψ_φ and z_x ,

$$\frac{\sigma}{\mu} \rightarrow \sqrt{\bar{p}_1 \left(\frac{w_1}{w}\right)^2 + \bar{p}_2 \left(\frac{w_2}{w}\right)^2} - 1 \quad (\text{VII-44})$$

and for z_φ ,

$$\frac{\sigma}{\mu} \rightarrow 0 \quad (\text{VII-45})$$

Thus, even though the average behavior of the system approaches the steady behavior as $(\lambda_1 + \lambda_2) \rightarrow \infty$, the variance of some of the outputs does not drop to zero.

Equation (VII-45) shows that, in the limit of large switching rates, the concentration response to an impulse in tracer input rate becomes completely deterministic. The tracer flow rate response, however, will still fluctuate as the total flow rate changes, as shown by equation (VII-44). The concentration response to an impulse in tracer concentration is not deterministic because the amount of tracer injected will vary from one realization to another.

The correlation functions of the various tracer responses can be calculated from equations corresponding to (IV-46). For the correlation of outlet tracer flow rate,

$$\frac{dq_1}{d\tau} = \frac{\varphi_1(t+\tau)}{v} [\pi_{11}(\tau) w_1 \mu_1(t) + \pi_{21}(\tau) w_2 \mu_2(t)] \quad (\text{VII-46})$$

$$- \left(\frac{w_1}{v} + \lambda_1 \right) q_1 + \lambda_2 q_2$$

$$\frac{dq_2}{d\tau} = \frac{\varphi_2(t+\tau)}{v} [\pi_{12}(\tau) w_1 \mu_1(t) + \pi_{22}(\tau) w_2 \mu_2(t)]$$

$$+ \lambda_1 q_1 - \left(\frac{w_2}{v} + \lambda_2 \right) q_2 ; \quad \tau=0: \begin{cases} q_1 = w_1 s_1(t) \\ q_2 = w_2 s_2(t) \end{cases}$$

Then

$$\langle \psi(t) \psi(t+\tau) \rangle = w_1 q_1 + w_2 q_2 \quad (\text{VII-47})$$

Similarly, for tracer outlet concentration,

$$\frac{dq_1}{d\tau} = \frac{\varphi_1(t+\tau)}{v} [\pi_{11}(\tau) \mu_1(t) + \pi_{21}(\tau) \mu_2(t)]$$

$$- \left(\frac{w_1}{v} + \lambda_1 \right) q_1 + \lambda_2 q_2$$

(VII-48)

$$\frac{dq_2}{d\tau} = \frac{\varphi_2(t+\tau)}{v} [\pi_{12}(\tau) \mu_1(t) + \pi_{22}(\tau) \mu_2(t)]$$

$$+ \lambda_1 q_1 - \left(\frac{w_2}{v} + \lambda_2 \right) q_2 ; \quad \tau=0: \begin{cases} q_1 = s_1(t) \\ q_2 = s_2(t) \end{cases}$$

Then

$$\langle \Xi(t) \Xi(t+\tau) \rangle = q_1 + q_2 \quad (\text{VII-49})$$

For impulse responses, the inhomogeneous terms drop out of the equations. To solve (VII-46) or (VII-48), $\mu_1(t)$, $\mu_2(t)$, $s_1(t)$ and $s_2(t)$ must already have been calculated from equations (VII-13) and (VII-34).

In this manner one obtains

$$\begin{aligned} \langle \psi(t) \psi(t+\tau) \rangle &= \langle \psi^2(t) \rangle \frac{b_1 e^{b_2 \tau} - b_2 e^{b_1 \tau}}{b_1 - b_2} \\ &- \left\{ \frac{w_1^3}{v} s_1(t) + \frac{w_2^3}{v} s_2(t) + (w_1 - w_2) [\lambda_1 s_1(t) w_1 \right. \\ &\quad \left. - \lambda_2 s_2(t) w_2] \right\} \frac{e^{b_1 \tau} - e^{b_2 \tau}}{b_1 - b_2} \end{aligned} \quad (\text{VII-50})$$

$$\langle z(t) z(t+\tau) \rangle = \langle z^2(t) \rangle \frac{b_1 e^{b_1 \tau} - b_2 e^{b_2 \tau}}{b_1 - b_2} - \frac{w_1 s_1(t) + w_2 s_2(t)}{\nu} \frac{e^{b_1 \tau} - e^{b_2 \tau}}{b_1 - b_2} \quad (\text{VII-51})$$

The quantities $\langle \psi^2(t) \rangle$, $\langle z^2(t) \rangle$, $s_1(t)$, $s_2(t)$, and $\langle \psi(t) \rangle$ are calculated as before. The corresponding autocorrelations, $\rho_t(\tau)$, can then be calculated from equation (IV-34) or (IV-35).

It is interesting to calculate the slope of $\rho_t(\tau)$ at $\tau=0$. Since $\rho_t(\tau) = 1$ when $\tau=0$, and since $\rho_t(\tau) \neq 1$ for all t and τ , a non-zero slope at $\tau=0$ indicates that the curve of $\rho_t(\tau)$ at constant t will have a corner point at $\tau=0$, whereas a slope of zero at $\tau=0$ allows the curve to be smooth. The autocorrelation function of the total flow rate given by equation (VII-9), for example, exhibits such a corner.

From the definition of $\rho_t(\tau)$, equation (IV-34),

$$\frac{\partial}{\partial \tau} \left\{ \rho_t(\tau) \right\}_{\tau=0} = \frac{1}{\sigma^2(t)} \left[\frac{\partial}{\partial \tau} \left\{ \langle \psi(t) \psi(t+\tau) \rangle \right\}_{\tau=0} - \frac{1}{2} \frac{d}{dt} \langle \psi^2(t) \rangle \right] \quad (\text{VII-52})$$

A similar relationship can be obtained from equation (IV-35).

Thus it is found that, for the correlation of ψ ,

$$\frac{\partial}{\partial \tau} \left\{ \rho_t(\tau) \right\}_{\tau=0} = -\frac{1}{2} (w_1 - w_2)^2 (\lambda_1 s_1(t) + \lambda_2 s_2(t)) \quad (\text{VII-53})$$

and for the correlation of z ,

$$\frac{\partial}{\partial \tau} \{ \rho_c(\tau) \}_{\tau=0} = 0 \quad (\text{VII-54})$$

The auto correlation of outlet concentration is, therefore, smooth at $\tau=0$, while that of outlet tracer flow rate has a corner. This fact is related to the smoothness of the corresponding realizations.

C. Moments of Conversion with First Order Reaction

In the case of first order reaction, the equation of change becomes

$$v \frac{dx}{dt} = \varphi_\alpha(t) - w_\alpha x - kx \quad (\text{VII-55})$$

corresponding to equation (VII-10) for tracer response.

The probability distribution then satisfies

$$\begin{aligned} \frac{\partial p_1(t,x)}{\partial t} + \frac{\partial}{\partial x} \left[\left(\frac{\varphi_1(t)}{v} - \frac{w_1}{v} x - kx \right) p_1(t,x) \right] \\ = -\lambda_1 p_1(t,x) + \lambda_2 p_2(t,x) \end{aligned} \quad (\text{VII-56})$$

$$\begin{aligned} \frac{\partial p_2(t,x)}{\partial t} + \frac{\partial}{\partial x} \left[\left(\frac{\varphi_2(t)}{v} - \frac{w_2}{v} x - kx \right) p_2(t,x) \right] \\ = \lambda_1 p_1(t,x) - \lambda_2 p_2(t,x) \end{aligned}$$

In the case with chemical reaction, the probability distribution of interest is the stationary one, which satisfies (VII-56) with $\frac{\partial p_1(t,x)}{\partial t} = \frac{\partial p_2(t,x)}{\partial t} = 0$. Equations (VII-56) then become ordinary differential equations which can be solved directly for the probability distribution:

$$\frac{d}{dx} \left[\left\{ \frac{\varphi_1}{v} - \left(\frac{w_1}{v} + k \right) x \right\} p_1(x) \right] = -\lambda_1 p_1(x) + \lambda_2 p_2(x) \quad (\text{VII-57})$$

$$\frac{d}{dx} \left[\left\{ \frac{\varphi_2}{v} - \left(\frac{w_2}{v} + k \right) x \right\} p_2(x) \right] = \lambda_1 p_1(x) - \lambda_2 p_2(x)$$

The solution to these will be described later. The moments of the steady state conversion will be calculated first.

Taking moments in (VII-57), one obtains

$$\begin{aligned} \left(\frac{w_1}{v} + \lambda_1 + k \right) m_1 - \lambda_2 m_2 &= \frac{\bar{P}_1}{v} \varphi_1 \\ -\lambda_1 m_1 + \left(\frac{w_2}{v} + \lambda_2 + k \right) m_2 &= \frac{\bar{P}_2}{v} \varphi_2 \end{aligned} \quad (\text{VII-58})$$

where $m_1 = \int x p_1(x) dx$, $m_2 = \int x p_2(x) dx$, corresponding to equation (V-6). Equation (VII-58) is a special case of equation (V-10). The expected outlet flow rate of unconverted reactant is given by

$$\langle \psi \rangle = w_1 m_1 + w_2 m_2 \quad (\text{VII-59})$$

Similarly, the expected outlet concentration of unconverted reactant is given by

$$\langle z \rangle = m_1 + m_2 \quad (\text{VII-60})$$

For constant reactant inlet concentration, the reactant feed rate is given by

$$\varphi_1 = w_1 x_0 \quad ; \quad \varphi_2 = w_2 x_0 \quad (\text{VII-61})$$

For constant reactant feed rate these become

$$\varphi_1 = \varphi_2 = \varphi \quad (\text{VII-62})$$

In discussing first order reactions it is useful to redefine some symbols. Let ψ_x and ψ_φ now stand for the outlet reactant flow rate for constant input concentration and for constant inlet reactant flow rate, respectively.

Also, let \bar{x}_x and \bar{x}_φ be the corresponding outlet reactant concentrations. Solving (VII-58), the following results are obtained:

$$\frac{\langle \psi_x \rangle}{\bar{w} x_0} = \frac{\frac{\bar{P}_1 w_1^2 + \bar{P}_2 w_2^2}{v \bar{w}} k + \frac{w_1 w_2}{v^2} + \frac{\bar{w}}{v} (\lambda_1 + \lambda_2)}{k^2 + \left[\frac{\bar{w}}{v} + \frac{\bar{w}}{v} + \lambda_1 + \lambda_2 \right] k + \frac{w_1 w_2}{v^2} + \frac{\bar{w}}{v} (\lambda_1 + \lambda_2)} \quad (\text{VII-63})$$

$$\frac{\langle \psi_\varphi \rangle}{\varphi} = \frac{\frac{\bar{w}}{v} k + \frac{w_1 w_2}{v^2} + \frac{\bar{w}}{v} (\lambda_1 + \lambda_2)}{k^2 + \left[\frac{\bar{w}}{v} + \frac{\bar{w}}{v} + \lambda_1 + \lambda_2 \right] k + \frac{w_1 w_2}{v^2} + \frac{\bar{w}}{v} (\lambda_1 + \lambda_2)} \quad (\text{VII-64})$$

$$\frac{\langle \bar{x}_x \rangle}{x_0} = \frac{\frac{\bar{w}}{v} k + \frac{w_1 w_2}{v^2} + \frac{\bar{w}}{v} (\lambda_1 + \lambda_2)}{k^2 + \left[\frac{\bar{w}}{v} + \frac{\bar{w}}{v} + \lambda_1 + \lambda_2 \right] k + \frac{w_1 w_2}{v^2} + \frac{\bar{w}}{v} (\lambda_1 + \lambda_2)} \quad (\text{VII-65})$$

$$\frac{\bar{w} \langle \bar{x}_\varphi \rangle}{\varphi} = \frac{\frac{\bar{w}}{v} k + \frac{w_1 w_2}{v^2} + \frac{\bar{w}}{v} (\lambda_1 + \lambda_2) + \bar{P}_1 \bar{P}_2 \left(\frac{w_1}{v} - \frac{w_2}{v} \right)^2}{k^2 + \left[\frac{\bar{w}}{v} + \frac{\bar{w}}{v} + \lambda_1 + \lambda_2 \right] k + \frac{w_1 w_2}{v^2} + \frac{\bar{w}}{v} (\lambda_1 + \lambda_2)} \quad (\text{VII-66})$$

The left hand sides of equations (VII-63) and (VII-64) are equal to the fraction of reactant that remains uncon-

verted. It may be noted that as $(\lambda_1 + \lambda_2) \rightarrow \infty$, the right hand sides of all four equations approaches $\frac{1}{1 + \frac{vk}{\bar{w}}}$, the unconverted fraction for steady flow. The unconverted fraction calculated from (VII-64) is always lower than that calculated from (VII-63).

In fact it can be seen that

$$\frac{\langle \psi_0 \rangle}{\bar{c}} < \frac{1}{1 + \frac{vk}{\bar{w}}} < \frac{\langle \psi_2 \rangle}{\bar{w} x_0} \quad (\text{VII-67})$$

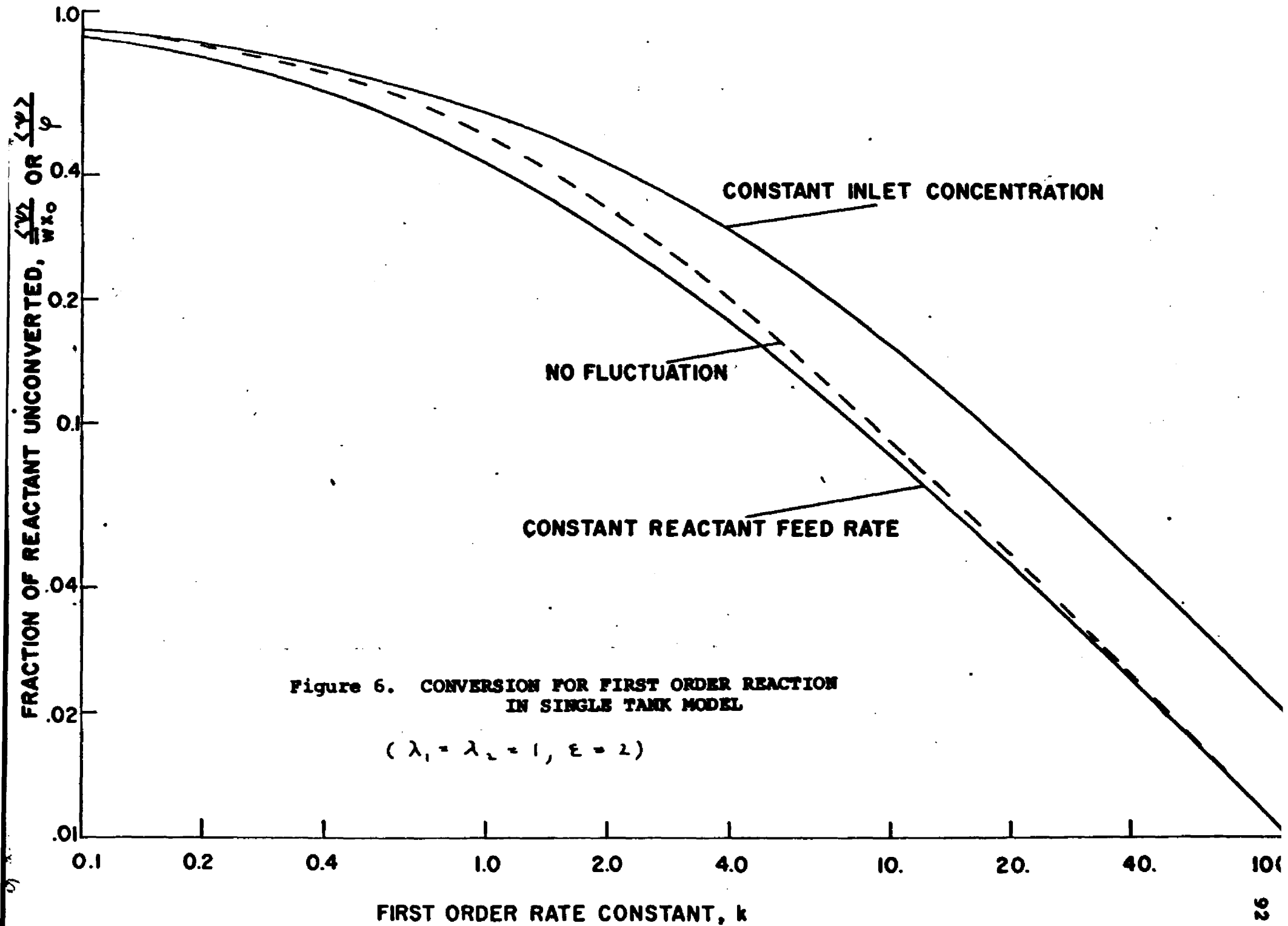
for any values of the parameters. A plot of equations (VII-63) and (VII-64) for typical values of the parameters is given in Figure 6 for illustration, along with the unconverted fraction at steady flow.

The implication of (VII-67) is that if reactant is fed at a constant rate, fluctuations in the flow rate will improve the conversion, while if reactant is fed at constant concentration, the fluctuations will make conversion worse.

The second moments for first order reactions are obtained from the following equations:

$$\begin{aligned} \left[2 \frac{\bar{w}_1}{V} + 2k + \lambda_1 \right] s_1 - \lambda_2 s_2 &= 2 \frac{c_1}{V} m_1 \\ -\lambda_1 s_1 + \left[2 \frac{\bar{w}_2}{V} + 2k + \lambda_2 \right] s_2 &= 2 \frac{c_2}{V} m_2 \end{aligned} \quad (\text{VII-68})$$

$$\langle \psi^2 \rangle = \bar{w}_1^2 s_1 + \bar{w}_2^2 s_2 \quad (\text{VII-69})$$

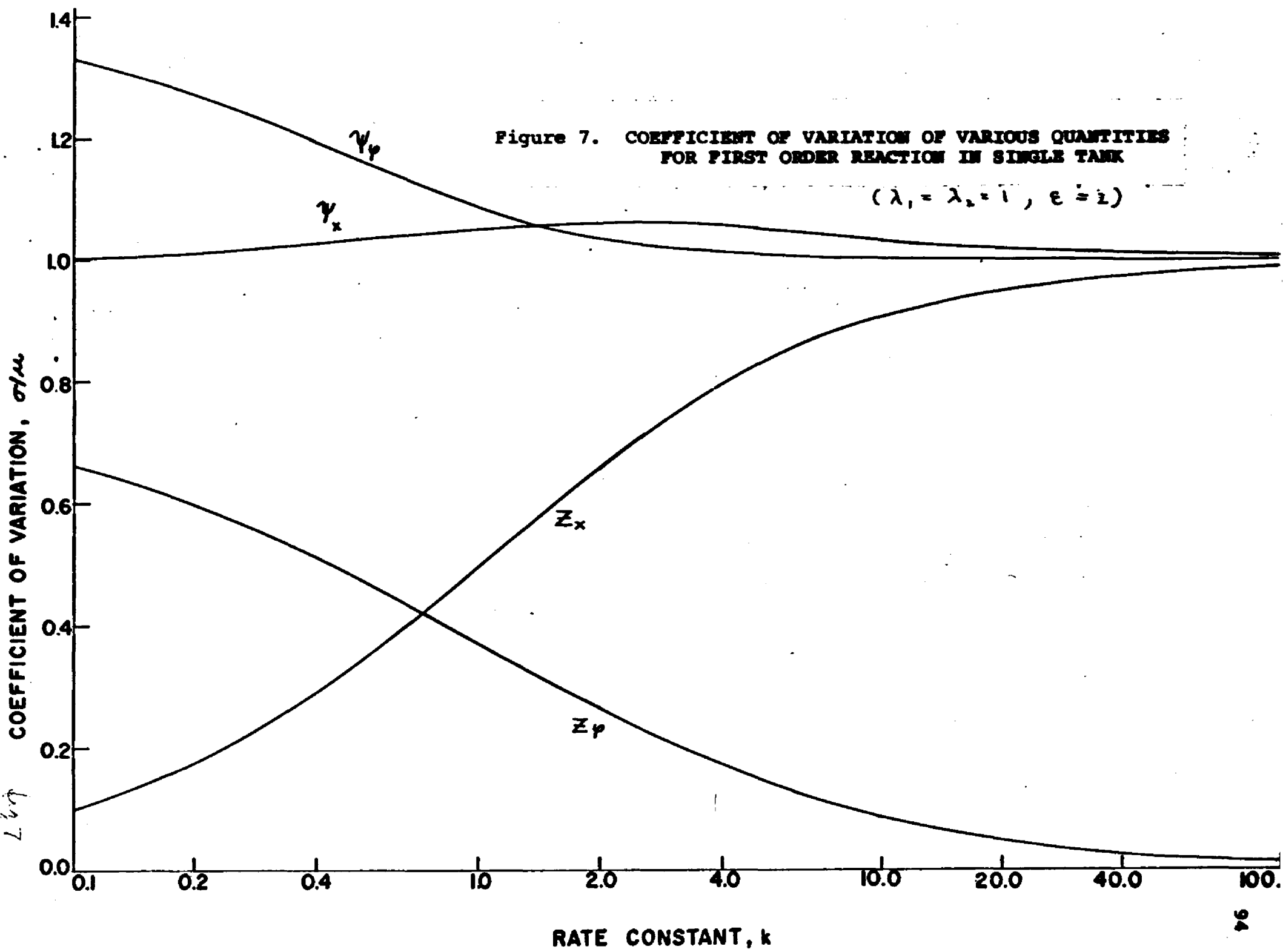


$$\langle \bar{z}^2 \rangle = S_1 + S_2 \quad (\text{VII-70})$$

These correspond to equation (V-20) for the general case. These are easily solved, but since the formulas are somewhat unwieldy they are not presented. The coefficient of variation, $\frac{\sigma}{\mu}$, of the various quantities are shown in Figure 7 for the same values of the system parameters as used in Figure 6.

It is seen in Figure 7 that the coefficient of variation of the outlet reactant flow rate is close to one for both inputs, while that of outlet concentration is appreciable smaller. It is also noted that the curves for the two inputs, constant inlet concentration and constant inlet reactant flow rate, cross over at some value of the rate constant for either measure of the output, \bar{z} or ψ . The value of one, that is asymptotically approached by three of the curves, occurs because of the parameter values used. At $\epsilon = 2$ the flow switches between 2.0 and 0.0, an extreme situation.

The equations for the autocorrelations of ψ and \bar{z} are quite similar to those for tracer response, (VII-46) and (VII-48). These become, for outlet reactant flow rate,



$$\begin{aligned} \frac{dq_1}{d\tau} = \frac{q_1}{v} [\pi_{11}(\tau) w_1 m_1 + \pi_{21}(\tau) w_2 m_2] \\ - \left(\frac{w_1}{v} + \lambda_1 + k \right) q_1 + \lambda_2 q_2 \end{aligned} \quad (\text{VII-71})$$

$$\begin{aligned} \frac{dq_2}{d\tau} = \frac{q_2}{v} [\pi_{12}(\tau) w_1 m_1 + \pi_{22}(\tau) w_2 m_2] \\ + \lambda_1 q_1 - \left(\frac{w_2}{v} + \lambda_2 + k \right) q_2 \end{aligned} \quad (\text{VII-72})$$

$$\tau = 0: \quad q_1 = w_1 s_1, \quad q_2 = w_2 s_2 \quad (\text{VII-72})$$

$$\langle \psi(t) \psi(t+\tau) \rangle = w_1 q_1 + w_2 q_2 \quad (\text{VII-73})$$

Similarly, for outlet reactant concentration,

$$\begin{aligned} \frac{dq_1}{d\tau} = \frac{q_1}{v} [\pi_{11}(\tau) m_1 + \pi_{21}(\tau) m_2] \\ - \left(\frac{w_1}{v} + \lambda_1 + k \right) q_1 + \lambda_2 q_2 \end{aligned} \quad (\text{VII-74})$$

$$\begin{aligned} \frac{dq_2}{d\tau} = \frac{q_2}{v} [\pi_{12}(\tau) m_1 + \pi_{22}(\tau) m_2] \\ + \lambda_1 q_1 - \left(\frac{w_2}{v} + \lambda_2 + k \right) q_2 \end{aligned}$$

$$\tau = 0: \quad q_1 = s_1, \quad q_2 = s_2 \quad (\text{VII-75})$$

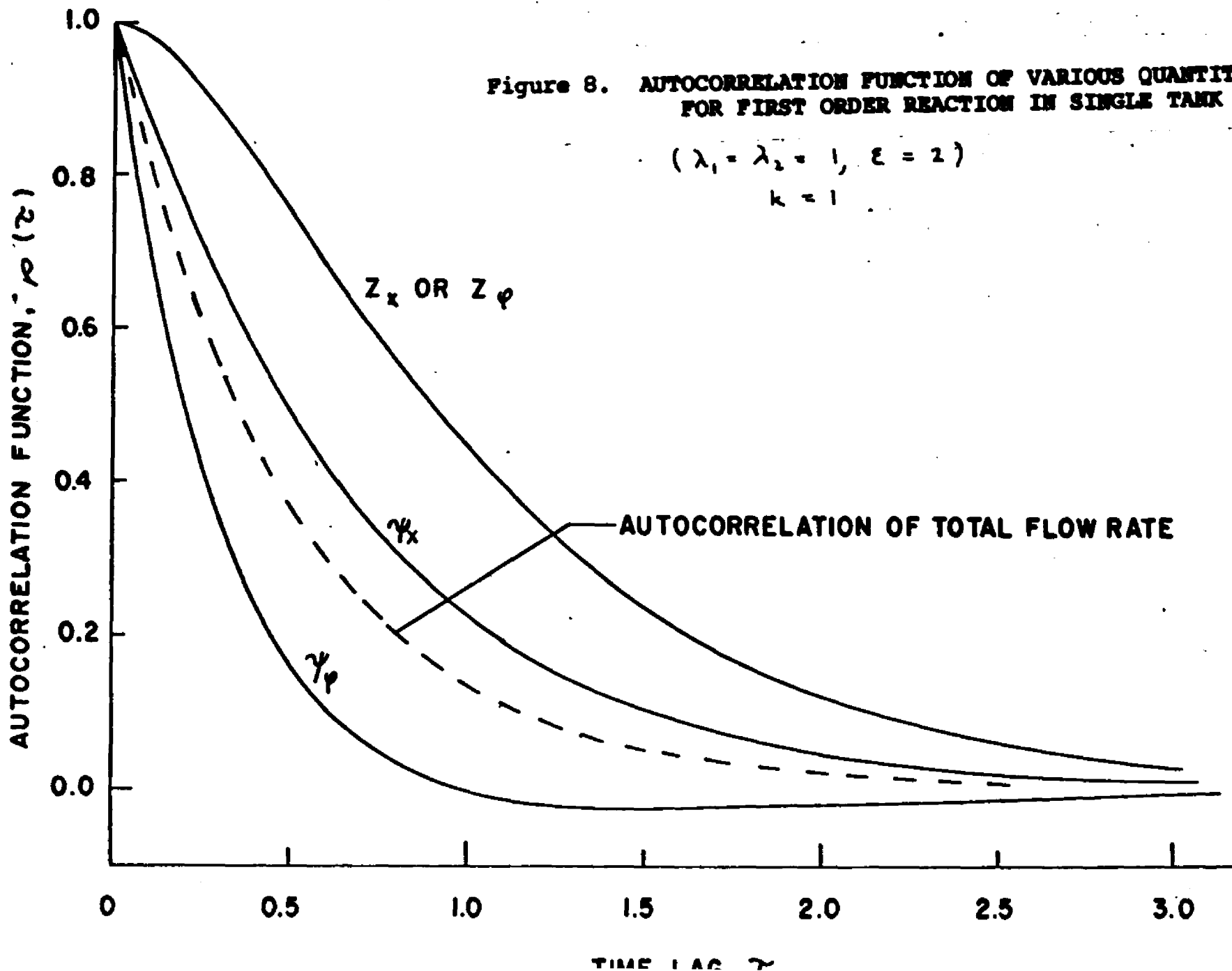
$$\langle z(t) z(t+\tau) \rangle = q_1 + q_2 \quad (\text{VII-76})$$

These were solved for some typical values and the results plotted in Figure 8. The curves for the auto-correlation of outlet concentration for the two inputs, z_x and z_φ , are seen to coincide, while those for outlet reactant flow rate, ψ_x and ψ_φ , differ. Again,

Figure 8. AUTOCORRELATION FUNCTION OF VARIOUS QUANTITIES FOR FIRST ORDER REACTION IN SINGLE TANK

$$(\lambda_1 = \lambda_2 = 1, \epsilon = 2)$$

$$k = 1$$



this is a peculiarity of the single tank model. In general all four curves would be different. As was the case for tracer response, the slope of $\rho(\tau)$ at $\tau = 0$ is equal to zero for the autocorrelation of concentration, but not for the autocorrelation of outlet reactant flow rate.

D. Probability Distribution for Single Tank with Reaction

The fact that equation (VII-48) is an ordinary differential equation makes its solution especially simple. In fact it can be solved just as easily for reactions with non-linear rate expressions. To see this let us rewrite (VII-46) more generally:

$$\frac{dx}{dt} = f_x(x) \quad (\text{VII-77})$$

Then, for two flow states, the stationary probability density satisfies

$$\begin{aligned} \frac{d}{dx} [f_1 p_1(x)] &= -\lambda_1 p_1(x) + \lambda_2 p_2(x) \\ \frac{d}{dx} [f_2 p_2(x)] &= \lambda_1 p_1(x) - \lambda_2 p_2(x) \end{aligned} \quad (\text{VII-78})$$

Adding the two equations in (VII-78) together,

$$\frac{d}{dx} [f_1 p_1 + f_2 p_2] = 0 \quad (\text{VII-79})$$

Thus

$$f_1 p_1 + f_2 p_2 = c \quad (\text{VII-80})$$

where c is some constant, independent of x .

If $f_1 + f_2$ are to have finite expectations, it is clear that $c=0$. Thus

$$f_1 p_1 = - f_2 p_2 \quad (\text{VII-71})$$

$$\frac{d}{dx} [f_1 p_1] + f_1 \left[\lambda_1 \frac{p_1}{f_1} - \lambda_2 \frac{p_2}{f_2} \right] = 0 \quad (\text{VII-72})$$

Using (VII-71) in (VII-72),

$$\frac{d}{dx} [f_1 p_1] + \left[\frac{\lambda_1}{f_1} + \frac{\lambda_2}{f_2} \right] f_1 p_1 = 0 \quad (\text{VII-73})$$

Note that because of (VII-71), p_1 and p_2 can be different from zero only where f_1 and f_2 have different signs. Define $g(x)$ so that

$$g(x) = |f_1(x) p_1(x)| = |f_2(x) p_2(x)| \quad (\text{VII-74})$$

Then

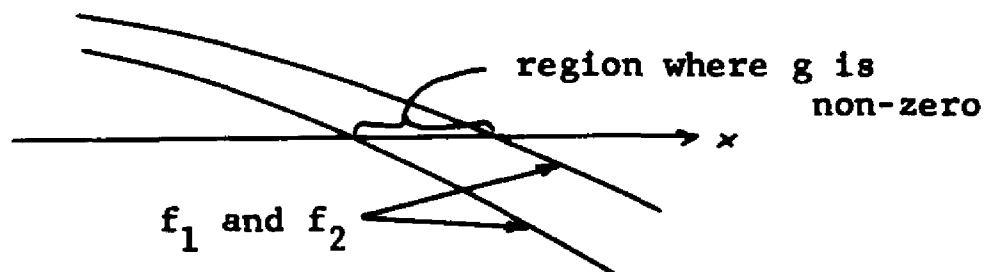
$$\frac{dg}{dx} + \left[\frac{\lambda_1}{f_1} + \frac{\lambda_2}{f_2} \right] g = 0 \quad (\text{VII-75})$$

Separating variables,

$$\frac{d}{dx} \ln g = - \left[\frac{\lambda_1}{f_1} + \frac{\lambda_2}{f_2} \right] \quad (\text{VII-76})$$

To find boundary conditions on g to use with (VII-76), consider the points where either $f_1(x)$ or $f_2(x)$ passes through zero. If p_1 is to be normalizable, it is necessary that $p_1(x) = \frac{g(x)}{|f_1(x)|}$ be integrable. Unless $f_1'(x) = \infty$ at

that point, an unusual situation, $g(x)$ must approach zero at such a point. Thus (VII-76) is applied to regions on the x -axis over which f_1 and f_2 are of opposite sign. The values of g at the end points of such a region, which are necessarily zeros of either f_1 or f_2 , are zero. Infact a further condition must be satisfied by f_1 and f_2 over the region. Since $g \rightarrow 0$ at each singular point (i.e. a zero of either f_1 or f_2), $\ln g \rightarrow -\infty$. Thus $\frac{d}{dx} \ln g$ must $\rightarrow +\infty$ at the left end of the region and $-\infty$ at the right end, so that the function that goes to zero at the left end (either f_1 or f_2) must be negative over the region, and that which goes to zero at the right end must be positive over the region. Therefore, in any region of the x -axis where $g(x)$ is non-zero, the functions $f_1(x)$ and $f_2(x)$ must appear as in the sketch:



Physically, the points where f_1 or f_2 pass through zero are steady states when the flow is fixed at w_1 or w_2 respectively. The requirement that the slopes of f_1 and f_2 be negative at these points for solutions to exist between them is just the same as the conditions for stability of

these steady states. At the stationary condition, then, the system will oscillate in a region bounded by stable steady states corresponding to the two different flow rates.

For first order reactions,

$$\begin{aligned} f_1(x) &= \frac{q_1}{v} - \left(\frac{w_1}{v} + k\right)x \\ f_2(x) &= \frac{q_2}{v} - \left(\frac{w_2}{v} + k\right)x \end{aligned} \quad (\text{VII-77})$$

Substituting in (VII-76) and integrating,

$$g(x) = c_1 \left| \frac{q_1}{v} - \left(\frac{w_1}{v} + k\right)x \right|^{\frac{\lambda_1}{w_1/v + k}} \left| \frac{q_2}{v} - \left(\frac{w_2}{v} + k\right)x \right|^{\frac{\lambda_2}{w_2/v + k}} \quad (\text{VII-78})$$

for values of x between $\frac{q_1}{w_1 + kv}$ and $\frac{q_2}{w_2 + kv}$. For values of x outside this region, $g(x) \equiv 0$. The value of the constant c_1 is determined by the fact that the integral of $p_1(x) + p_2(x)$ is one.

It is convenient to define a new variable, y , as follows:

$$y(x) = \frac{x - \frac{q_1}{w_1 + kv}}{\frac{q_2}{w_2 + kv} - \frac{q_1}{w_1 + kv}} \quad (\text{VII-79})$$

The probability distribution of the variable y is then given for $0 < y < 1$ by

$$\begin{aligned} p_1(y) &= \bar{p}_1 \frac{y^{r-1}(1-y)^s}{B(r, s+1)} \\ p_2(y) &= \bar{p}_2 \frac{y^r(1-y)^{s-1}}{B(r+1, s)} \end{aligned} \quad (\text{VII-80})$$

where

$$r = \frac{\lambda_1}{\frac{w_1}{v} + k}, \quad s = \frac{\lambda_2}{\frac{w_2}{v} + k} \quad (\text{VII-81})$$

and $B(r,s)$ is the beta-function of r and s defined as follows:

$$B(r,s) = \int_0^1 t^{r-1} (1-t)^{s-1} dt \quad (\text{VII-82})$$

The distributions (VII-80) are called beta-distributions, and the indefinite integrals are tabulated functions, called incomplete beta-functions.

The probability that outlet concentration z is between z_1 , and z_2 is then given by

$$\text{Pr} \{ z_1 < z < z_2 \} = \int_{y(z_1)}^{y(z_2)} [p_1(t) + p_2(t)] dt \quad (\text{VII-83})$$

Similarly, the probability that outlet reactant flow rate, ψ , is between ψ_1 and ψ_2 is given by

$$\text{Pr} \{ \psi_1 < \psi < \psi_2 \} = \int_{y(\frac{\psi_1}{w_1})}^{y(\frac{\psi_2}{w_1})} p_1(t) dt + \int_{y(\frac{\psi_1}{w_2})}^{y(\frac{\psi_2}{w_2})} p_2(t) dt \quad (\text{VII-84})$$

In both (VII-83) and (VII-84) it must be kept in mind that $p_1(y)$ and $p_2(y)$ are zero unless $0 < y < 1$

The shape of the probability distribution depends on the values of r and s . If r is less than one, there will

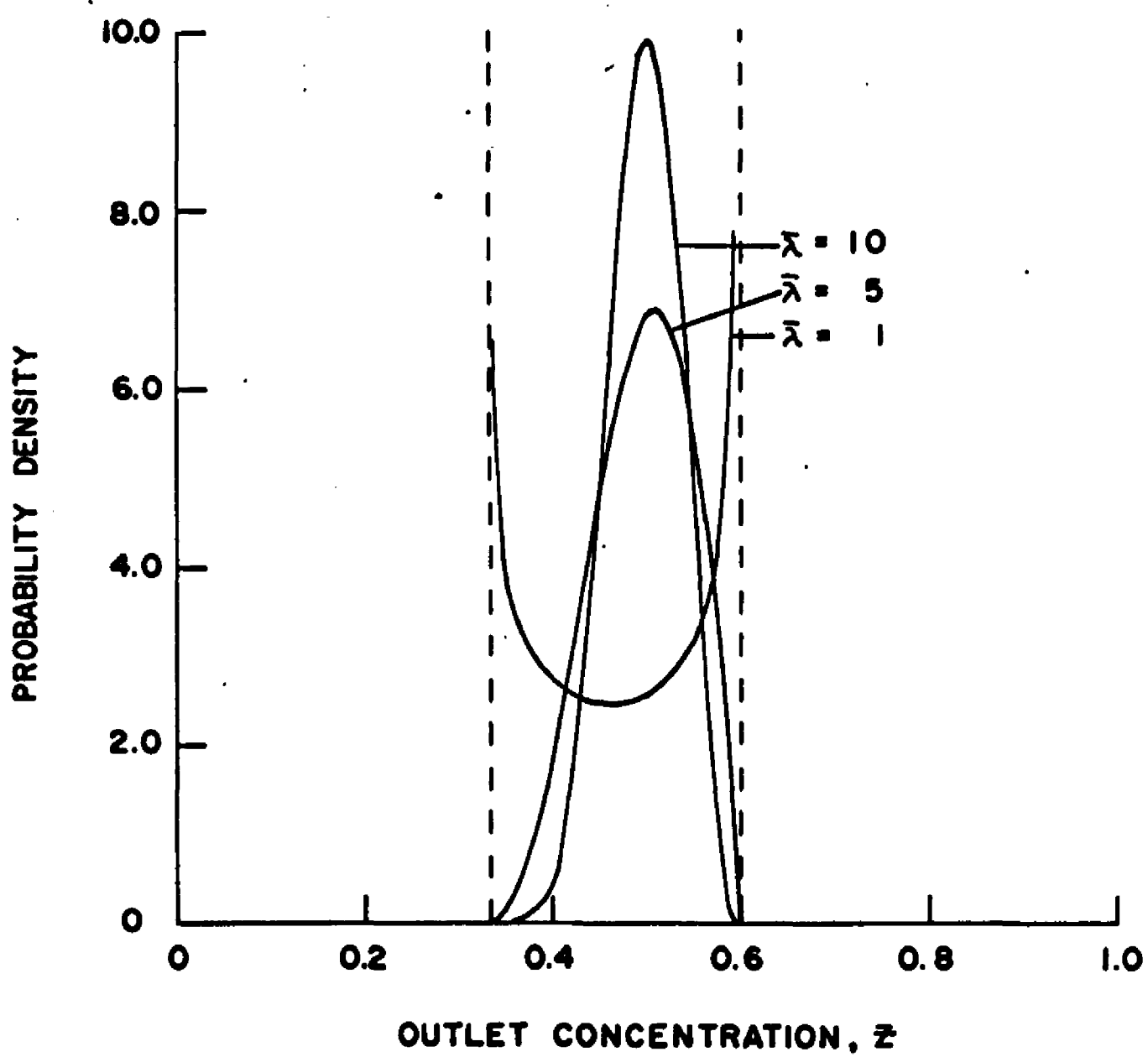
be an infinity in the probability distribution at $y=0$, and if s is less than one, there will be an infinity at $y=1$. Values of r or s greater than one give zeros at the corresponding points. For large values of r and s the distribution becomes very peaked and narrow, which corresponds to large values of λ_1 and λ_2 . For small values the probability becomes concentrated near the steady states at the edges of the region. Density functions for x or ψ are easily calculated by differentiating (VII-83) or (VII-84) with respect to x_1 or ψ_1 , respectively. Note that the density for ψ may split into two regions if w_1 and w_2 are sufficiently different. If one of the flow rates, say w_1 , is zero, then the distribution of ψ will have an atom of probability at $\psi = 0$, of weight \bar{p}_1 .

The shape of the distribution of y does not depend on whether reactant is fed at constant concentration or at constant rate, since r and s are independent of this condition. It is simply a question of how the switching rates, λ_1 and λ_2 , compare with the characteristic response rates of the system, $\frac{w_1}{V} + k$ and $\frac{w_2}{V} + k$, respectively. The density function of outlet concentration for some typical values of the parameters is shown in Figure 9. The quantity $\bar{\lambda}$ is defined as $\frac{1}{2}(\lambda_1 + \lambda_2)$, which is the

Figure 9

Figure 9. PROBABILITY DENSITY OF OUTLET CONCENTRATION FOR
FOR FIRST ORDER REACTION IN SINGLE TANK

$$(\lambda_1 = \lambda_2, \epsilon = 1, \kappa = 1)$$



mean switching rate. Note how the distribution narrows with increasing switching rate.

For second order reactions, the corresponding $f_1(x)$ and $f_2(x)$ are

$$\begin{aligned} f_1(x) &= \frac{q_1}{v} - \frac{w_1}{v} x - k x^2 \\ f_2(x) &= \frac{q_2}{v} - \frac{w_2}{v} x - k x^2 \end{aligned} \quad (\text{VII-85})$$

In this case,

$$\begin{aligned} g(x) &= c_1 \left| \frac{2 k x + \frac{w_1}{v} - \sqrt{\left(\frac{w_1}{v}\right)^2 + 4 k \frac{q_1}{v}}}{2 k x + \frac{w_1}{v} + \sqrt{\left(\frac{w_1}{v}\right)^2 + 4 k \frac{q_1}{v}}} \right|^{\frac{\lambda_1}{\sqrt{\left(\frac{w_1}{v}\right)^2 + 4 k \frac{q_1}{v}}}} \\ &\cdot \left| \frac{2 k x + \frac{w_2}{v} - \sqrt{\left(\frac{w_2}{v}\right)^2 + 4 k \frac{q_2}{v}}}{2 k x + \frac{w_2}{v} + \sqrt{\left(\frac{w_2}{v}\right)^2 + 4 k \frac{q_2}{v}}} \right|^{\frac{\lambda_2}{\sqrt{\left(\frac{w_2}{v}\right)^2 + 4 k \frac{q_2}{v}}}} \end{aligned} \quad (\text{VII-86})$$

where, again, the constant c_1 must be determined by the condition that $\int [p_1(x) + p_2(x)] dx = 1$. Equation (VII-86) may be written

$$g(x) = c_1 \left| \frac{x - a_1}{x + b_1} \right|^r \left| \frac{x - a_2}{x + b_2} \right|^s \quad (\text{VII-87})$$

where

$$r = \frac{\lambda_1}{\frac{w_1}{v} + 2 k a_1}, \quad s = \frac{\lambda_2}{\frac{w_2}{v} + 2 k a_2} \quad (\text{VII-88})$$

The quantities a_1 and a_2 are the steady solutions corres-

ponding to w_1 and w_2 , respectively, and $-b_1$ and $-b_2$ are the extraneous roots of f_1 and f_2 . Thus, in these terms,

$$f_1(x) = -k(x - a_1)(x + b_1) \quad (\text{VII-89})$$

$$f_2(x) = -k(x - a_2)(x + b_2)$$

so that

$$p_1(x) = \frac{c_1}{k} \frac{|x - a_1|^{r-1} |x - a_2|^s}{|x + b_1|^{r+1} |x + b_2|^s} \quad (\text{VII-90})$$

$$p_2(x) = \frac{c_2}{k} \frac{|x - a_1|^r |x - a_2|^{s-1}}{|x + b_1|^r |x + b_2|^{s+1}}$$

The shape of the density functions given by (VII-90) are quite similar to those for first order reactions, as given by (VII-80). The constant c_1 must be determined by numerical integration. The density function $p_1(x) + p_2(x)$ from equation (VII-90) is shown in Figure 10 for some typical parameter values.

It can be seen that the values for r and s given by equation (VII-88) and those given by equation (VII-81) may both be expressed by the relationship

$$r = \frac{\lambda_1}{|f_1'(a_1)|} \quad , \quad s = \frac{\lambda_2}{|f_2'(a_2)|} \quad (\text{VII-91})$$

Figure 10

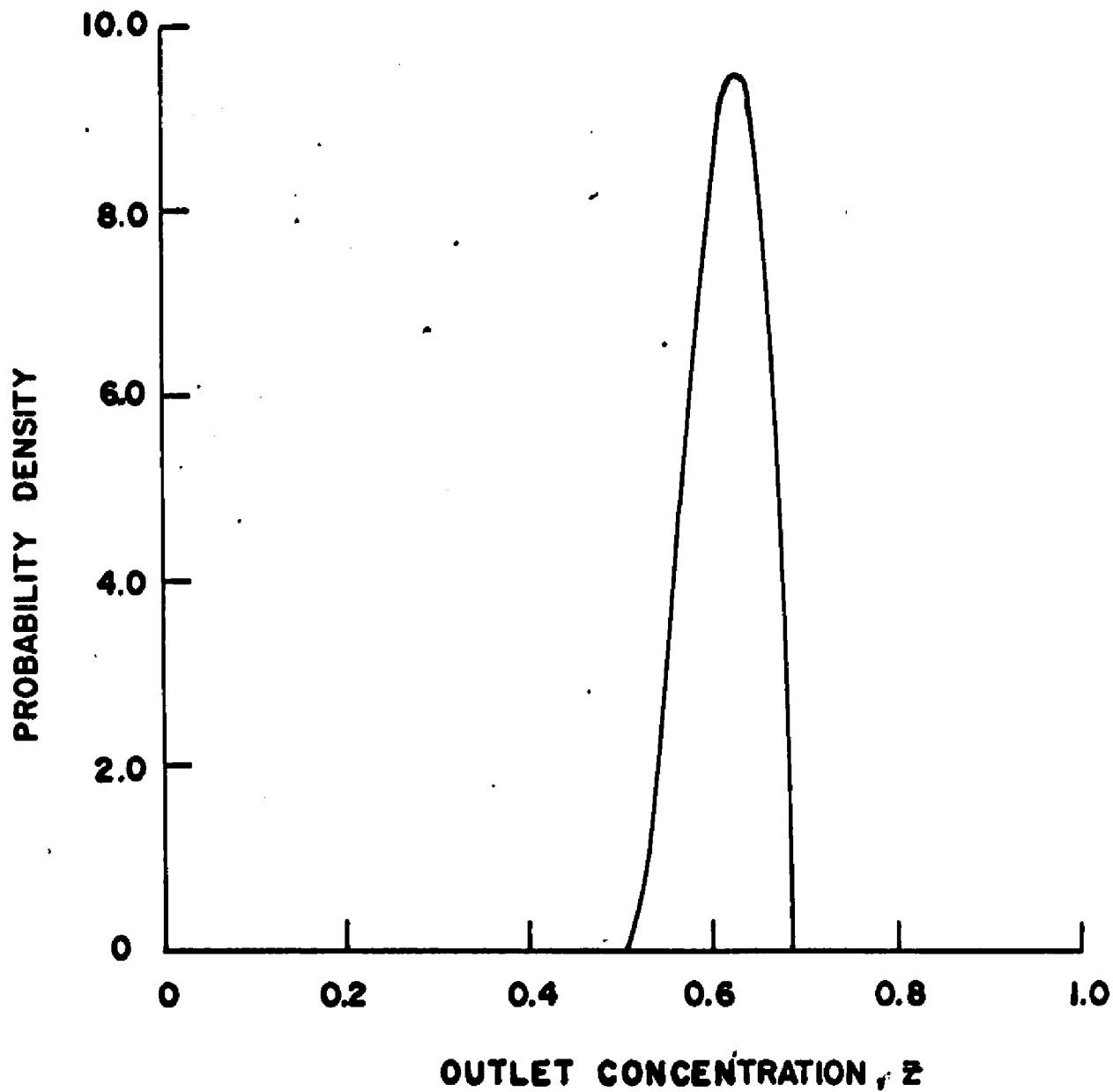


Figure 10. PROBABILITY DENSITY OF OUTLET CONCENTRATION FOR SECOND ORDER REACTION IN SINGLE TANK

$$(\lambda_1 = \lambda_2 = 5, \epsilon = 1, k = 1)$$

The shape of the probability density for more general kinetics may be inferred by considering its behavior near the roots of f_1 and f_2 . Near the roots of f_1 , for example,

$$f_1(x) \approx f_1'(a_1)(x - a_1) \quad (\text{VII-92})$$

If the root a_1 is stable, then $f_1'(a_1)$ will be negative.

For values of x near a_1 , equation (VII-76) then becomes

$$\frac{d}{dx} \ln g \approx \frac{-\lambda_1}{f_1'(a_1)(x - a_1)} \quad (\text{VII-93})$$

since $\frac{\lambda_2}{f_2(x)}$ will be negligible by comparison to $\frac{\lambda_1}{f_1'(a_1)(x - a_1)}$

This gives

$$g(x) \approx c_1 |x - a_1|^{\frac{\lambda_1}{|f_1'(a_1)|}} \quad (\text{VII-94})$$

Similarly, near $x = a_2$, where a_2 is a stable root of f_2 ,

$$g(x) \approx c_2 |x - a_2|^{\frac{\lambda_2}{|f_2'(a_2)|}} \quad (\text{VII-95})$$

Thus the quantities r and s given by equation (VII-91) are seen to determine the behavior of the probability density near the ends of the range for arbitrary kinetics. Again, if r and s have values less than one, the probability density will have infinities at the corresponding points, and if r and s are greater than one, it will have zeros at the corresponding points.

Another case of interest is an exothermic reaction under adiabatic conditions. For this situation both the material and energy balance must be considered. The material balance is, for constant x_0 ,

$$v \frac{dx}{dt} = w(x_0 - x) - v R(x, T) \quad (\text{VII-96})$$

and the energy balance is

$$v \frac{dT}{dt} = w(T_0 - T) + v \frac{\Delta T^*}{x_0} R(x, T) \quad (\text{VII-97})$$

where T is temperature, $R(x, T)$ is the reaction rate, and ΔT^* is the temperature increase resulting from complete conversion. Multiplying (VII-96) by $\frac{\Delta T^*}{x_0}$ and adding to (VII-91),

$$v \frac{d}{dt} \left[\frac{x \Delta T^*}{x_0} + T \right] = w \left\{ [\Delta T^* + T_0] - \left[\frac{x \Delta T^*}{x_0} + T \right] \right\} \quad (\text{VII-98})$$

Since w is always positive, the quantity $\left[\frac{x \Delta T^*}{x_0} + T \right]$ will approach $[\Delta T^* + T_0]$ monotonically, even though w fluctuates, so that after a long time, when the process becomes stationary,

$$T = T_0 + \Delta T^* \left(1 - \frac{x}{x_0} \right)$$

or, scaling x so that $x_0 = 1$,

$$T = T_0 + \Delta T^* (1 - x) \quad (\text{VII-99})$$

Actually, it can be shown using the general stability criterion for Markov Processes [25] that (VII-99) would be true for the stationary solution even if one of the states of w were negative, provided only that

$$\begin{aligned} -\frac{w_1}{\nu} &< \frac{1}{2}(\lambda_1 + \lambda_2) \\ -\frac{w_2}{\nu} &< \frac{1}{2}(\lambda_1 + \lambda_2) \\ -\frac{\bar{w}}{\nu} &< \frac{2w_1w_2}{\nu^2(\lambda_1 + \lambda_2)} \end{aligned}$$

These relations are automatically true if w_1 and w_2 are both positive. The reaction rate, $R(x,T)$, may be taken as

$$R(x,T) = k_{\infty} e^{-\frac{E}{RT}} x^n \quad (\text{VII-100})$$

Substituting (VII-99) into (VII-100),

$$R(x,T) = k_{\infty} e^{-\left\{\frac{\alpha}{1+\theta(1-x)}\right\}} x^n \quad (\text{VII-101})$$

where

$$\alpha = \frac{E}{RT_0} \quad , \quad \theta = \frac{\Delta T}{T_0}$$

Thus, for this case,

$$\begin{aligned} f_1(x) &= \frac{w_1}{\nu} - \frac{w_1}{\nu} x - k_{\infty} e^{-\left\{\frac{\alpha}{1+\theta(1-x)}\right\}} x^n \\ f_2(x) &= \frac{w_2}{\nu} - \frac{w_2}{\nu} x - k_{\infty} e^{-\left\{\frac{\alpha}{1+\theta(1-x)}\right\}} x^n \end{aligned} \quad (\text{VII-102})$$

The interesting feature of this system is the existence of multiple roots of $f_1(x)$ and $f_2(x)$, allowing the possibility of disjoint regions of non-zero probability. Figure 11, for example, shows a case where both $f_1(x)$ and $f_2(x)$ have three roots. In this case the entire probability distribution would be contained in two small regions. One region is bounded by the smallest root of $f_1(x)$ and the smallest root of $f_2(x)$, and the other by the largest root of $f_1(x)$ and the largest root of $f_2(x)$. The latter two points are very close together and also very close to $x=1$, so that they cannot be seen distinctly on the graph. Note that there will be no probability of being between the two middle roots, since $f_1(x)$ and $f_2(x)$ cross the axis with positive slope at these points. The middle roots of the two curves represent unstable steady states of the system with constant flow rates. The relative weights of the two regions are arbitrary, depending on the initial probability distribution of the system. The fact that the probability of being anywhere between the two regions is zero, together with the fact that the concentration varies continuously with time, shows that once the concentration is within one of the two stable regions, it will never leave that region.

The stable region at low concentration, or high

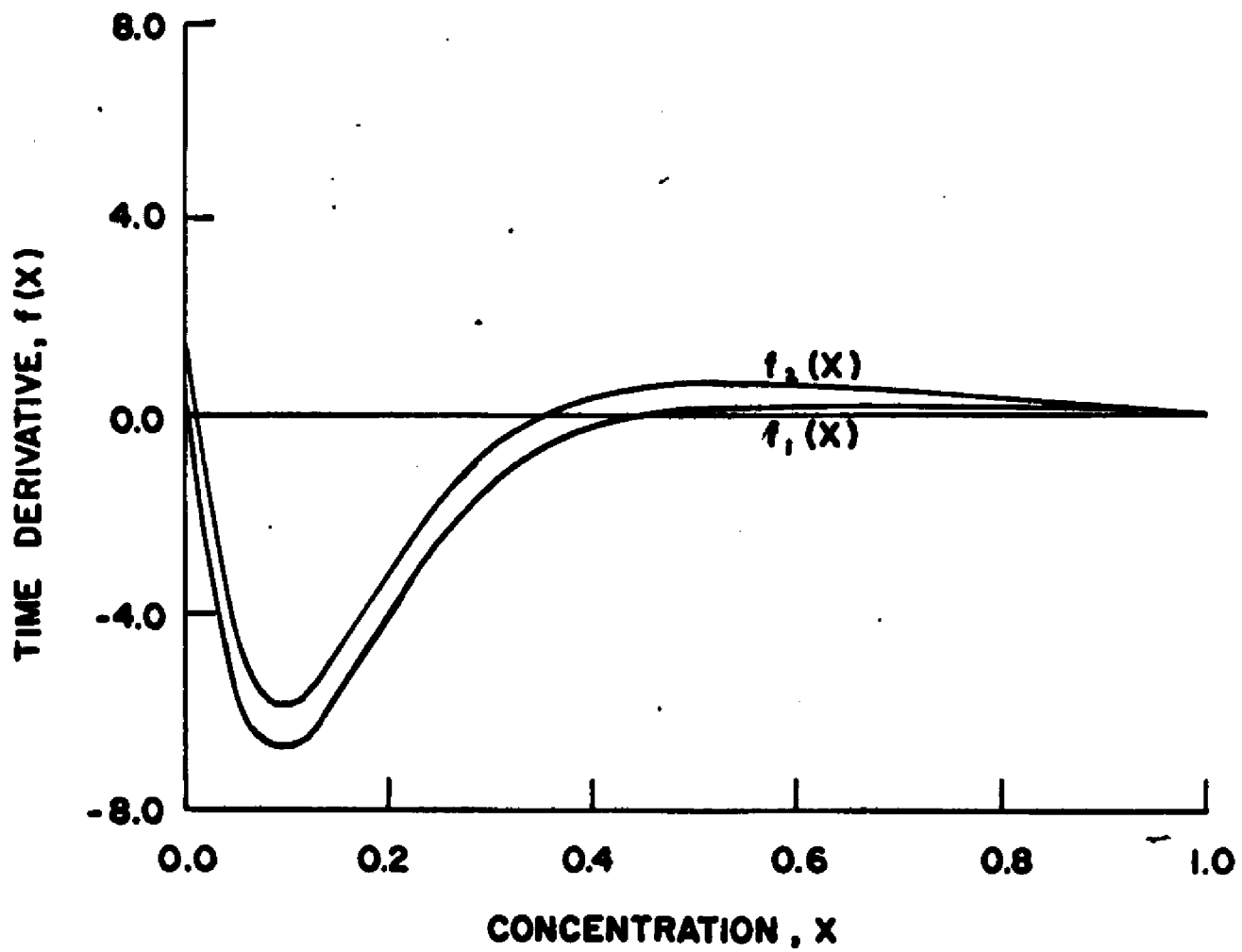


Figure 11. RATE OF CHANGE FOR FIRST ORDER ADIABATIC REACTION IN SINGLE TANK (two stable regions)

$$(E=1, k_{\infty} = 10^{11}, E/RT_0 = 40, \Delta T^*/T_0 = 1)$$

conversion, corresponds to an ignited state of a combustion process, while the stable region at high concentration, or low conversion, corresponds to an unignited state. Thus, under conditions where each of the allowable flow rates through the stirred tank result in both ignited and unignited steady states when held steady, the probability distribution will be concentrated over two stable regions. If the system is once ignited it will not become extinguished, and if it is not ignited it will not spontaneously ignite.

Another situation is shown in Figure 12. Here the function $f_1(x)$ has three roots, but $f_2(x)$ has only one, very close to $x=1$. In this case the entire stationary distribution will be concentrated in the very narrow region between the highest root of $f_1(x)$ and the only root of $f_2(x)$. This means that the system, which may begin in an ignited state, will eventually become extinguished with probability one. Thus, in cases where the range of allowable flow rates is such that at one extreme of flow rate the system has both ignited and unignited steady states, the system will eventually become extinguished and will not ignite spontaneously.

Other configurations are possible. It could happen that $f_2(x)$ has three roots, but $f_1(x)$ has only an ignited

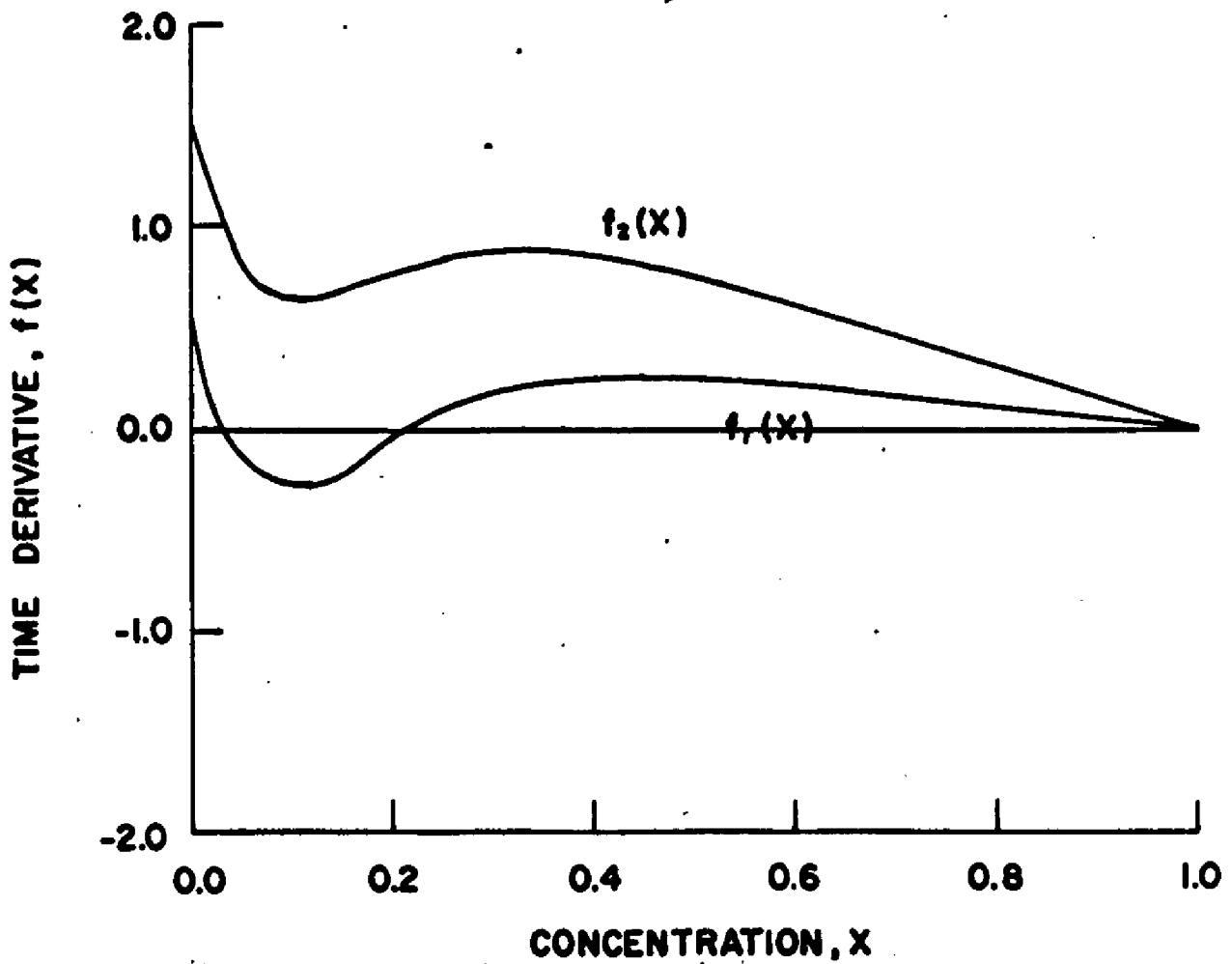


Figure 12. RATE OF CHANGE FOR FIRST ORDER ADIABATIC REACTION IN SINGLE TANK (one stable region)

$$(\epsilon = 1, k_{\infty} = 10^{10}, E/RT_0 = 40, \Delta T^*/T_0 = 1)$$

solution, in which case there would be only one stable region, corresponding to an ignited state of the system. A case where the details of stationary distribution within stable regions is of somewhat more interest is where $f_1(x)$ has only an ignited solution, and $f_2(x)$ only an unignited one.

The time derivatives $f_1(x)$ and $f_2(x)$, are shown for such a case in Figure 13, along with the resulting probability distribution, computed numerically from equation (VII-69). The distribution is concentrated mostly at the high concentration end of the scale for these values of the parameters. This occurs because the absolute value of the negative derivative, $f_1(x)$, is somewhat less than that of the positive derivative, $f_2(x)$, over most of the range. A slight change in the parameters which shifts both $f_1(x)$ and $f_2(x)$ down slightly changes the shape of the distribution markedly as seen in Figure 14. Here the value of $\frac{\Delta T^*}{T_0}$, which is proportional to the heat release of the reaction, is changed from 0.22 to 0.23. Comparing the curve for $\bar{\lambda} = 5$ in Figure 14 to the curve in Figure 13, one notes that the distribution shifts toward the low concentration end of the scale when $\frac{\Delta T^*}{T_0}$ is increased. It is also seen that the

Figure 13. PROBABILITY DISTRIBUTION FOR SINGLE TANK WITH FIRST ORDER ADIABATIC REACTION SHOWING LARGE STABLE REGION

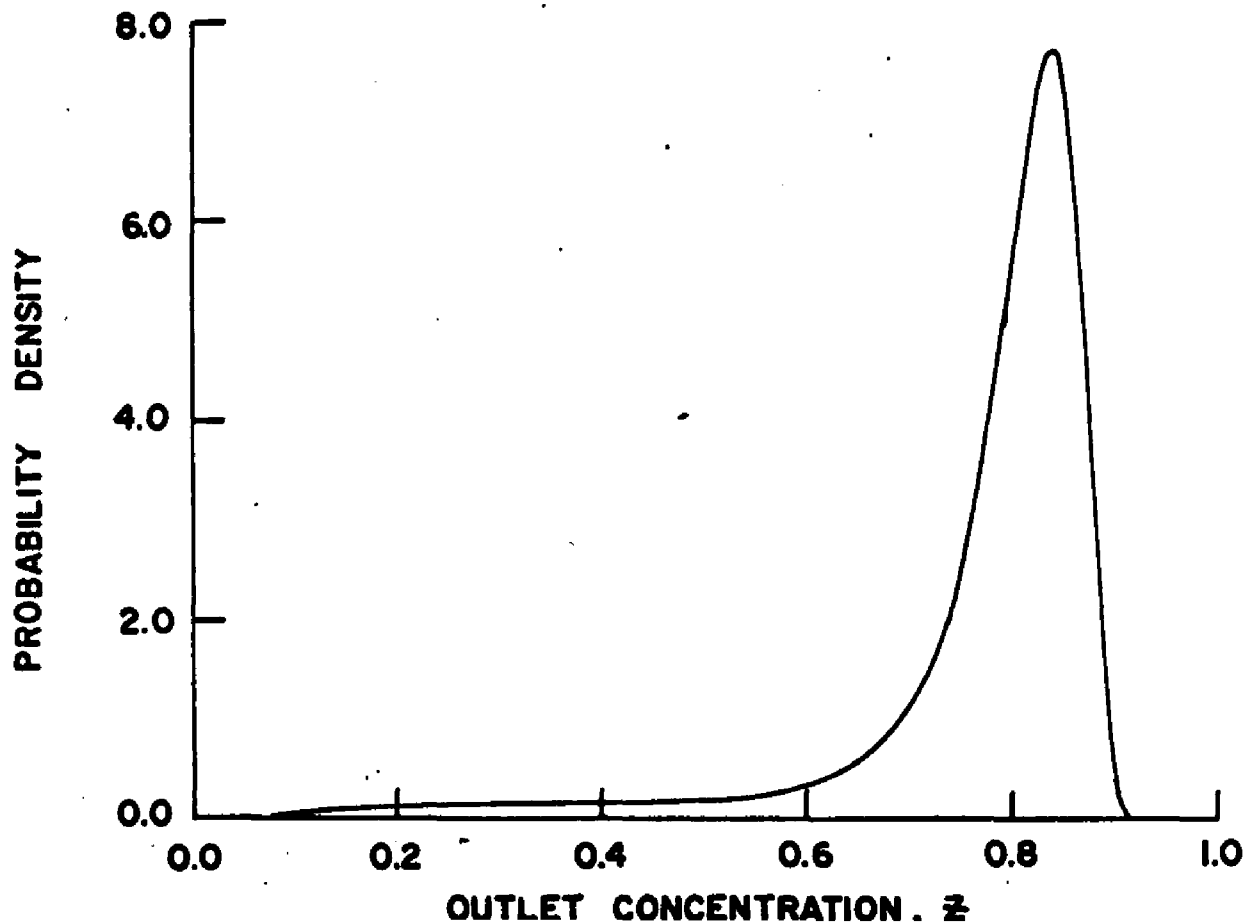
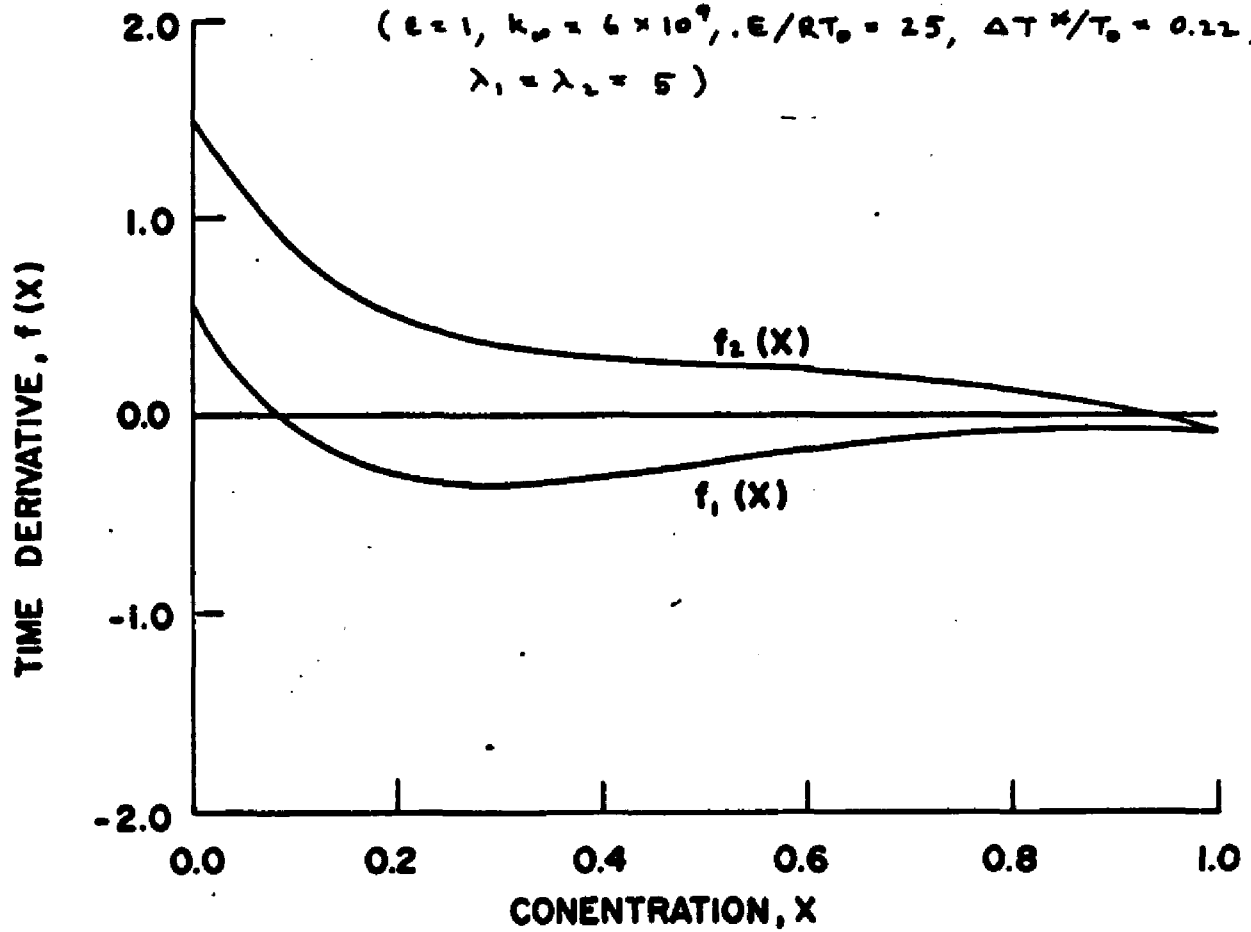
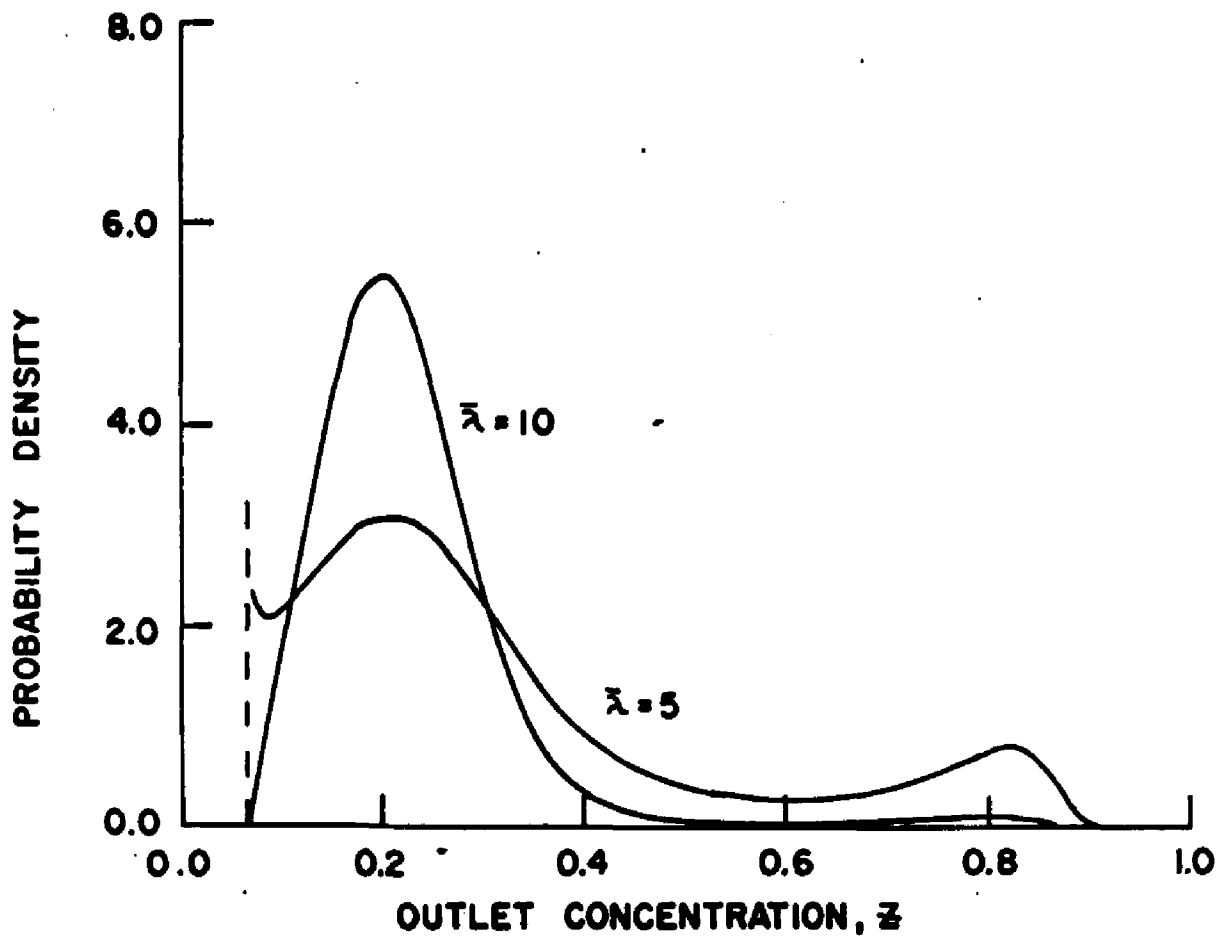
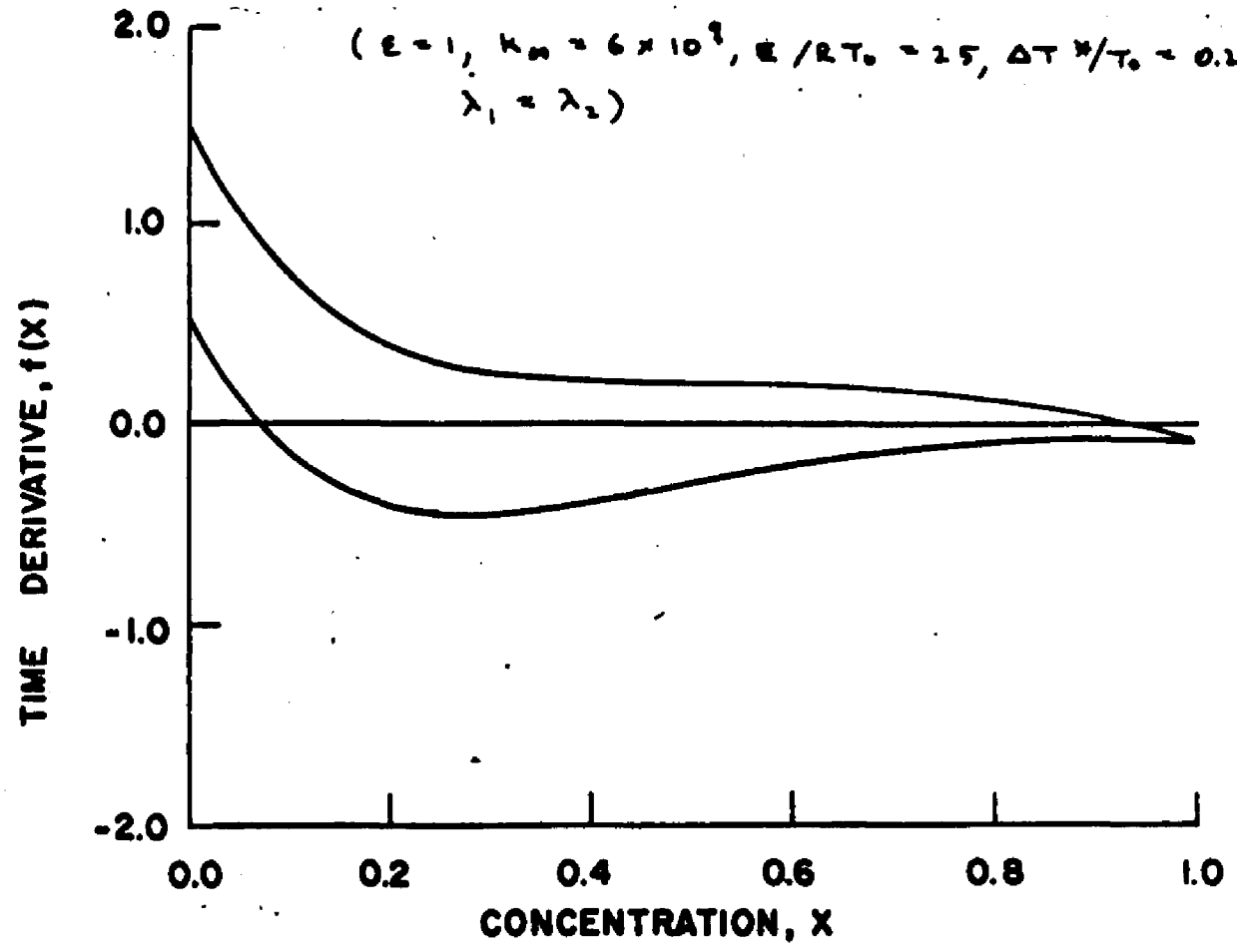


Figure 14. PROBABILITY DISTRIBUTIONS FOR SINGLE TANK WITH FIRST ORDER ADIABATIC REACTION SHOWING LARGE STABLE REGION 116



distribution becomes bimodal, with one peak at the low concentration end and one at the high concentration end. This means that the system will spend relatively little time in the central region of the concentration scale, compared to the ends of the scale. Increasing the switching rate, $\bar{\lambda}$, tends to narrow the distribution, as is seen for $\bar{\lambda} = 10$ in Figure 14. It is also seen that the probability of being at high concentrations decreases sharply with increasing switching rate, for the parameter values shown.

VIII. Series and Parallel Models

A. Formulation

Two special cases of the general model will be treated in this section. One consists of two tanks connected in parallel, as shown in Figure 15, and the other consists of two tanks in series, shown in Figure 16. In both cases it is assumed that the total flow rate through the system, w , is constant, so that the different tracer experiments described previously are identical. In the parallel model, the proportion of the total flow that enters each tank fluctuates. Denoting the fraction of the total flow entering tank one when the flow state is α by r_α , the various flow rates become

$$w_{01\alpha} = w_{13\alpha} = r_\alpha w$$

$$w_{02\alpha} = w_{23\alpha} = (1 - r_\alpha)w$$
(VIII-1)

In the series model, the rate of mixing between the two tanks fluctuates. Again, the various flow rates can be expressed in terms of a random quantity r_α :

$$w_{12\alpha} = (1 + r_\alpha)w$$

$$w_{21\alpha} = r_\alpha w$$
(VIII-2)

It will be assumed in both cases that the random flow

Figure 15: PARALLEL MODEL

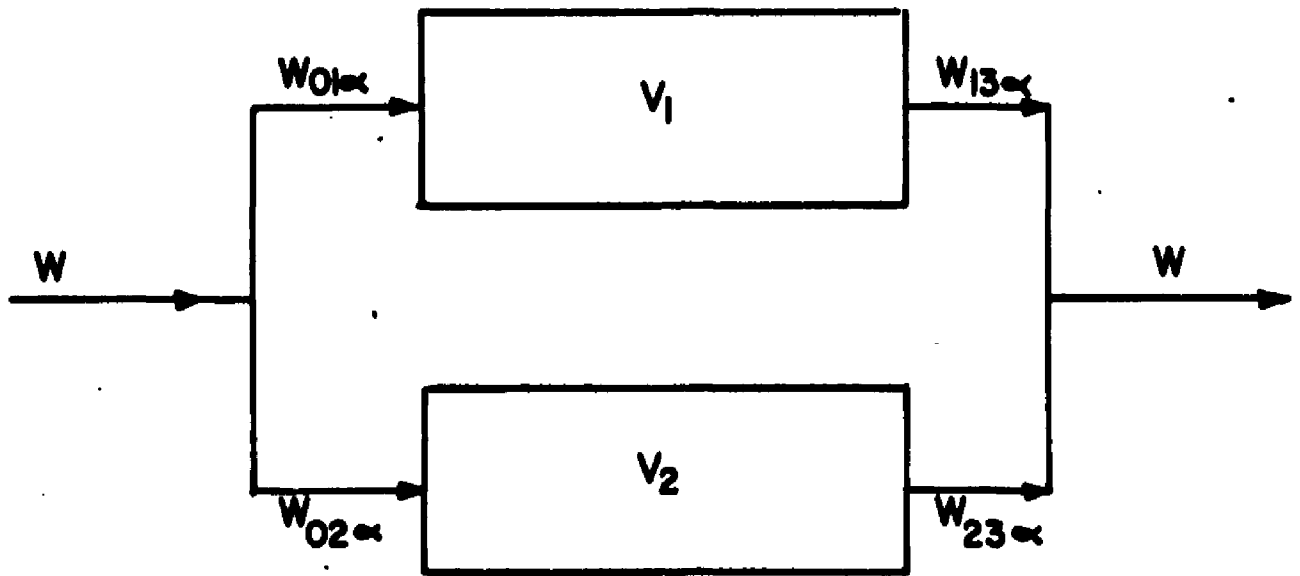
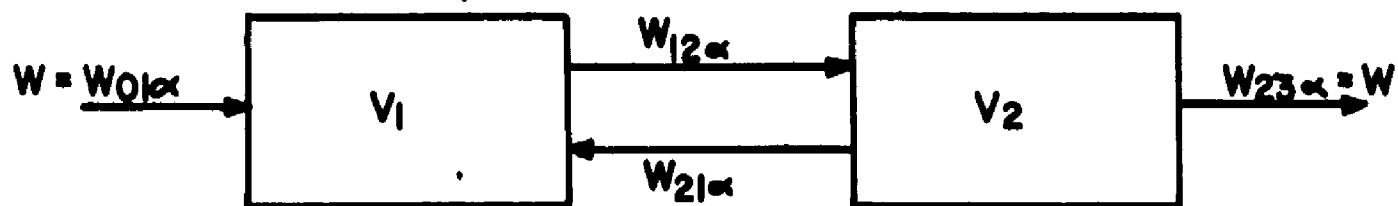


Figure 16: SERIES MODEL



state index, α , takes on only two values, so that the probability structure of the mixing flows will be the same as that described in section VII A.

B. Tracer Experiments

The tracer material balance, equation (IV-4), becomes for the parallel case

$$\begin{aligned} v_1 \frac{dx_1}{dt} &= \varphi_{\alpha_1}(t) - w r_{\alpha} x_1 \\ v_2 \frac{dx_2}{dt} &= \varphi_{\alpha_2}(t) - w(1-r_{\alpha}) x_2 \end{aligned} \quad (\text{VIII-3})$$

Since the total flow rate, w , is constant, inputs in tracer concentration are equivalent to inputs in tracer feed rate, the outputs differing only by a constant scale factor. Thus the input tracer feed rate, $\varphi(t)$, and the input tracer concentration, $x_0(t)$, are related by

$$\varphi(t) = w x_0(t) \quad (\text{VIII-4})$$

Writing the $\varphi_{\alpha_j}(t)$ in terms of $x_0(t)$, equation (VIII-3) becomes

$$\begin{aligned} v_1 \frac{dx_1}{dt} &= w r_{\alpha} [x_0(t) - x_1] \\ v_2 \frac{dx_2}{dt} &= w(1-r_{\alpha}) [x_0(t) - x_2] \end{aligned} \quad (\text{VIII-5})$$

The outlet concentration, \bar{x} , is then given by

$$\bar{x} = r_{\alpha} x_1 + (1-r_{\alpha}) x_2 \quad (\text{VIII-6})$$

and the outlet tracer flow rate, ψ , by

$$\psi = w z \quad (\text{VIII-7})$$

The nature of the output of the parallel model is shown by a typical response to a step input, shown in Figure 17. This curve was calculated by a Monte-Carlo procedure. It is seen that switches in flow state produce discontinuous changes in outlet concentration.

For the series case, the material balance becomes

$$\begin{aligned} v_1 \frac{dx_1}{dt} &= w x_0(t) - w(1+r_\alpha) x_1 + w r_\alpha x_2 \\ v_2 \frac{dx_2}{dt} &= w(1+r_\alpha) [x_1 - x_2] \end{aligned} \quad (\text{VIII-8})$$

In this case the outlet concentration is equal to the concentration in tank two:

$$z = x_2 \quad (\text{VIII-9})$$

A typical step response of the series model is shown in Figure 18. Here the switches cause discontinuous changes in the first derivative of the output concentration, but not in the output concentration itself.

For either case, equations describing the probability density, $p(t,x)$, may be written, corresponding to equation (IV-5). For the parallel model it is found that

Figure 17: TYPICAL STEP RESPONSE FOR PARALLEL CASE

$$(v_1 = v_2, \bar{r} = 1/2, \lambda_1 = \lambda_2, \bar{\lambda} = 1, \varepsilon = 1/2)$$

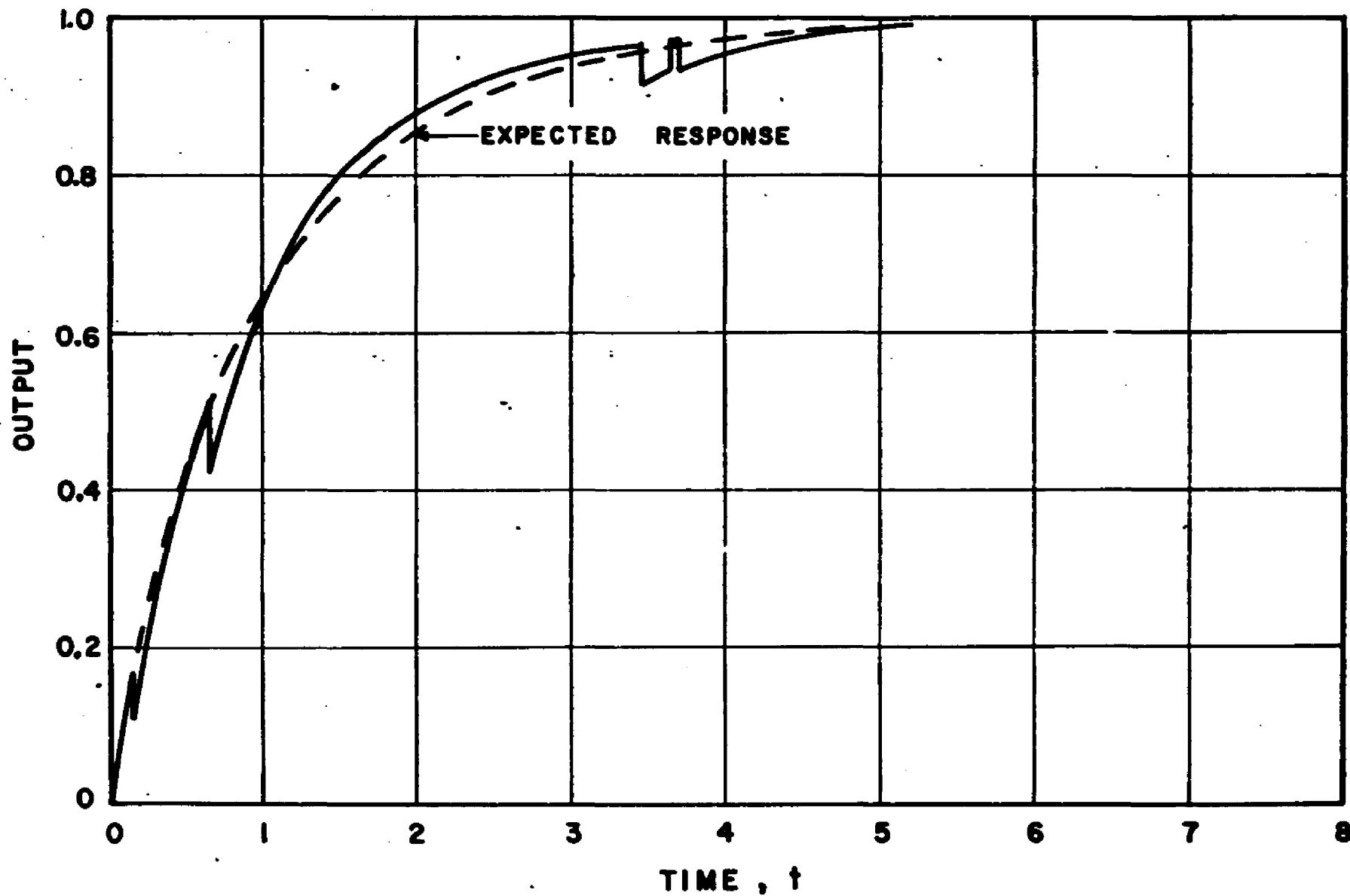
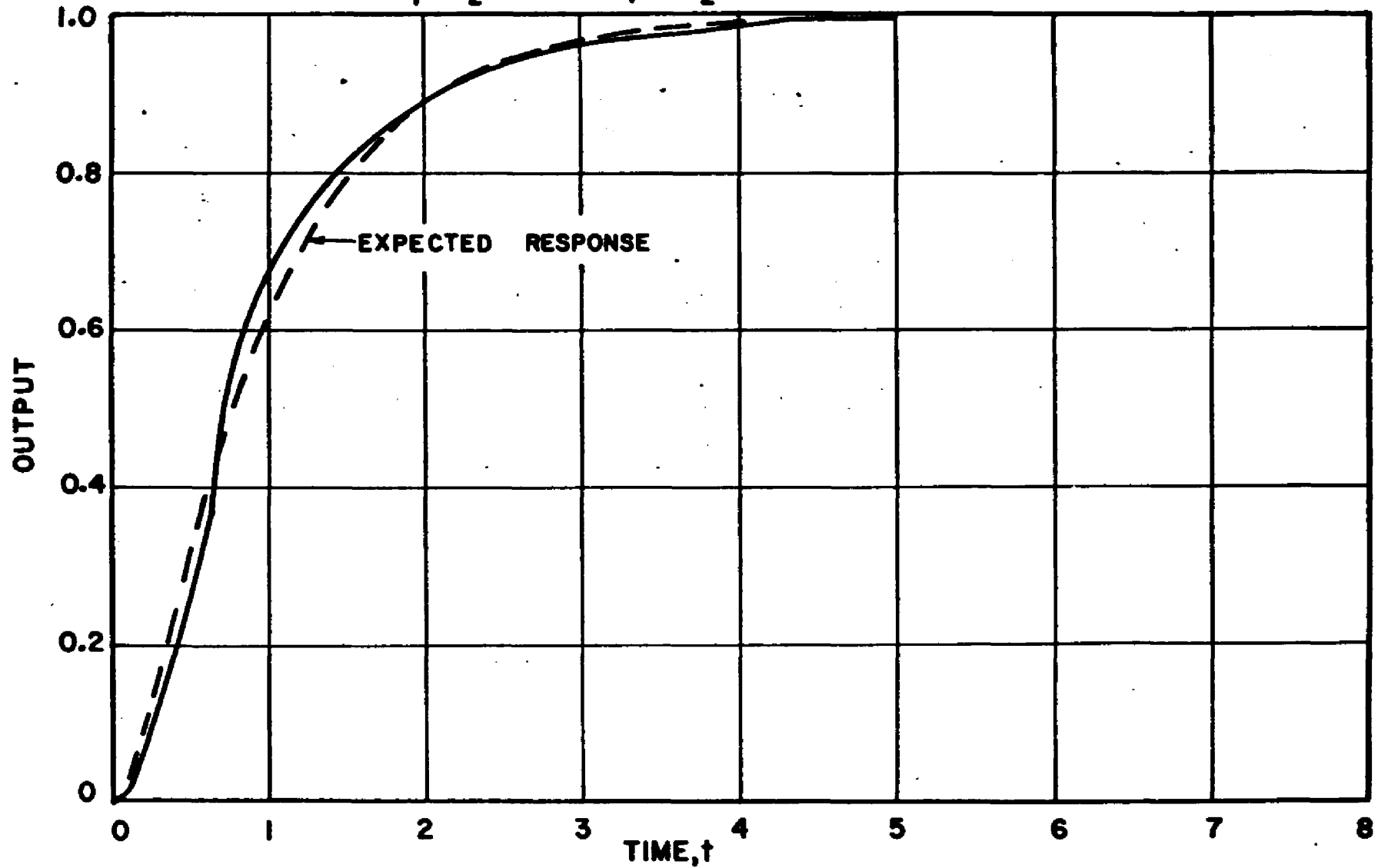


Figure 18: TYPICAL STEP RESPONSE FOR SERIES CASE

$$(v_1 = v_2, \bar{r} = 1, \lambda_1 = \lambda_2, \bar{\lambda} = 1, \epsilon = 2)$$



$$\begin{aligned}
& \frac{\partial p_1(t, \underline{x})}{\partial t} + \frac{\partial}{\partial x_1} \left\{ \frac{w r_1}{v_1} [x_0(t) - x_1] p_1(t, \underline{x}) \right\} \\
& + \frac{\partial}{\partial x_2} \left\{ \frac{w(1-r_1)}{v_2} [x_0(t) - x_2] p_2(t, \underline{x}) \right\} \\
& = -\lambda_1 p_1(t, \underline{x}) + \lambda_2 p_2(t, \underline{x}) \quad (\text{VIII-10})
\end{aligned}$$

$$\begin{aligned}
& \frac{\partial p_2(t, \underline{x})}{\partial t} + \frac{\partial}{\partial x_1} \left\{ \frac{w r_2}{v_1} [x_0(t) - x_1] p_2(t, \underline{x}) \right\} \\
& + \frac{\partial}{\partial x_2} \left\{ \frac{w(1-r_2)}{v_2} [x_0(t) - x_2] p_2(t, \underline{x}) \right\} \\
& = \lambda_1 p_1(t, \underline{x}) - \lambda_2 p_2(t, \underline{x})
\end{aligned}$$

with initial conditions

$$p_1(0, \underline{x}) = \bar{p}_1 \delta(x_1) \delta(x_2)$$

$$p_2(0, \underline{x}) = \bar{p}_2 \delta(x_1) \delta(x_2) \quad (\text{VIII-11})$$

The corresponding equation for the series case is

$$\begin{aligned}
& \frac{\partial p_1(t, \underline{x})}{\partial t} + \frac{\partial}{\partial x_1} \left\{ \left[\frac{w}{v_1} x_0(t) - \frac{w}{v_1} (1+r_1) x_1 + \frac{w}{v_1} r_1 x_2 \right] p_1(t, \underline{x}) \right\} \\
& + \frac{\partial}{\partial x_2} \left\{ \frac{w}{v_2} (1+r_1) (x_1 - x_2) p_2(t, \underline{x}) \right\} \\
& = -\lambda_1 p_1(t, \underline{x}) + \lambda_2 p_2(t, \underline{x})
\end{aligned}$$

$$\begin{aligned}
& \frac{\partial p_2(t, \underline{x})}{\partial t} + \frac{\partial}{\partial x_1} \left\{ \left[\frac{w}{v_1} x_0(t) - \frac{w}{v_1} (1+r_2) x_1 + \frac{w}{v_1} r_2 x_2 \right] p_2(t, \underline{x}) \right\} \\
& + \frac{\partial}{\partial x_2} \left\{ \frac{w}{v_2} (1+r_2) (x_1 - x_2) p_2(t, \underline{x}) \right\} \\
& = \lambda_1 p_1(t, \underline{x}) - \lambda_2 p_2(t, \underline{x}) \quad (\text{VIII-12})
\end{aligned}$$

with the same initial conditions, (VIII-11). As in the previous case, ordinary differential equations describing the time behavior of the first and second moments of tracer concentration can be written, corresponding to equations (IV-14) and (IV-28). Thus for the parallel case, the first moments are given by

$$\begin{aligned}\frac{d\mu_{11}}{dt} &= \bar{p}_1 \frac{w}{v_1} r_1 x_0(t) - \left(\frac{w}{v_1} r_1 + \lambda_1 \right) \mu_{11} + \lambda_2 \mu_{21} \\ \frac{d\mu_{21}}{dt} &= \bar{p}_2 \frac{w}{v_1} r_2 x_0(t) + \lambda_1 \mu_{11} - \left(\frac{w}{v_1} r_2 + \lambda_2 \right) \mu_{21} \\ \frac{d\mu_{12}}{dt} &= \bar{p}_1 \frac{w}{v_2} (1-r_1) x_0(t) - \left[\frac{w}{v_2} (1-r_1) + \lambda_1 \right] \mu_{12} + \lambda_2 \mu_{22} \\ \frac{d\mu_{22}}{dt} &= \bar{p}_2 \frac{w}{v_2} (1-r_2) x_0(t) + \lambda_1 \mu_{12} - \left[\frac{w}{v_2} (1-r_2) + \lambda_2 \right] \mu_{22}\end{aligned}\tag{VIII-13}$$

where $\mu_{pj}(t) = \int x_j p_p(t, \mathbf{x}) d\mathbf{x}$. The initial conditions for (VIII-13) are

$$\mu_{11}(0) = \mu_{21}(0) = \mu_{12}(0) = \mu_{22}(0) = 0 \tag{VIII-14}$$

The expected outlet concentration, $\langle \mathbf{z}(t) \rangle$, is then given by

$$\begin{aligned}\langle \mathbf{z}(t) \rangle &= r_1 \mu_{11}(t) + r_2 \mu_{21}(t) + (1-r_1) \mu_{12}(t) \\ &\quad + (1-r_2) \mu_{22}(t)\end{aligned}\tag{VIII-15}$$

which is the same as equation (IV-16). Similarly, the first moments for the series case satisfy

$$\begin{aligned}\frac{d\mu_{11}}{dt} &= \bar{p}_1 \frac{W}{V_1} x_o(t) - \left[\frac{W}{V_1} (1+r_1) + \lambda_1 \right] \mu_{11} + \lambda_2 \mu_{21} + \frac{W}{V_1} r_1 \mu_{12} \\ \frac{d\mu_{21}}{dt} &= \bar{p}_2 \frac{W}{V_1} x_o(t) + \lambda_1 \mu_{11} - \left[\frac{W}{V_1} (1+r_2) + \lambda_2 \right] \mu_{21} + \frac{W}{V_1} r_2 \mu_{22} \\ \frac{d\mu_{12}}{dt} &= \frac{W}{V_2} (1+r_1) \mu_{11} - \left[\frac{W}{V_2} (1+r_1) + \lambda_1 \right] \mu_{12} + \lambda_2 \mu_{22} \\ \frac{d\mu_{22}}{dt} &= \frac{W}{V_2} (1+r_2) \mu_{21} + \lambda_1 \mu_{12} - \left[\frac{W}{V_2} (1+r_2) + \lambda_2 \right] \mu_{22}\end{aligned}\tag{VIII-16}$$

with initial conditions (VIII-14). Then

$$\langle z(t) \rangle = \mu_{12}(t) + \mu_{22}(t)\tag{VIII-17}$$

Comparison of equations (VIII-13) with (VII-13) shows that, as far as first moments are concerned, each tank in the parallel model behaves independently. The expected response of the parallel model is just the superposition of the expected responses of the two individual tanks to the appropriate concentration input. Because the total flow rate through both the series and parallel models is constant, all the impulse responses described in the previous section, ψ_x , ψ_φ , z_x , z_φ ,

are identical. The expected impulse response is equal to the (unique) residence time density function. From the residence time density the escape intensity, $h(t)$, can be calculated, as explained previously. This quantity is shown for the parallel model in Figures 19 and 20, and for the series model in Figure 21 and 22. In these graphs, $\epsilon = r_1 - r_2$ and $\bar{\lambda} = \frac{1}{2}(\lambda_1 + \lambda_2)$. The parameters for the parallel case are chosen so that the model is symmetrical with respect to the two tanks. This makes the responses of the parallel system identical to those of a single tank with the same concentration inputs. In fact the curve of $h(t)$ for $\epsilon = 1$ in Figure 19 is identical to $h_x(t)$ in Figure 3, the intensity of the distribution $f_x(t)$ of the single tank.

It is seen in Figure 19 that increasing the size of the fluctuation, ϵ , increases the departure of $h(t)$ from its value with steady flow and, as noted in connection with the single tank response, behaves in a manner that indicates bypassing. In Figure 20 it is shown that switching rate, $\bar{\lambda}$, has a pronounced effect on $h(t)$ for the parallel case. At high switching rates the behavior approaches that for steady flow, which in this case is given by $h(t) = 1$. At low switching rates a large bypass

Figure 19: EFFECT OF FLUCTUATION MAGNITUDE ON ESCAPE INTENSITY FOR PARALLEL CASE

$$(v_1 = v_2, F = \frac{1}{2}, \lambda_1 = \lambda_2, \bar{\lambda} = 1)$$

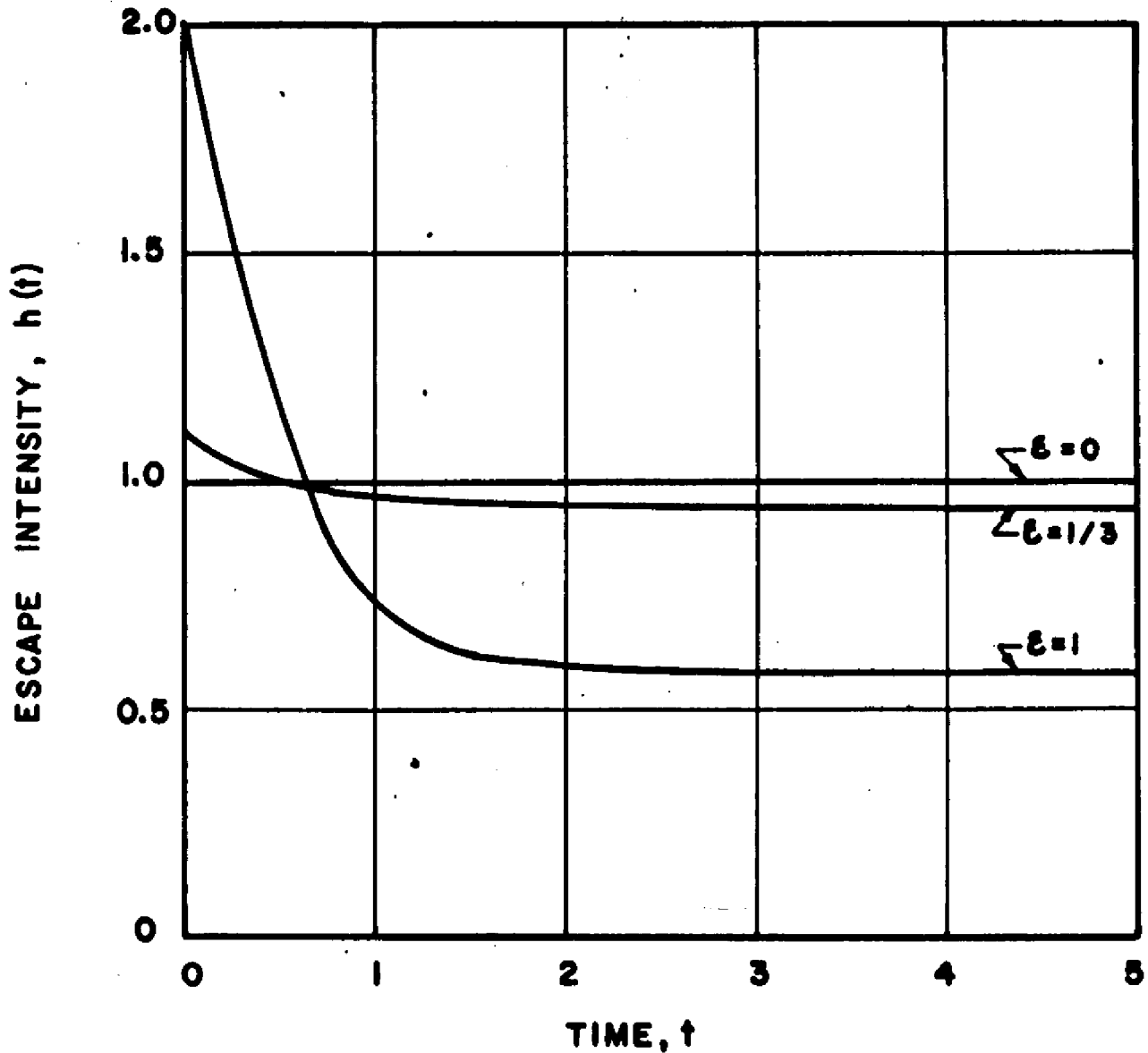


Figure 20: EFFECT OF SWITCHING RATE ON ESCAPE INTENSITY FOR PARALLEL CASE

$$(\nu_1 = \nu_2, \bar{P} = 1/2, \lambda_1 = \lambda_2, \epsilon = 1)$$

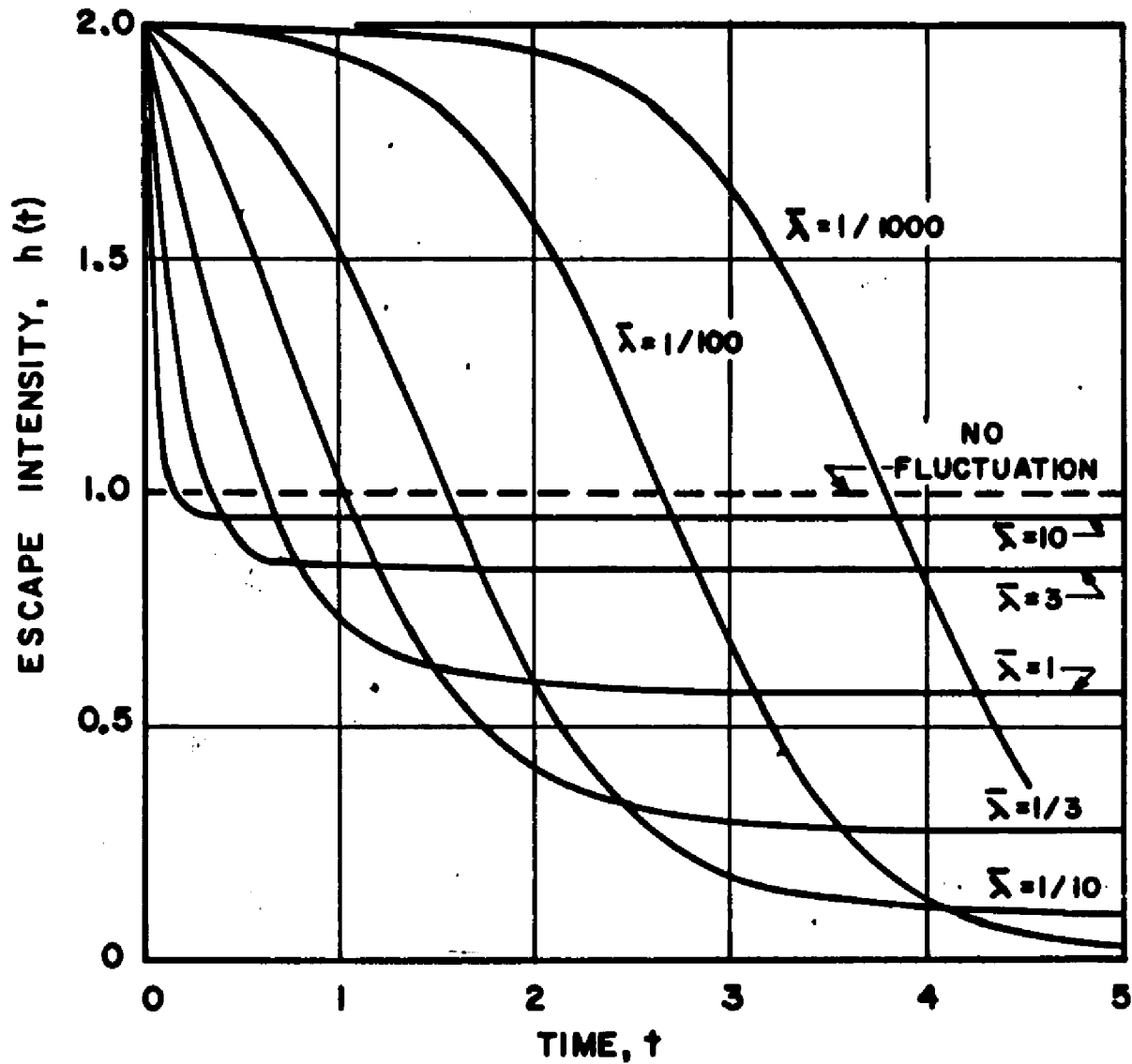


Figure 21: EFFECT OF FLUCTUATION MAGNITUDE ON ESCAPE INTENSITY FOR SERIES CASE

$$(v_1 = v_2, \bar{r} = 1, \lambda_1 = \lambda_2, \bar{\lambda} = 1)$$

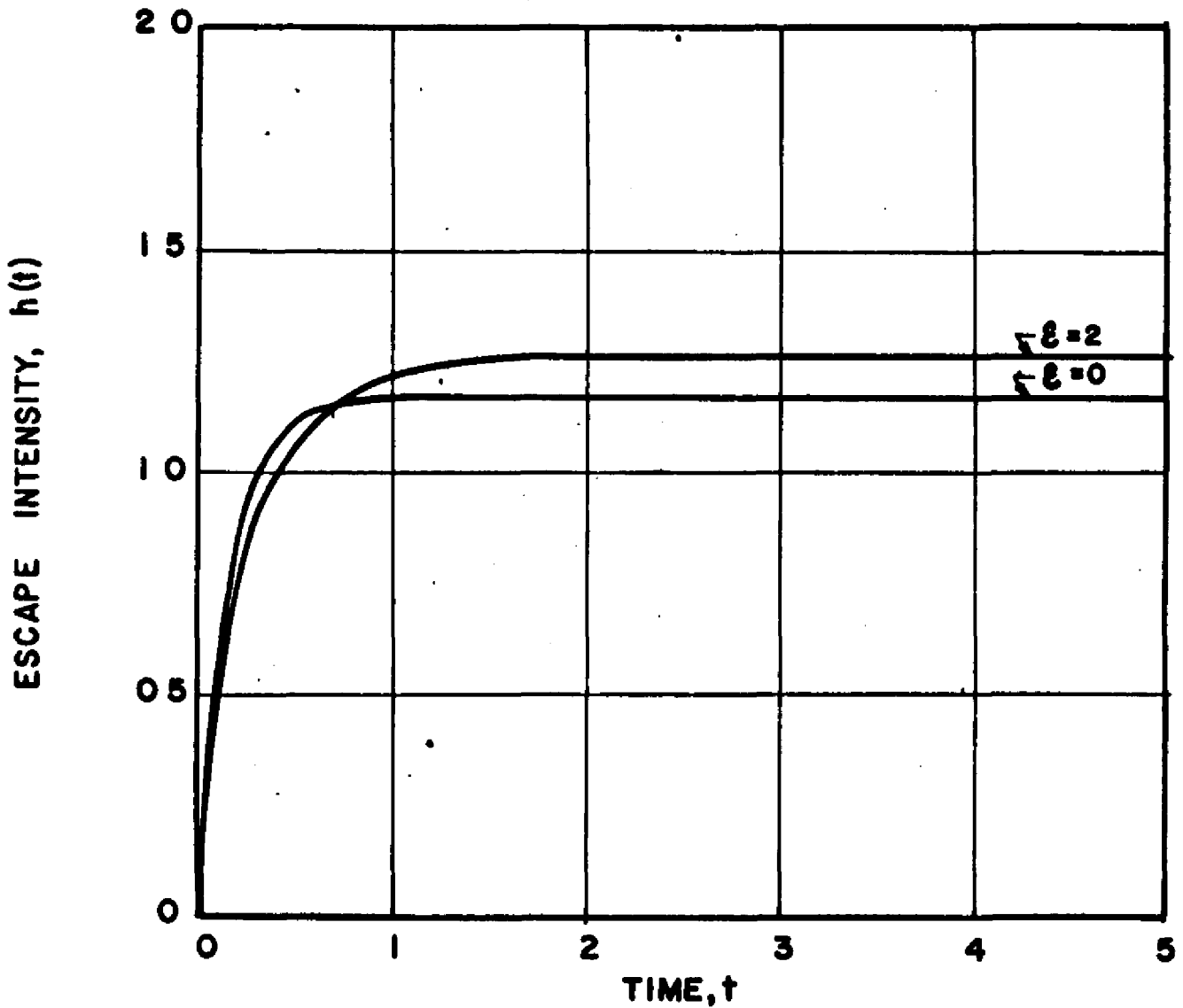
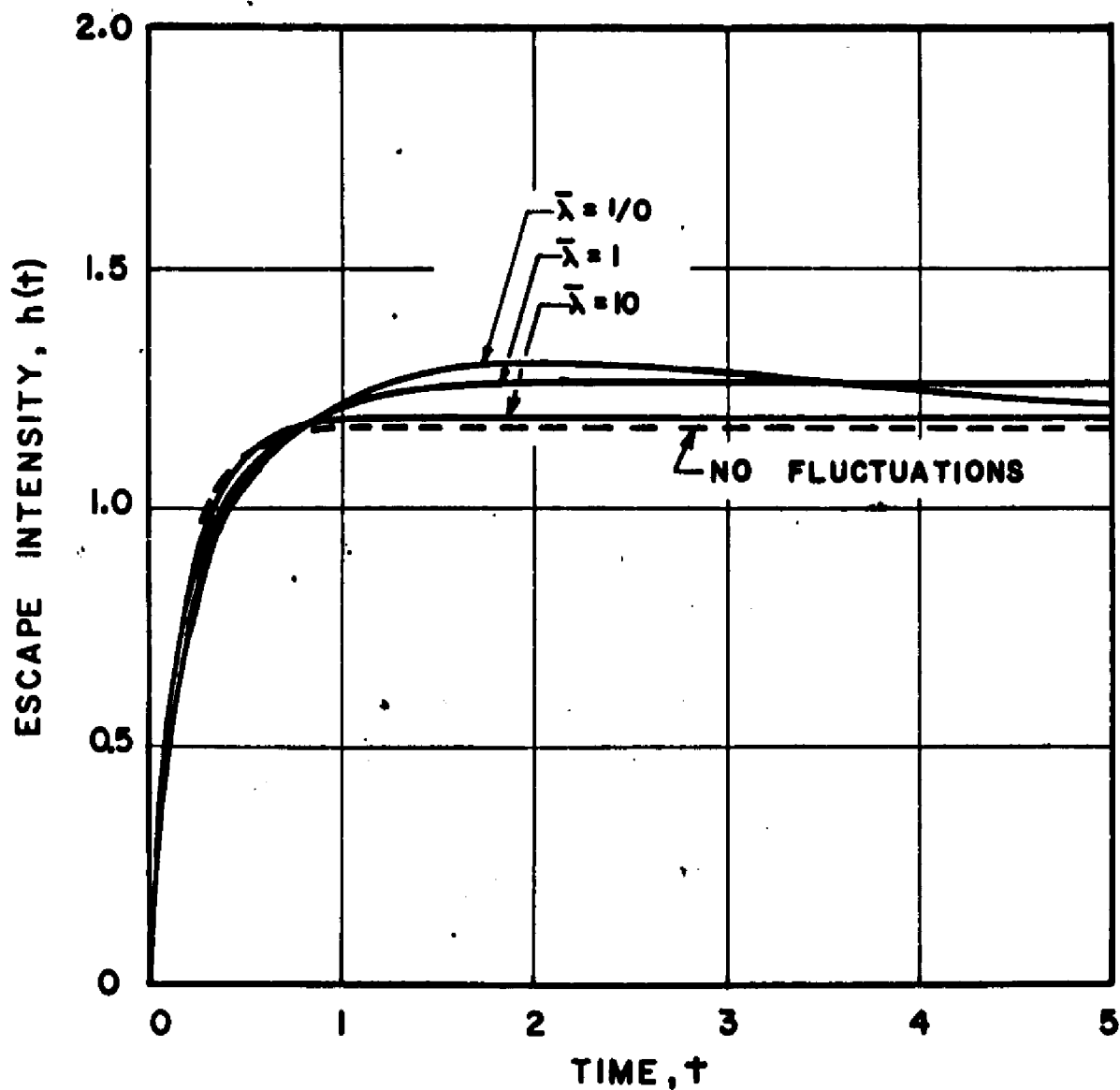


Figure 22: EFFECT OF SWITCHING RATE ON ESCAPE INTENSITY FOR SERIES CASE

$$(\nu_1 = \nu_2, \bar{r} = 1, \lambda_1 = \lambda_2, \xi = 2)$$



effect is observed. The curves for the series model, Figures 21 and 22, show a much smaller effect of the flow fluctuations on $h(t)$. In this case the main effect is a slight increase in the limiting value of $h(t)$ as $t \rightarrow \infty$. Again, at large switching rates the effects become small and the steady behavior is approached.

The equations satisfied by the second moments for the parallel case are

$$\frac{ds_{111}}{dt} = 2 \frac{w}{v_1} r_1 \mu_{11}(t) x_0(t) - \left[2 \frac{w}{v_1} r_1 + \lambda_1 \right] s_{111} + \lambda_2 s_{211}$$

$$\frac{ds_{211}}{dt} = 2 \frac{w}{v_1} r_2 \mu_{21}(t) x_0(t) + \lambda_1 s_{111} - \left[2 \frac{w}{v_1} r_2 + \lambda_2 \right] s_{211}$$

$$\frac{ds_{122}}{dt} = 2 \frac{w}{v_2} (1-r_1) \mu_{12}(t) x_0(t) - \left[2 \frac{w}{v_2} (1-r_1) + \lambda_1 \right] s_{122} + \lambda_2 s_{222}$$

$$\frac{ds_{222}}{dt} = 2 \frac{w}{v_2} (1-r_2) \mu_{22}(t) x_0(t) + \lambda_1 s_{122} - \left[2 \frac{w}{v_2} (1-r_2) + \lambda_2 \right] s_{222}$$

$$\begin{aligned} \frac{ds_{112}}{dt} = & \frac{w}{v_1} r_1 \mu_{12}(t) x_0(t) + \frac{w}{v_2} (1-r_1) \mu_{11}(t) x_0(t) \\ & - \left[\frac{w}{v_1} r_1 + \frac{w}{v_2} (1-r_1) + \lambda_1 \right] s_{112} + \lambda_2 s_{212} \end{aligned}$$

$$\begin{aligned} \frac{ds_{212}}{dt} = & \frac{w}{v_1} r_2 \mu_{22}(t) x_0(t) + \frac{w}{v_2} (1-r_2) \mu_{21}(t) x_0(t) \\ & + \lambda_1 s_{112} - \left[\frac{w}{v_1} r_2 + \frac{w}{v_2} (1-r_2) + \lambda_2 \right] s_{212} \end{aligned} \quad (\text{VIII-18})$$

where $s_{ijk}(t) = \int x_j x_k p_i(t, \underline{x}) d\underline{x}$. The mean-square outlet concentration, $\langle z^2(t) \rangle$, is then given by

$$\begin{aligned} \langle z^2(t) \rangle = & r_1^2 S_{111} + r_2^2 S_{211} + (1-r_1)^2 S_{122} \\ & + (1-r_2)^2 S_{222} + 2r_1(1-r_1)S_{112} + 2r_2(1-r_2)S_{212} \end{aligned} \quad (\text{VIII-19})$$

which corresponds to equation (IV-31). Because of the presence of the mixed moments, s_{112} and s_{212} , the superposition principle, which works for first moments, fails for second moments. The variance of the output cannot be calculated from the variances of the individual tank concentrations. The second moments for the series case are given by

$$\frac{ds_{111}}{dt} = 2 \frac{W}{V_1} \mu_{11}(t) x_0(t) - [2 \frac{W}{V_1} (1+r_1) + \lambda] s_{111} + \lambda_2 s_{211} + 2 \frac{W}{V_1} r_1 s_{112}$$

$$\frac{ds_{211}}{dt} = 2 \frac{W}{V_1} \mu_{21}(t) x_0(t) + \lambda_1 s_{111} - [2 \frac{W}{V_1} (1+r_2) + \lambda_2] s_{211} + 2 \frac{W}{V_1} r_2 s_{212}$$

$$\frac{ds_{122}}{dt} = - [2 \frac{W}{V_2} (1+r_1) + \lambda_1] s_{122} + \lambda_2 s_{222} + 2 \frac{W}{V_2} (1+r_1) s_{112}$$

$$\frac{ds_{222}}{dt} = \lambda_1 s_{122} - [2 \frac{W}{V_2} (1+r_2) + \lambda_2] s_{222} + 2 \frac{W}{V_2} (1+r_2) s_{212}$$

(VIII-20)

$$\begin{aligned}
\frac{ds_{112}}{dt} &= \frac{W}{V_1} \mu_{12}(t) x_o(t) + \frac{W}{V_2} (1+r_1) S_{111} + \frac{W}{V_1} r_1 S_{122} \\
&\quad - \left[\frac{W}{V_1} (1+r_1) + \frac{W}{V_2} (1+r_1) + \lambda_1 \right] S_{112} + \lambda_2 S_{212} \\
\frac{ds_{212}}{dt} &= \frac{W}{V_1} \mu_{22}(t) x_o(t) + \frac{W}{V_2} (1+r_2) S_{211} + \frac{W}{V_1} r_2 S_{222} \\
&\quad + \lambda_1 S_{112} - \left[\frac{W}{V_1} (1+r_2) + \frac{W}{V_2} (1+r_2) + \lambda_2 \right] S_{212}
\end{aligned} \tag{VIII-20}$$

Then

$$\langle \bar{x}^2(t) \rangle = S_{122} + S_{212} \tag{VIII-21}$$

The second moments of the step response for some typical values of the parameters were calculated for both models. The results, presented in the form of curves of $\sigma(t)/\mu(t)$, the coefficient of variation of the outlet concentration, are shown in Figures 23 and 24 for the parallel case and in Figures 25 and 26 for the series case. Figure 23 shows that increasing fluctuation magnitude increases the coefficient of variation of the output for the parallel system in a non-linear way, the effect being slight until the fluctuation size becomes substantial. It is seen in Figure 25, however, that the relationship between $\sigma(t)/\mu(t)$ and ϵ is practically linear for the series case. It is also seen that the output for the parallel case fluctuates more strongly than that for the series case. In Figure 24, it is seen that the

Figure 23: EFFECT OF FLUCTUATION MAGNITUDE ON COEFFICIENT OF VARIATION OF STEP RESPONSE FOR PARALLEL CASE

$$(\nu_1 = \nu_2, \tau = 1/2, \lambda_1 = \lambda_2, \bar{\lambda} = 1)$$

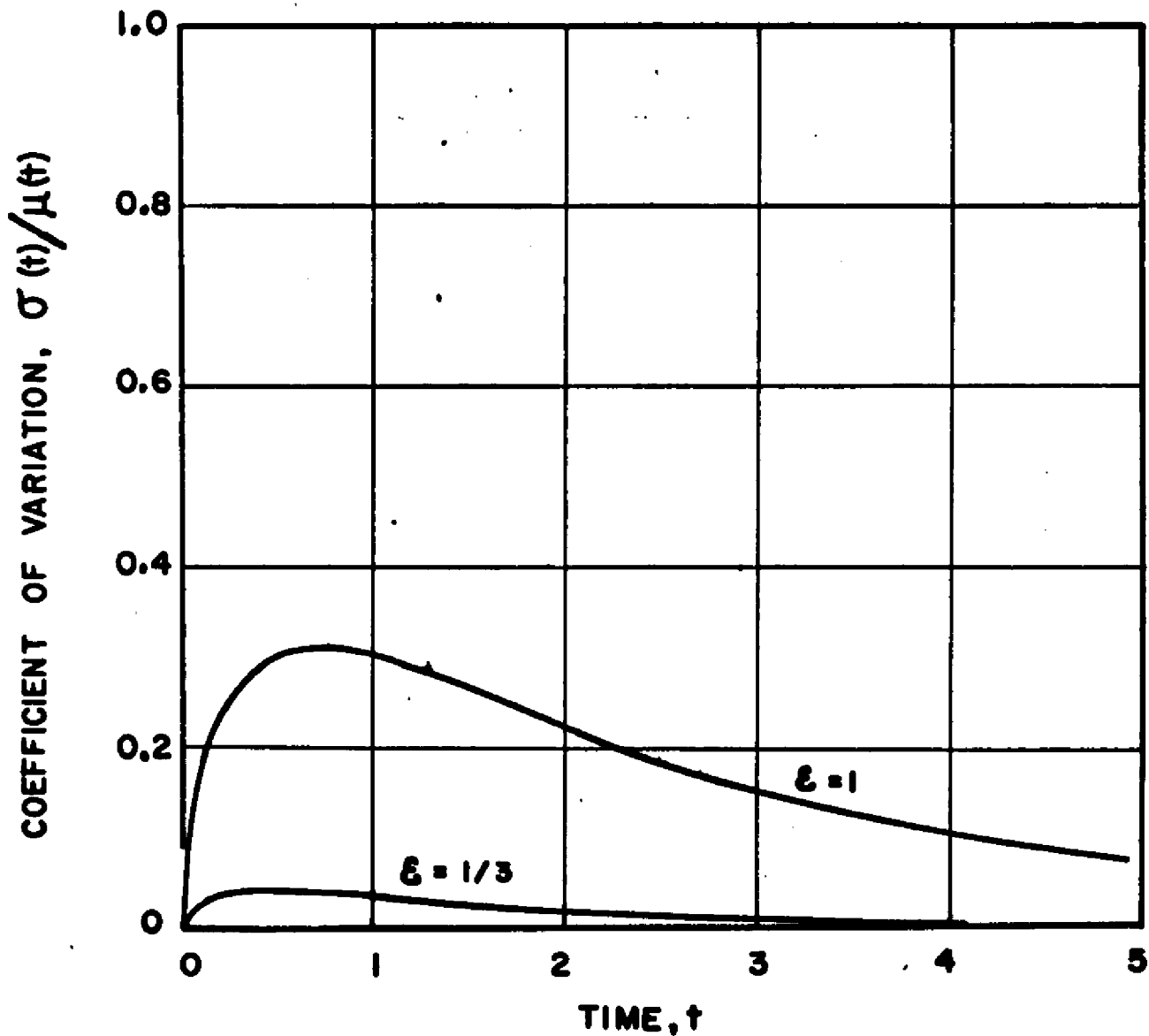


Figure 24: EFFECT OF SWITCHING RATE ON COEFFICIENT OF VARIATION OF STEP RESPONSE FOR PARALLEL CASE

$$(v_1 = v_2, F = \frac{1}{2}, \lambda_1 = \lambda_2, \xi = 1)$$

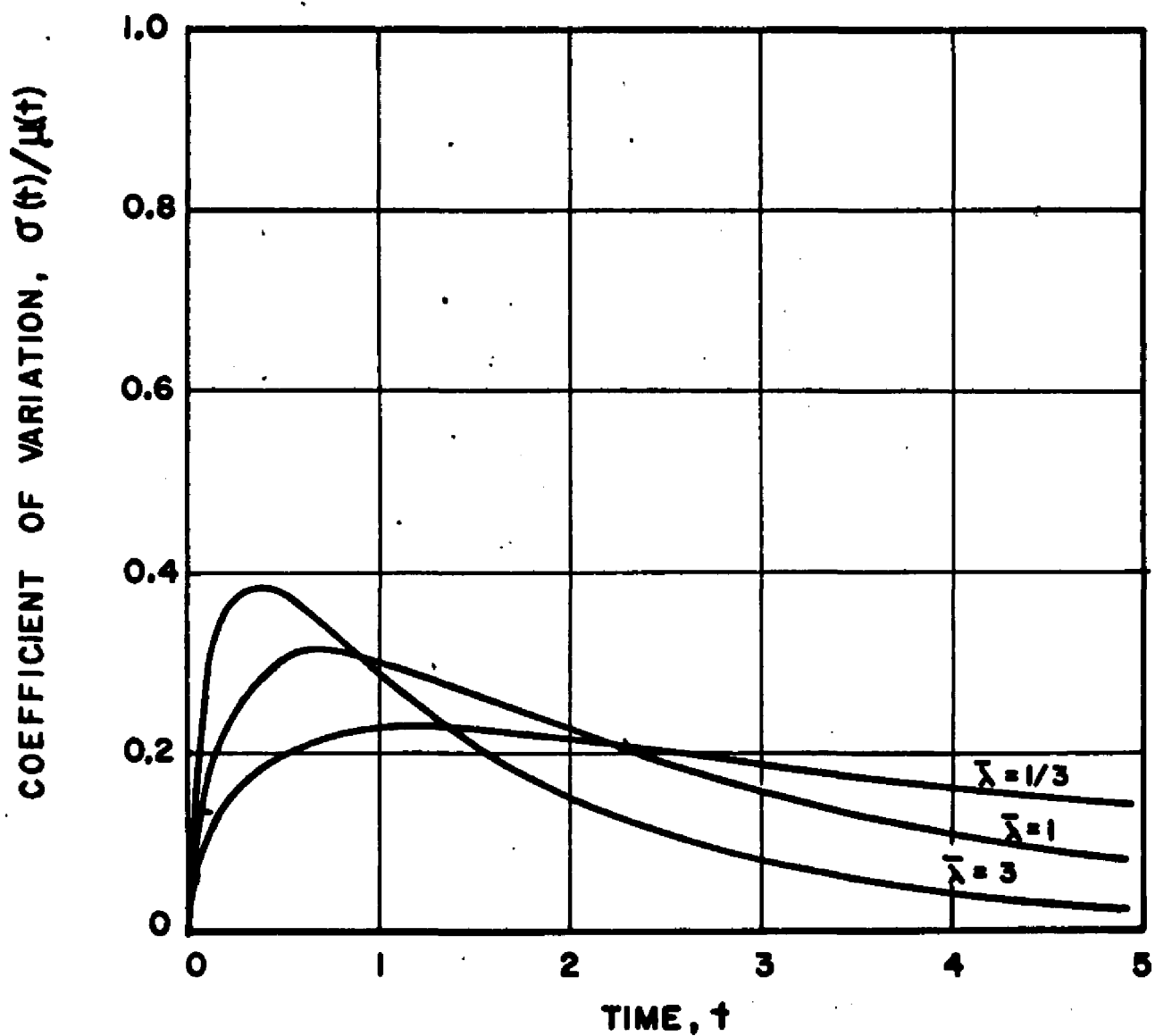


Figure 25: EFFECT OF FLUCTUATION MAGNITUDE ON COEFFICIENT OF VARIATION OF STEP RESPONSE FOR SERIES CASE

$$(\nu_1 = \nu_2, \bar{P} = 1, \lambda_1 = \lambda_2, \bar{\lambda} = 1)$$

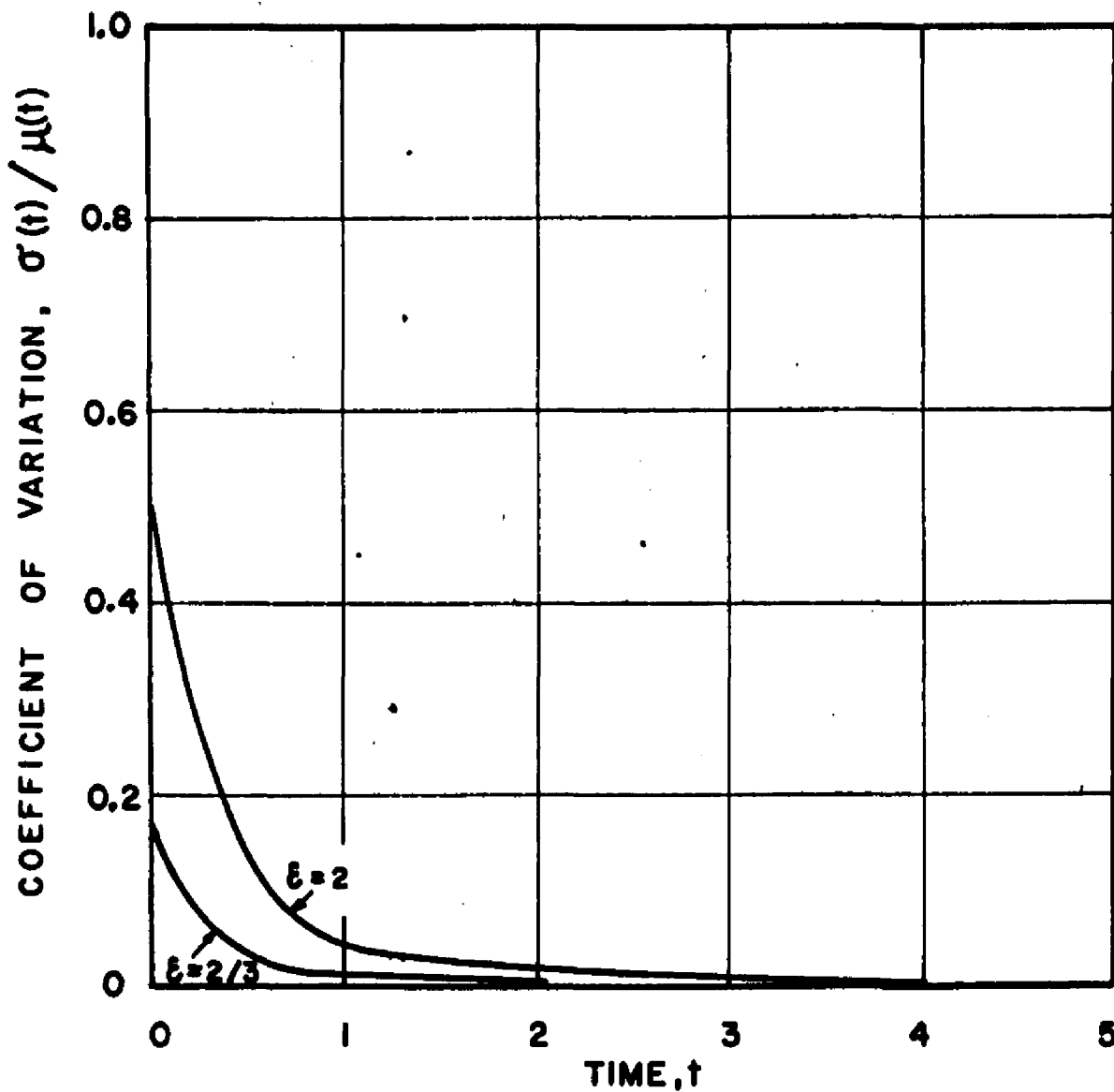
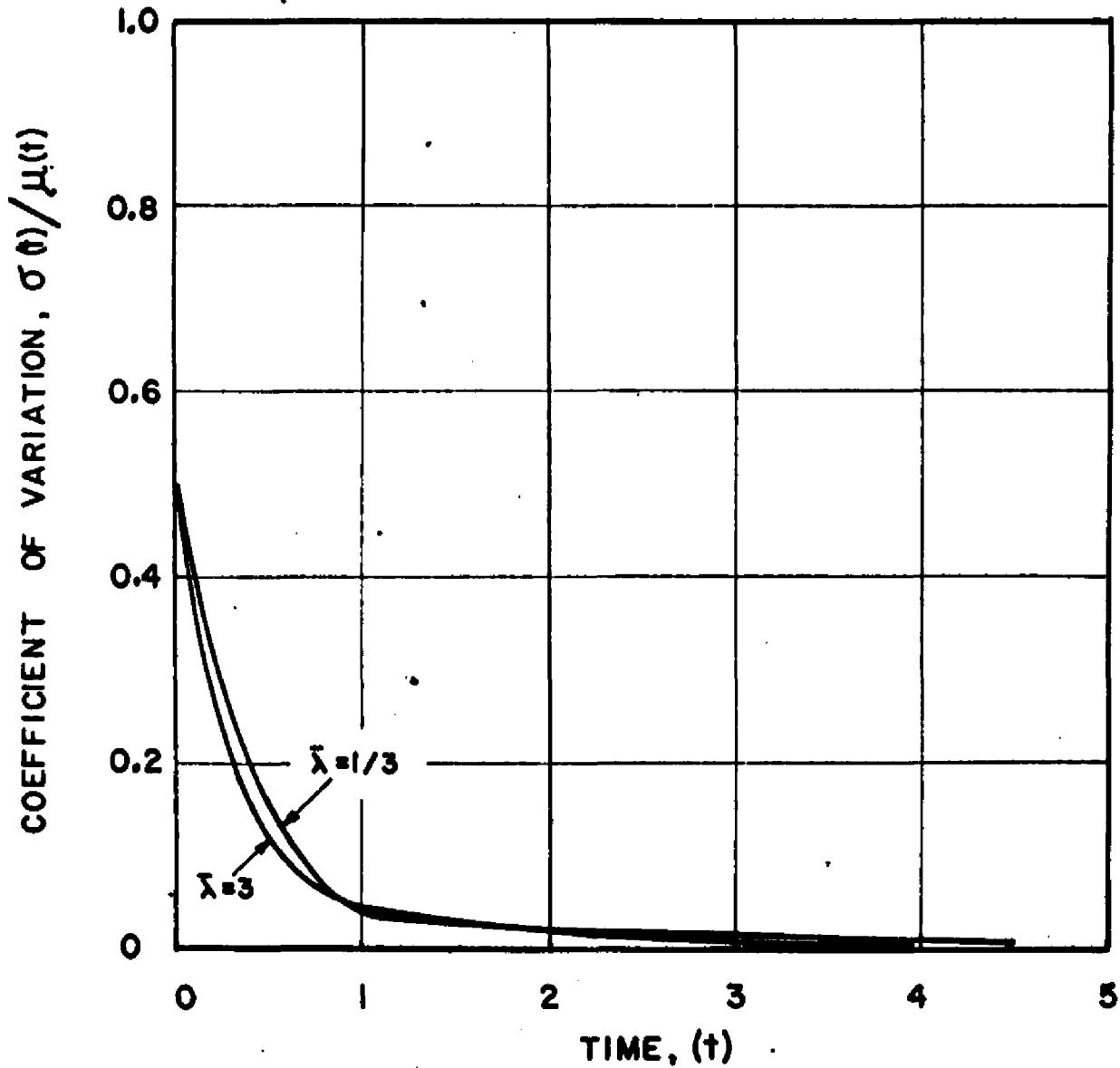


FIGURE 26

EFFECT OF SWITCHING RATE ON COEFFICIENT OF VARIATION

Figure 26: EFFECT OF SWITCHING RATE ON COEFFICIENT OF VARIATION OF STEP RESPONSE FOR SERIES CASE

$$(\nu_1 = \nu_2, \bar{r} = 1, \lambda_1 = \lambda_2, \varepsilon = 2)$$



switching rate has a strong effect on the shape of the curve for the parallel case. Figure 26 shows that switching rate has a relatively minor effect on the curve for the series case.

The autocorrelation function of outlet concentration, defined by equation (IV-35), can be calculated from equations corresponding to (IV-46). For the parallel case these become

$$\begin{aligned} \frac{dq_{11}}{d\tau} = & \frac{w}{v_1} r_1 \left\{ \pi_{11}(\tau) [r_1 \mu_{11}(t) + (1-r_1) \mu_{12}(t)] \right. \\ & \left. + \pi_{21}(\tau) [r_2 \mu_{21}(t) + (1-r_2) \mu_{22}(t)] \right\} \\ & - \left(\frac{w}{v_1} r_1 + \lambda_1 \right) q_{11} + \lambda_2 q_{21} \end{aligned}$$

$$\begin{aligned} \frac{dq_{21}}{d\tau} = & \frac{w}{v_1} r_2 \left\{ \pi_{12}(\tau) [r_1 \mu_{11}(t) + (1-r_1) \mu_{12}(t)] \right. \\ & \left. + \pi_{22}(\tau) [r_2 \mu_{21}(t) + (1-r_2) \mu_{22}(t)] \right\} \\ & + \lambda_1 q_{11} - \left(\frac{w}{v_1} r_2 + \lambda_2 \right) q_{21} \end{aligned}$$

$$\begin{aligned} \frac{dq_{12}}{d\tau} = & \frac{w}{v_2} (1-r_1) \left\{ \pi_{11}(\tau) [r_1 \mu_{11}(t) + (1-r_1) \mu_{12}(t)] \right. \\ & \left. + \pi_{21}(\tau) [r_2 \mu_{21}(t) + (1-r_2) \mu_{22}(t)] \right\} \\ & - \left[\frac{w}{v_2} (1-r_1) + \lambda_1 \right] q_{12} + \lambda_2 q_{22} \end{aligned}$$

(VIII-22)

$$\begin{aligned}
\frac{dq_{22}}{d\tau} = & \frac{w}{v_2} (1-r_2) \left\{ \pi_{12}(\tau) [r_1 \mu_{11}(t) + (1-r_1) \mu_{12}(t)] \right. \\
& \left. + \pi_{22}(\tau) [r_2 \mu_{21}(t) + (1-r_2) \mu_{22}(t)] \right\} \\
& + \lambda_1 q_{12} - \left[\frac{w}{v_2} (1-r_2) + \lambda_2 \right] q_{22}
\end{aligned}
\tag{VIII-22}$$

with initial conditions given by

$$\begin{aligned}
\tau = 0 : \quad q_{11} &= r_1 s_{11}(t) + (1-r_1) s_{112}(t) \\
q_{21} &= r_2 s_{21}(t) + (1-r_2) s_{212}(t) \\
q_{12} &= r_1 s_{112}(t) + (1-r_1) s_{122}(t) \\
q_{22} &= r_2 s_{212}(t) + (1-r_2) s_{222}(t)
\end{aligned}
\tag{VIII-23}$$

Then

$$\langle z(t) z(t+\tau) \rangle = r_1 q_{11} + r_2 q_{21} + (1-r_1) q_{12} + (1-r_2) q_{22} \tag{VIII-24}$$

The corresponding expressions for the series case are

$$\begin{aligned}
\frac{dq_{11}}{d\tau} = & \frac{w}{v_1} [\pi_{11}(\tau) \mu_{12}(t) + \pi_{21}(\tau) \mu_{22}(t)] \\
& - \left[\frac{w}{v_1} (1+r_1) + \lambda_1 \right] q_{11} + \lambda_2 q_{21} + \frac{w}{v_1} r_1 q_{12}
\end{aligned}$$

$$\frac{dq_{21}}{d\tau} = \frac{w}{v_1} [\pi_{12}(\tau)\mu_{12}(t) + \pi_{22}(\tau)\mu_{22}(t)]$$

$$+ \lambda_1 q_{11} - \left[\frac{w}{v_1}(1+r_2) + \lambda_2 \right] q_{21} + \frac{w}{v_1} r_2 q_{22}$$

$$\frac{dq_{12}}{d\tau} = - \left[\frac{w}{v_2}(1+r_1) + \lambda_1 \right] q_{12} + \lambda_2 q_{22}$$

$$+ \frac{w}{v_2}(1+r_1) q_{11}$$

$$\frac{dq_{22}}{d\tau} = \lambda_1 q_{12} - \left[\frac{w}{v_2}(1+r_2) + \lambda_2 \right] q_{22}$$

$$+ \frac{w}{v_2}(1+r_2) q_{21}$$

(VIII-25)

with initial conditions

$$\tau = 0: \quad q_{11} = S_{112}(t)$$

$$q_{21} = S_{212}(t)$$

$$q_{12} = S_{122}(t)$$

$$q_{22} = S_{222}(t)$$

(VIII-26)

Then

$$\langle z(t)z(t+\tau) \rangle = q_{12} + q_{22}$$

(VIII-27)

The autocorrelation function of the step response, $\rho_s(\tau)$, is shown for the parallel case in Figure 27 and for the series case in Figure 28. In both cases the function depends strongly on t , although for a stationary process it would depend on τ only. Also in both cases, the curves approach zero more slowly than does the correlation function of the flow rates, equation (VII-9). This indicates a long "memory time" of the process compared with that of the flow. Comparison of the two graphs shows that the curves for the series case approach zero considerably more slowly than those for the parallel case.

The coefficient of variation for an impulse response is shown in Figure 29 for the parallel model and in Figure 30 for the series model. These become large at large values of time in both cases. The curves for the parallel case are considerable higher than those for the series case (note difference in scales). At large switching rates, $\frac{t}{\tau}$ for the parallel model approaches a value of one for the parameters shown, while that for the series case approaches zero for any parameter values. Actually, the behavior of the concentration in each tank becomes deterministic at large switching rates for either model. In the parallel case, however, the outlet concentration will rapidly oscillate between two values of

Figure 27: AUTOCORRELATION FUNCTION OF STEP RESPONSE FOR PARALLEL CASE

$$(v_1 = v_2, \bar{r} = \frac{1}{2}, \lambda_1 = \lambda_2, \bar{\lambda} = 1, \varepsilon = 1)$$

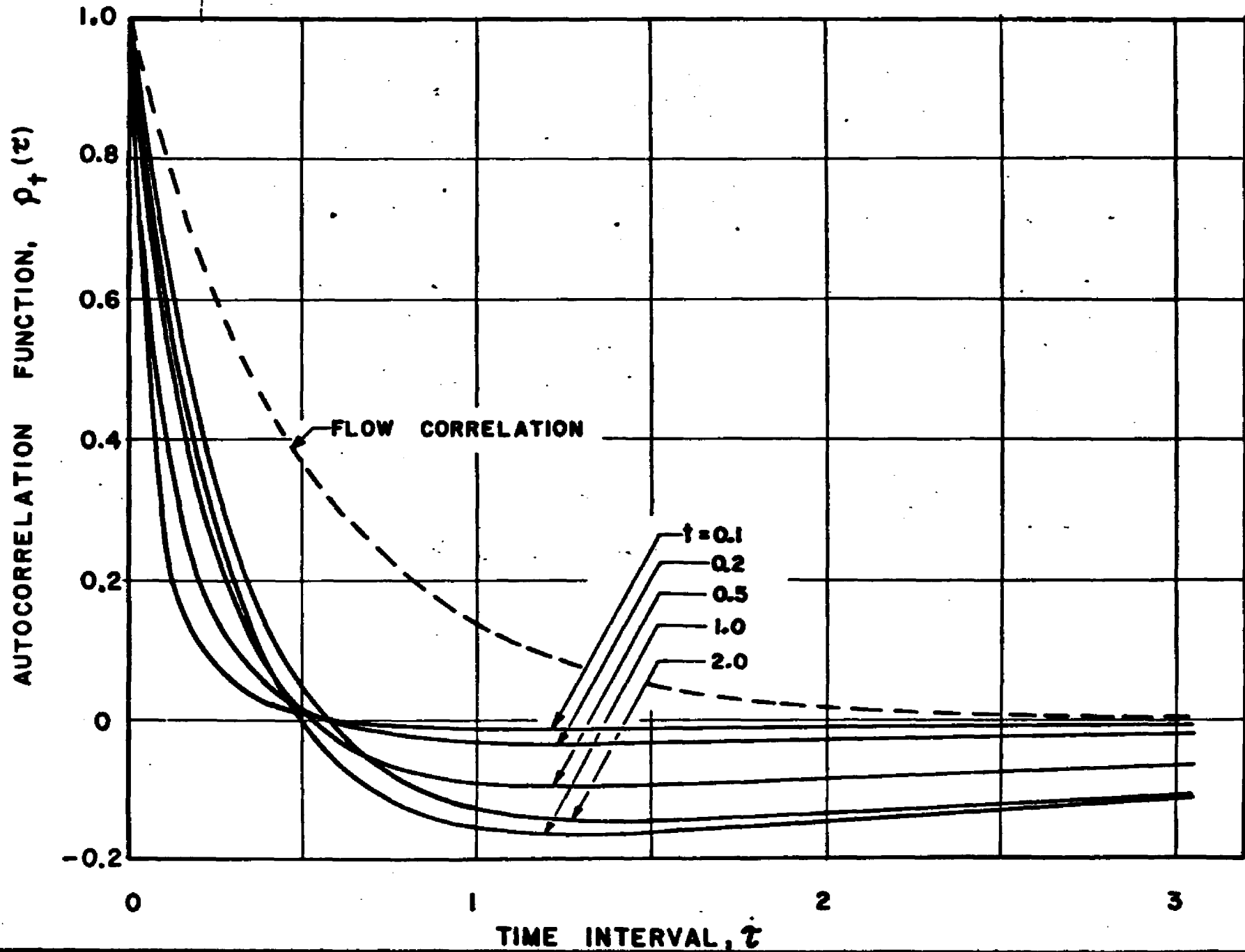


Figure 28: AUTOCORRELATION FUNCTION OF STEP RESPONSE FOR SERIES CASE

$$(v_1 = v_2, \bar{F} = 1, \lambda_1 = \lambda_2, \lambda = 1, \varepsilon = 2)$$

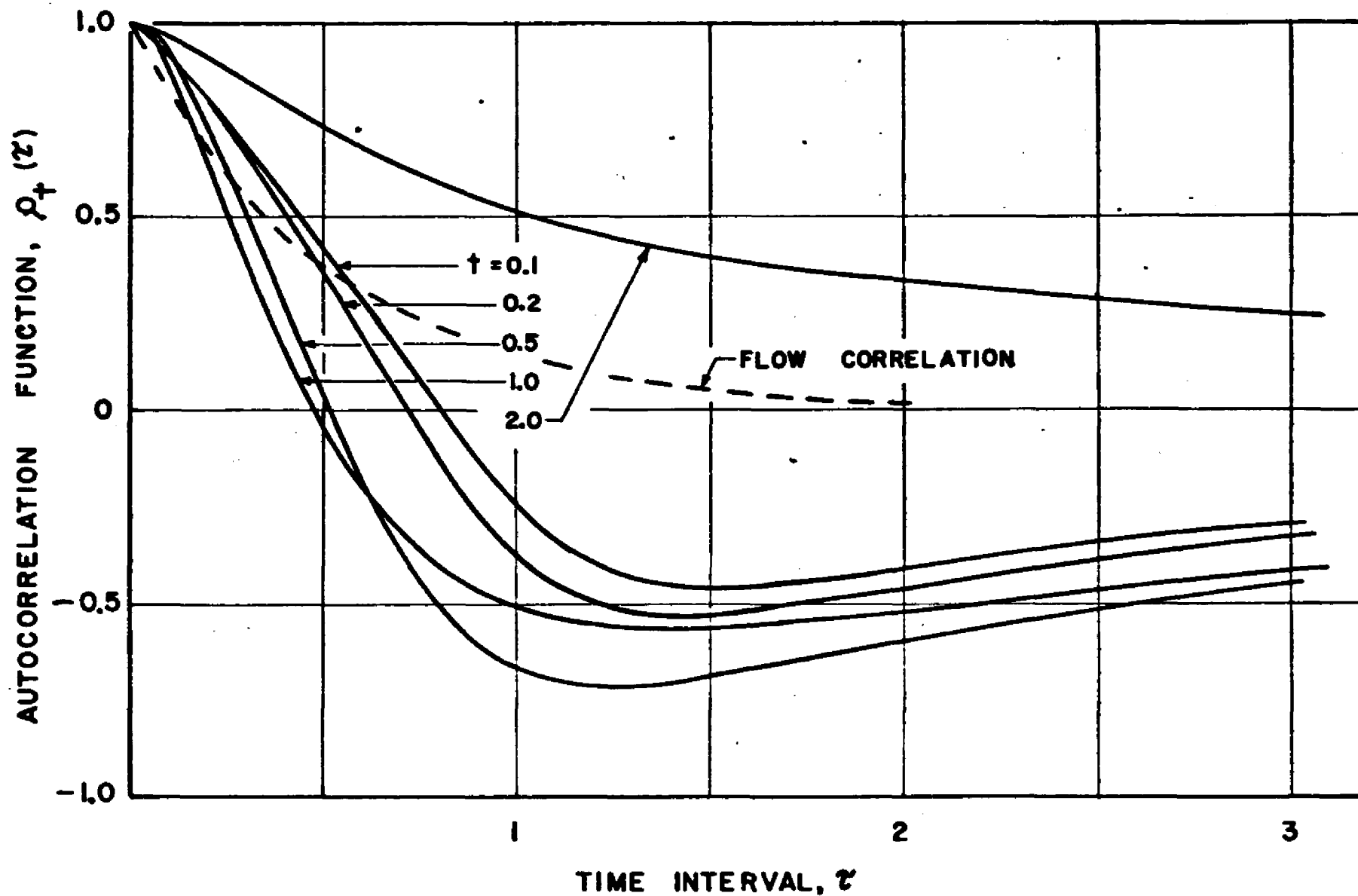
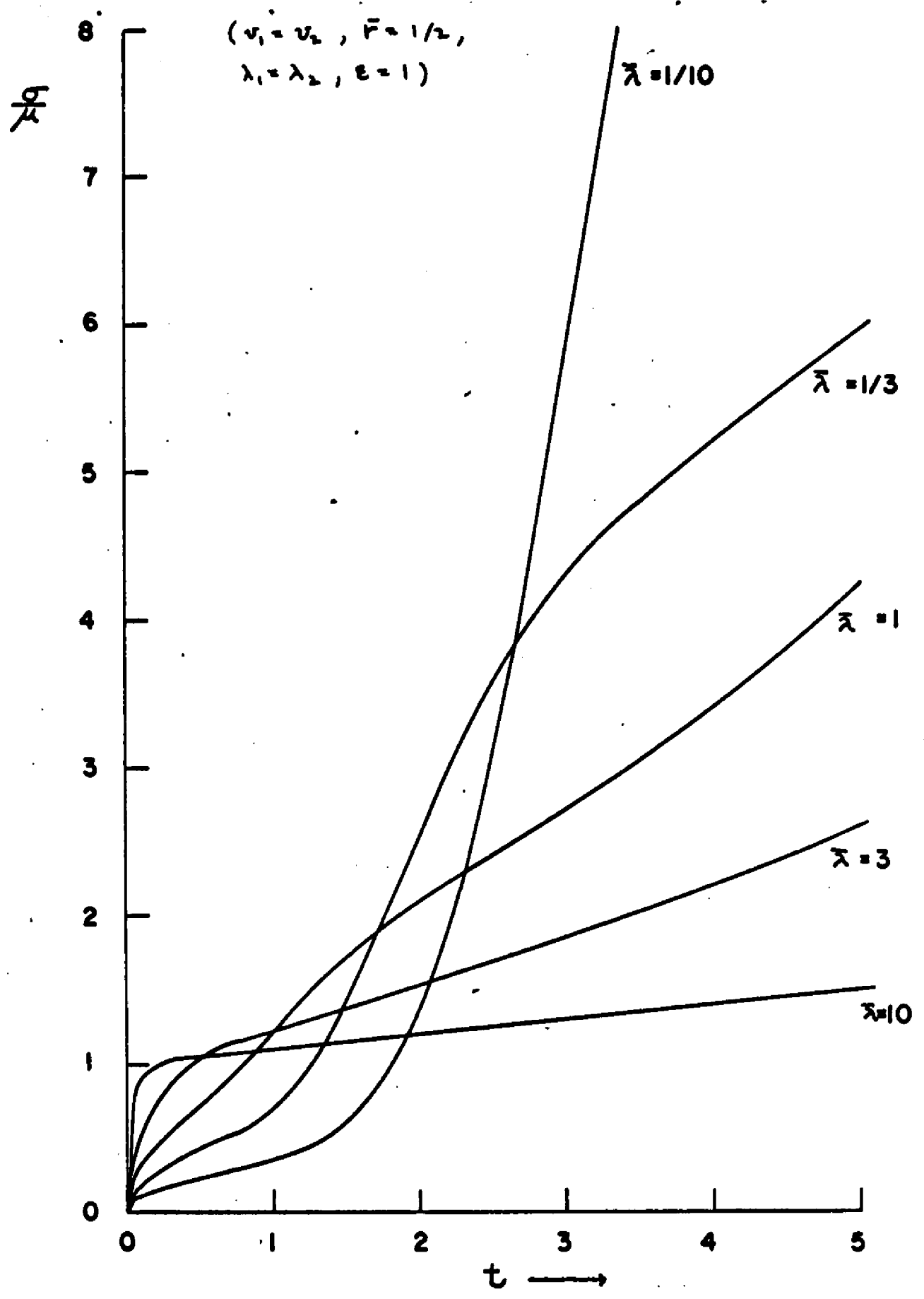


Figure 29. COEFFICIENT OF VARIATION OF IMPULSE RESPONSE FOR PARALLEL CASE



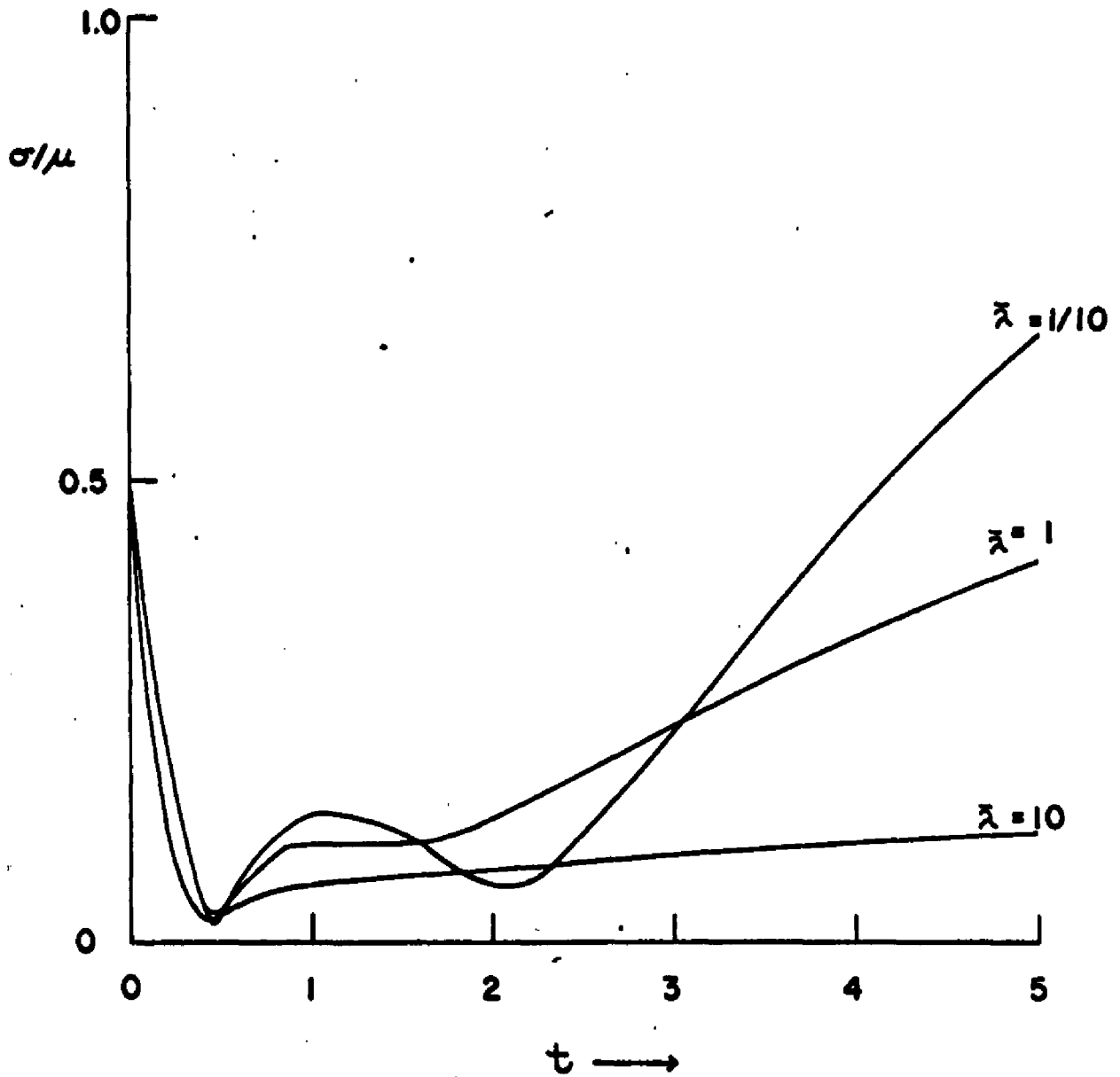


Figure 30. COEFFICIENT OF VARIATION OF IMPULSE RESPONSE FOR SERIES CASE

$$(\nu_1 = \nu_2, \bar{\nu} = 1, \lambda_1 = \lambda_2, \varepsilon = 2)$$

concentration.

C. Moments with First Order Reaction

When a first order reaction occurs and the inlet concentration is constant, the equations of change of the parallel model become

$$\begin{aligned}v_1 \frac{dx_1}{dt} &= w r_a x_0 - w r_a x_1 - k x_1 \\v_2 \frac{dx_2}{dt} &= w(1-r_a) x_0 - w(1-r_a) x_2 - k x_2\end{aligned}\quad (\text{VIII-28})$$

For the series model, the corresponding equations are

$$\begin{aligned}v_1 \frac{dx_1}{dt} &= w x_0 - w(1+r_a) x_1 + w r_a x_2 - k x_1 \\v_2 \frac{dx_2}{dt} &= w(1+r_a)(x_1 - x_2) - k x_2\end{aligned}\quad (\text{VIII-29})$$

The stationary distribution for the parallel case satisfies

$$\begin{aligned}&\frac{\partial}{\partial x_1} \left\{ \left[\frac{w}{v_1} r_a x_0 - \left(\frac{w}{v_1} r_a + k \right) x_1 \right] p_1(t, x) \right\} \\&+ \frac{\partial}{\partial x_2} \left\{ \left[\frac{w}{v_2} (1-r_a) x_0 - \left(\frac{w}{v_2} (1-r_a) + k \right) x_2 \right] p_1(t, x) \right\} \\&= -\lambda_1 p_1(t, x) + \lambda_2 p_2(t, x) \\&\frac{\partial}{\partial x_1} \left\{ \left[\frac{w}{v_1} r_a x_0 - \left(\frac{w}{v_1} r_a + k \right) x_1 \right] p_2(t, x) \right\} \\&+ \frac{\partial}{\partial x_2} \left\{ \left[\frac{w}{v_2} (1-r_a) x_0 - \left(\frac{w}{v_2} (1-r_a) + k \right) x_2 \right] p_2(t, x) \right\} \\&= \lambda_1 p_1(t, x) - \lambda_2 p_2(t, x)\end{aligned}\quad (\text{VIII-30})$$

The distribution for the series case satisfies

$$\begin{aligned} & \frac{\partial}{\partial x_1} \left\{ \left[\frac{W}{v_1} x_0 - \left(\frac{W}{v_1} (1+r_1) + k \right) x_1 + \frac{W}{v_1} r_1 x_2 \right] p_1(t, x) \right\} \\ & + \frac{\partial}{\partial x_2} \left\{ \left[\frac{W}{v_2} (1+r_1) x_1 - \left(\frac{W}{v_2} (1+r_1) + k \right) x_2 \right] p_1(t, x) \right\} \\ & = -\lambda_1 p_1(t, x) + \lambda_2 p_2(t, x) \end{aligned}$$

$$\begin{aligned} & \frac{\partial}{\partial x_1} \left\{ \left[\frac{W}{v_1} x_0 - \left(\frac{W}{v_1} (1+r_2) + k \right) x_1 + \frac{W}{v_1} r_2 x_2 \right] p_2(t, x) \right\} \\ & + \frac{\partial}{\partial x_2} \left\{ \left[\frac{W}{v_2} (1+r_2) x_1 - \left(\frac{W}{v_2} (1+r_2) + k \right) x_2 \right] p_2(t, x) \right\} \\ & = \lambda_1 p_1(t, x) - \lambda_2 p_2(t, x) \end{aligned}$$

(VIII-31)

In both cases the resulting partial differential equations are difficult to solve. The nature of the solutions to these equations will be discussed in the next section. The first and second moments of reactant concentration are easily calculated, however, using the methods of section V. The first and second moments for the parallel

case are calculated from

$$\left[\frac{W}{v_1} r_1 + k + \lambda_1 \right] m_{11} - \lambda_2 m_{21} = \bar{p}_1 \frac{W}{v_1} r_1$$

$$-\lambda_1 m_{11} + \left[\frac{W}{v_1} r_2 + k + \lambda_2 \right] m_{21} = \bar{p}_2 \frac{W}{v_1} r_2$$

$$\left[\frac{W}{v_2} (1-r_1) + k + \lambda_1 \right] m_{12} - \lambda_2 m_{22} = \bar{p}_1 \frac{W}{v_2} (1-r_1)$$

$$-\lambda_1 m_{12} + \left[\frac{W}{v_2} (1-r_2) + k + \lambda_2 \right] m_{22} = \bar{p}_2 \frac{W}{v_2} (1-r_2)$$

$$\left[2 \frac{W}{v_1} r_1 + 2k + \lambda_1 \right] s_{111} - \lambda_2 s_{211} = 2 \frac{W}{v_1} r_1 m_{11}$$

$$-\lambda_1 s_{111} + \left[2 \frac{W}{v_1} r_2 + 2k + \lambda_2 \right] s_{211} = 2 \frac{W}{v_1} r_2 m_{21}$$

$$\left[2 \frac{W}{v_2} (1-r_1) + 2k + \lambda_1 \right] s_{122} - \lambda_2 s_{222} = 2 \frac{W}{v_2} (1-r_1) m_{12}$$

$$-\lambda_1 s_{122} + \left[2 \frac{W}{v_2} (1-r_2) + 2k + \lambda_2 \right] s_{222} = 2 \frac{W}{v_2} (1-r_2) m_{22}$$

$$\left[\frac{W}{v_1} r_1 + \frac{W}{v_2} (1-r_1) + 2k + \lambda_1 \right] s_{112} - \lambda_2 s_{212} = \frac{W}{v_1} r_1 m_{12} + \frac{W}{v_2} (1-r_1) m_{11}$$

$$-\lambda_1 s_{112} + \left[\frac{W}{v_1} r_2 + \frac{W}{v_2} (1-r_2) + 2k + \lambda_2 \right] s_{212} = \frac{W}{v_1} r_2 m_{22} + \frac{W}{v_2} (1-r_2) m_{21}$$

(VIII-32)

Then

$$\langle Z \rangle = r_1 m_{11} + r_2 m_{21} + (1-r_1) m_{12} + (1-r_2) m_{22} \quad (\text{VIII-33})$$

and

$$\begin{aligned} \langle Z^2 \rangle = & r_1^2 S_{111} + r_2^2 S_{211} + (1-r_1)^2 S_{122} + (1-r_2)^2 S_{222} \\ & + 2r_1(1-r_1) S_{112} + 2r_2(1-r_2) S_{212} \end{aligned} \quad (\text{VIII-34})$$

Similarly, the moments for the series case are calculated from

$$\begin{aligned} & \left[\frac{W}{V_1}(1+r_1) + k + \lambda_1 \right] m_{11} - \lambda_2 m_{21} - \frac{W}{V_1} r_1 m_{12} = \frac{W}{V_1} \bar{p}_1 \\ & -\lambda_1 m_{11} + \left[\frac{W}{V_2}(1+r_2) + k + \lambda_2 \right] m_{21} - \frac{W}{V_2} r_2 m_{22} = \frac{W}{V_2} \bar{p}_2 \\ & -\frac{W}{V_2}(1+r_2) m_{21} - \lambda_1 m_{12} + \left[\frac{W}{V_1}(1+r_1) + k + \lambda_1 \right] m_{12} - \lambda_2 m_{22} = 0 \\ & -\frac{W}{V_1}(1+r_1) m_{11} - \lambda_1 m_{12} + \left[\frac{W}{V_2}(1+r_2) + k + \lambda_2 \right] m_{22} = 0 \\ & \left[2\frac{W}{V_1}(1+r_1) + 2k + \lambda_1 \right] S_{111} - \lambda_2 S_{211} - 2\frac{W}{V_1} r_1 S_{112} = 2\frac{W}{V_1} m_{11} \\ & -\lambda_1 S_{111} + \left[2\frac{W}{V_2}(1+r_2) + 2k + \lambda_2 \right] S_{211} - 2\frac{W}{V_2} r_2 S_{212} = 2\frac{W}{V_2} m_{21} \\ & \left[2\frac{W}{V_2}(1+r_2) + 2k + \lambda_2 \right] S_{122} - \lambda_2 S_{222} - 2\frac{W}{V_1}(1+r_1) S_{112} = 0 \\ & -\lambda_1 S_{122} + \left[2\frac{W}{V_2}(1+r_2) + 2k + \lambda_2 \right] S_{222} - 2\frac{W}{V_2}(1+r_2) S_{212} = 0 \end{aligned} \quad (\text{VIII-35})$$

$$\begin{aligned}
& -\frac{W}{v_2}(1+r_1)S_{111} - \frac{W}{v_1}r_1S_{122} + \left[\frac{W}{v_1}(1+r_1) + \frac{W}{v_2}(1+r_1) \right. \\
& \quad \left. + 2k + \lambda_1 \right] S_{112} - \lambda_2 S_{212} = \frac{W}{v_1}m_{12} \\
& -\frac{W}{v_2}(1+r_2)S_{211} - \frac{W}{v_1}r_2S_{222} - \lambda_1 S_{112} + \left[\frac{W}{v_1}(1+r_2) \right. \\
& \quad \left. + \frac{W}{v_2}(1+r_2) + 2k + \lambda_2 \right] S_{212} = \frac{W}{v_1}m_{22}
\end{aligned} \tag{VIII-35}$$

Then

$$\langle z \rangle = m_{12} + m_{22} \tag{VIII-36}$$

and

$$\langle z^2 \rangle = S_{122} + S_{222} \tag{VIII-37}$$

The mean outlet concentration, μ , and the standard deviation of outlet concentration, σ , are shown for the parallel case in Figure 31 and 32, and for the series case in Figure 33, for some typical parameter values.

It is seen in Figure 31 that the effect of the fluctuations in flow rate on the parallel case is to decrease conversion. For the series case, however, the result is a very slight increase in conversion, as shown in Figure 33. The fluctuations in outlet concentration are lower for the series than for the parallel case. Figure 32 shows that increasing the switching rate, λ , makes the

Figure 31

Figure 31. EFFECT OF FLUCTUATION SIZE ON FIRST ORDER REACTION BEHAVIOR OF PARALLEL MODEL

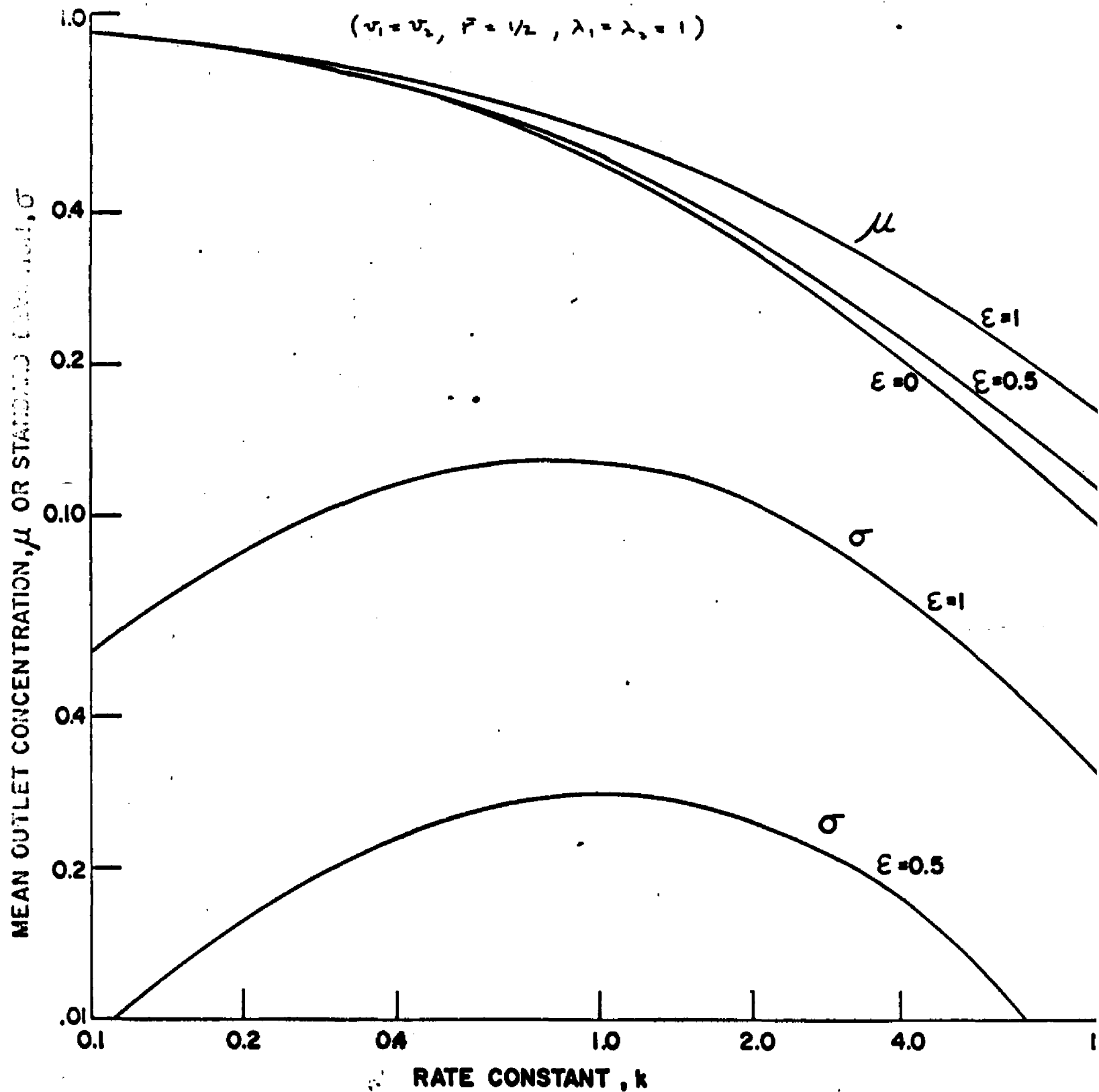


Figure 32. EFFECT OF SWITCHING RATE ON FIRST ORDER REACTION BEHAVIOR OF PARALLEL MODEL

$$(v_1 = v_2, p = 1/2, z = 1, \lambda_1 = \lambda_2)$$

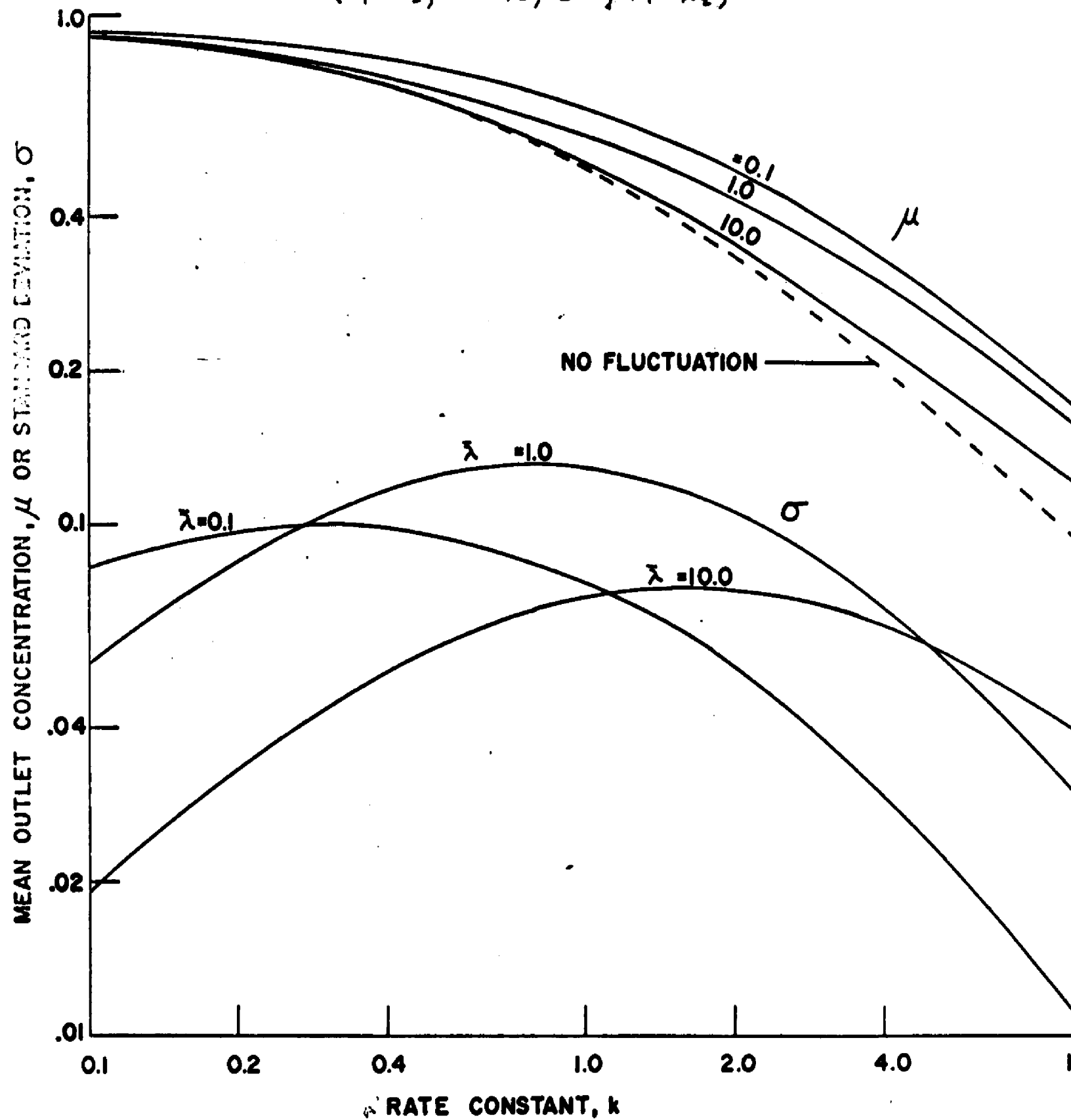
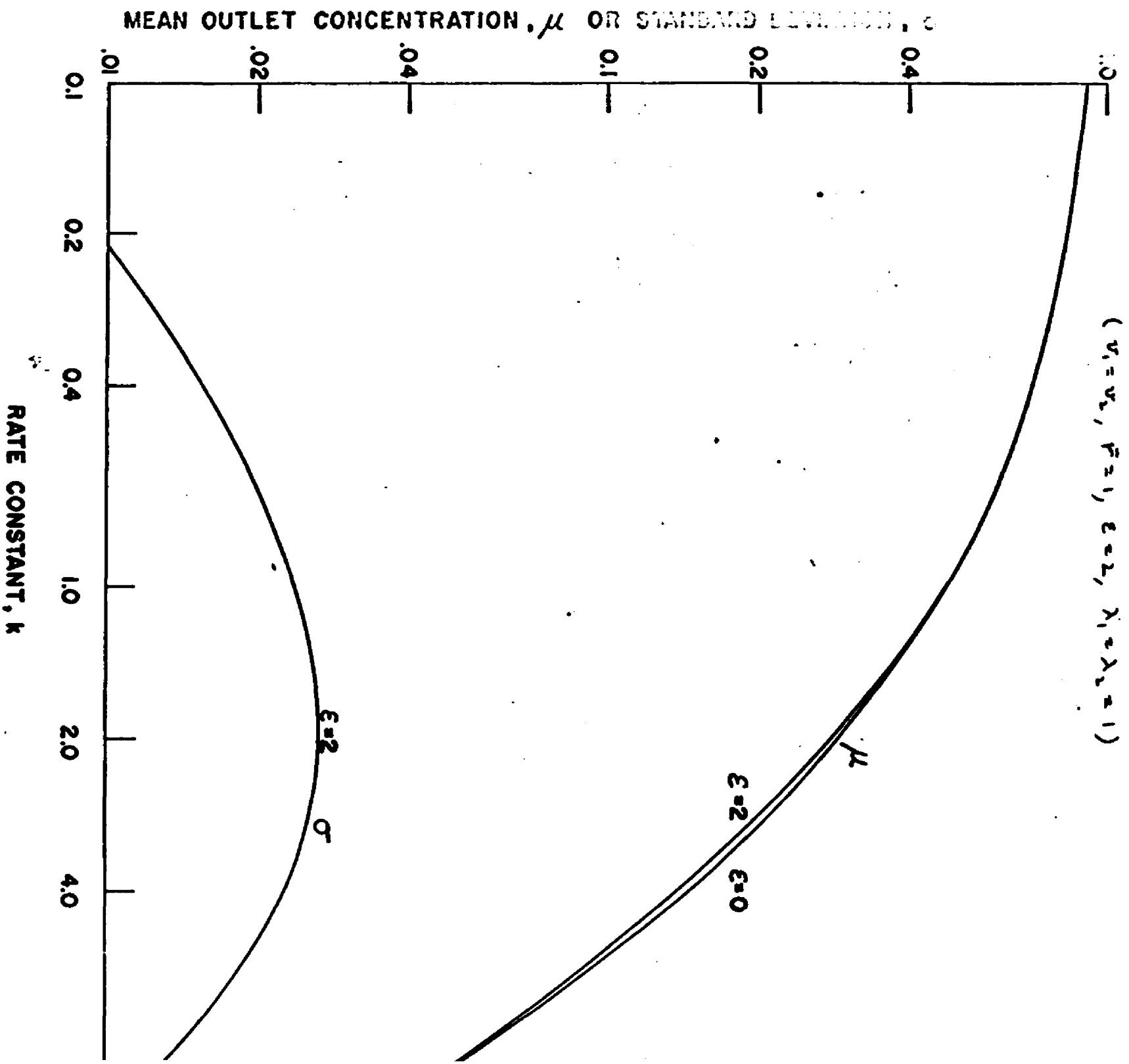


FIGURE 33. FIRST ORDER REACTION BEHAVIOR OF SERIES MODEL



conversion approach that for steady flow. The fluctuations in outlet concentration do not decrease very rapidly, however, with increasing switching rate. It is seen that the fluctuations in output concentration are greatest at values of $\bar{\lambda}$ of about one. Smaller or greater values of $\bar{\lambda}$ do not give σ vs. k curves with as high a peak. The value of k which gives the peak in the σ vs. k curve increases with increasing switching rate. Since the mean conversion for a first order reaction depends only on the first moment of the tracer response, and since the values of the parameters shown for the parallel model make this first moment identical to the single tank case, the curves for conversion shown for the parallel model are identical to those for the single tank model with constant inlet concentration.

The autocorrelation of outlet concentration may be calculated for the series and parallel models by equations similar to (VIII-22) and (VIII-25) for the autocorrelations of the tracer responses. Thus, for the parallel model

$$\begin{aligned} \frac{dq''}{d\tau} = & \sum_i r_i \left\{ \pi_{i1}(\tau) [r_1 m_{11} + (1-r_1) m_{12}] \right. \\ & \left. + \pi_{i2}(\tau) [r_2 m_{21} + (1-r_2) m_{22}] \right\} \\ & - \left(\sum_i r_i + k + \lambda_1 \right) q_{11} + \lambda_2 q_{21} \end{aligned} \quad \text{(VIII-38)}$$

$$\begin{aligned} \frac{dq_{21}}{d\tau} = & \frac{w}{v_1} r_2 \left\{ \pi_{12}(\tau) [r_1 m_{11} + (1-r_1) m_{12}] \right. \\ & \left. + \pi_{22}(\tau) [r_2 m_{21} + (1-r_2) m_{22}] \right\} \\ & + \lambda_1 q_{11} - \left(\frac{w}{v_1} r_2 + k + \lambda_2 \right) q_{21} \end{aligned}$$

$$\begin{aligned} \frac{dq_{12}}{d\tau} = & \frac{w}{v_1} (1-r_1) \left\{ \pi_{11}(\tau) [r_1 m_{11} + (1-r_1) m_{12}] \right. \\ & \left. + \pi_{21}(\tau) [r_2 m_{21} + (1-r_2) m_{22}] \right\} \\ & - \left[\frac{w}{v_2} (1-r_1) + k + \lambda_1 \right] q_{12} + \lambda_2 q_{22} \end{aligned}$$

$$\begin{aligned} \frac{dq_{22}}{d\tau} = & \frac{w}{v_2} (1-r_2) \left\{ \pi_{12}(\tau) [r_1 m_{11} + (1-r_1) m_{12}] \right. \\ & \left. + \pi_{22}(\tau) [r_2 m_{21} + (1-r_2) m_{22}] \right\} \\ & + \lambda_1 q_{12} - \left[\frac{w}{v_2} (1-r_2) + k + \lambda_2 \right] q_{22} \end{aligned}$$

(VIII-38)

with initial conditions given by

$$\begin{aligned}
\tau = 0: \quad q_{11} &= r_1 s_{111} + (1-r_1) s_{112} \\
q_{21} &= r_2 s_{211} + (1-r_2) s_{212} \\
q_{12} &= r_1 s_{112} + (1-r_1) s_{122} \\
q_{22} &= r_2 s_{212} + (1-r_2) s_{222}
\end{aligned}
\tag{VIII-39}$$

Then

$$\langle z(t) z(t+\tau) \rangle = r_1 q_{11} + r_2 q_{21} + (1-r_1) q_{12} + (1-r_2) q_{22}
\tag{VIII-40}$$

The corresponding equations for the series case are

$$\begin{aligned}
\frac{dq_{11}}{d\tau} &= \frac{w}{v_1} [\pi_{11}(\tau) m_{12} + \pi_{21}(\tau) m_{22}] \\
&\quad - \left[\frac{w}{v_1} (1+r_1) + k + \lambda_1 \right] q_{11} + \lambda_2 q_{21} + \frac{w}{v_1} r_1 q_{12} \\
\frac{dq_{21}}{d\tau} &= \frac{w}{v_1} [\pi_{12}(\tau) m_{12} + \pi_{22}(\tau) m_{22}] \\
&\quad + \lambda_1 q_{11} - \left[\frac{w}{v_1} (1+r_2) + k + \lambda_2 \right] q_{21} + \frac{w}{v_1} r_2 q_{22} \\
\frac{dq_{12}}{d\tau} &= - \left[\frac{w}{v_2} (1+r_1) + k + \lambda_1 \right] q_{12} + \lambda_2 q_{22} + \frac{w}{v_2} (1+r_1) q_{11} \\
\frac{dq_{22}}{d\tau} &= \lambda_1 q_{12} - \left[\frac{w}{v_2} (1+r_2) + k + \lambda_2 \right] q_{22} + \frac{w}{v_2} (1+r_2) q_{21}
\end{aligned}
\tag{VIII-41}$$

with initial conditions

$$\begin{aligned} \tau = 0: \quad q_{11} &= s_{112} \\ q_{21} &= s_{212} \\ q_{12} &= s_{122} \\ q_{22} &= s_{222} \end{aligned} \quad (\text{VIII-42})$$

Then

$$\langle z(t) z(t+\tau) \rangle = q_{12} + q_{22} \quad (\text{VIII-43})$$

The autocorrelation of outlet reactant concentration for some typical parameter values is shown in Figures 34 and 35 for the parallel case and in Figure 36 for the series case. Figure 34 is for the same parameter values as used previously. In Figure 35, the ratio of the volume in tank one to the total volume has been changed from 0.5 to 0.677. The curves in the two figures differ markedly. This is due to the fact that when the parallel system is symmetrical, so that the steady-state conversion in either flow state is the same, the effect of the flow fluctuations becomes small as the response time of the system becomes small, which occurs at large values of k . It is seen that in Figure 34 as k becomes large the correlation

Figure 34. AUTOCORRELATION FOR FIRST ORDER REACTION
IN PARALLEL CASE
(symmetrical)

$$(v_1 = v_2, F = 1/2, \epsilon = 1, \lambda_1 = \lambda_2 = 1)$$

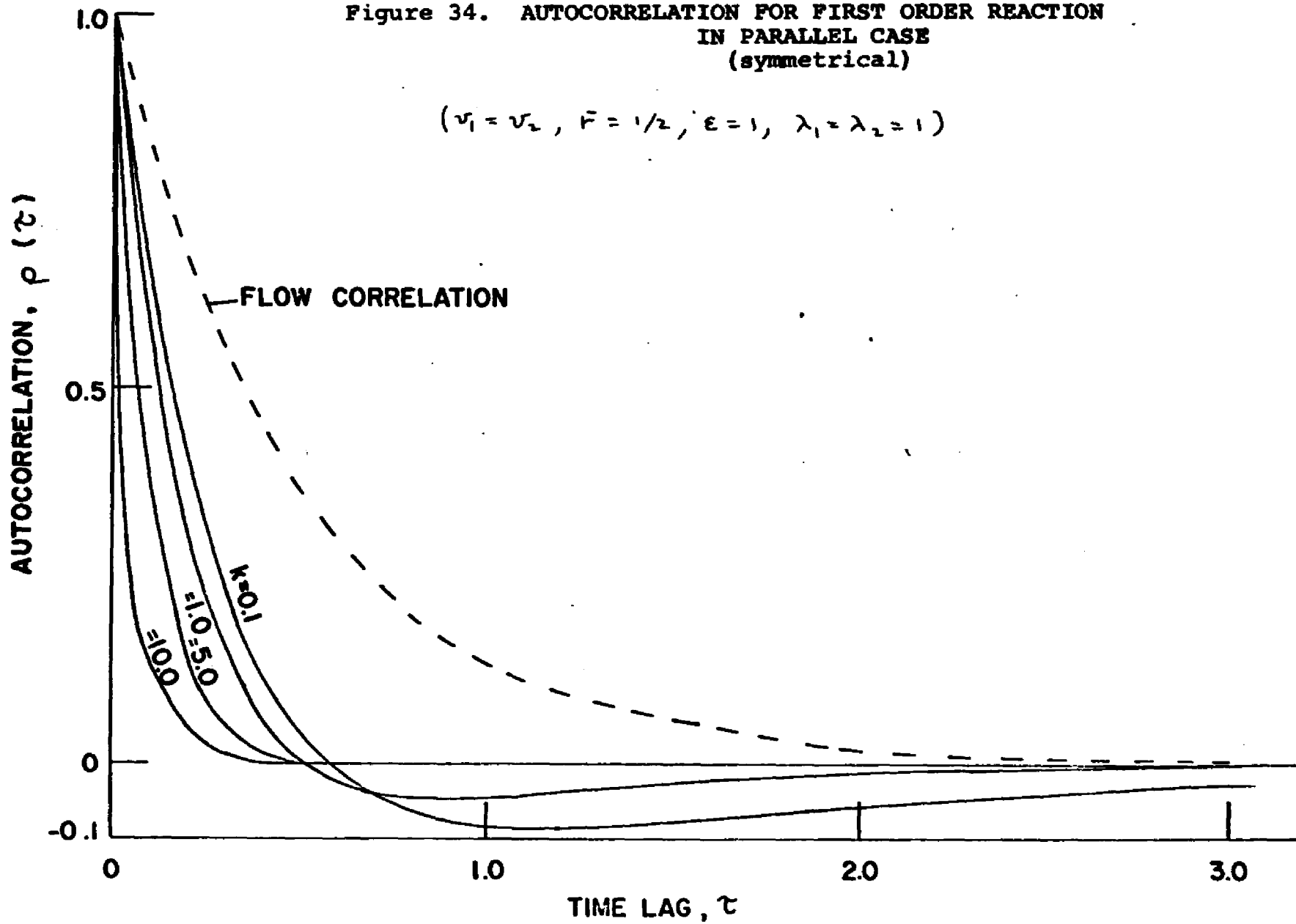
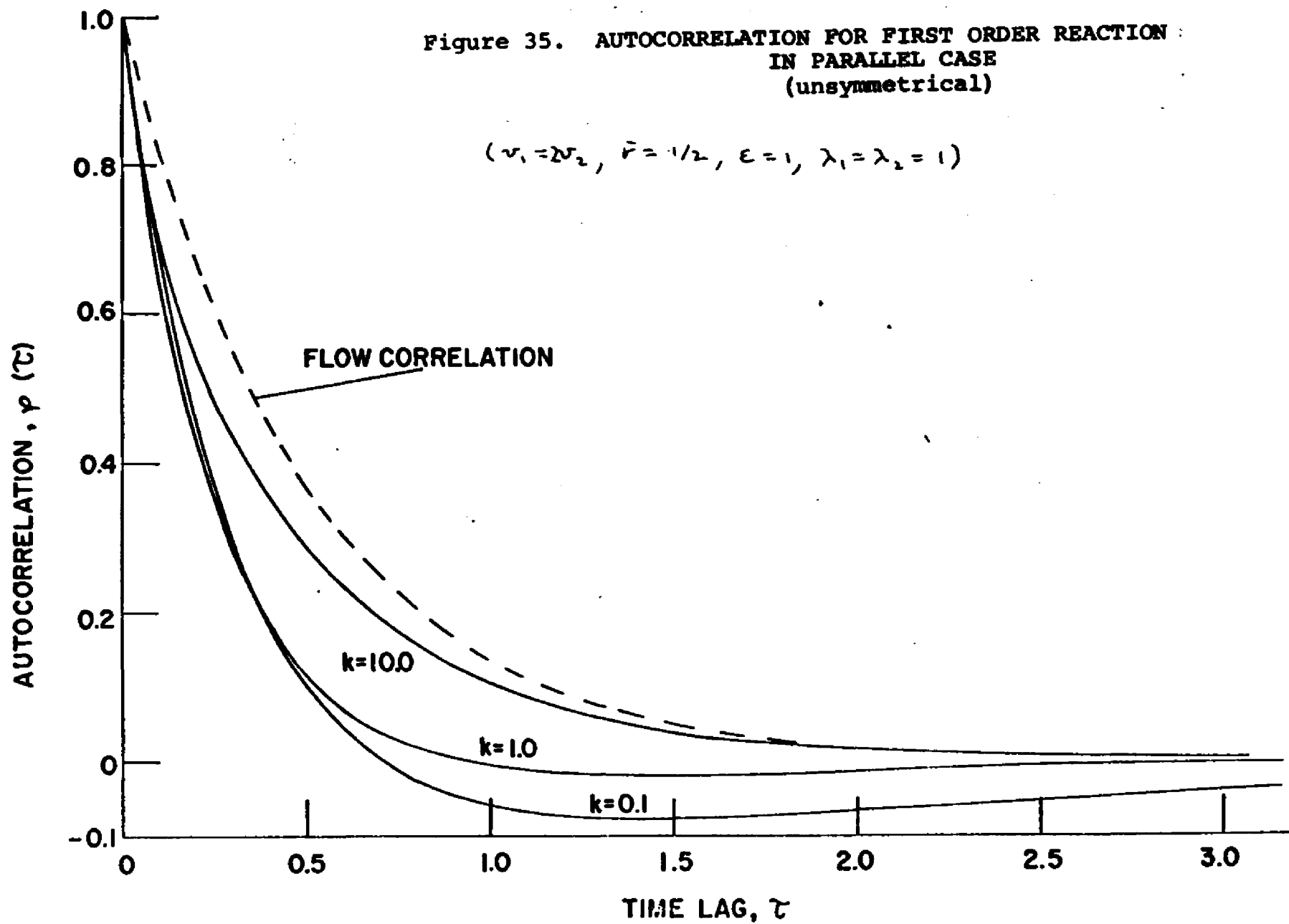
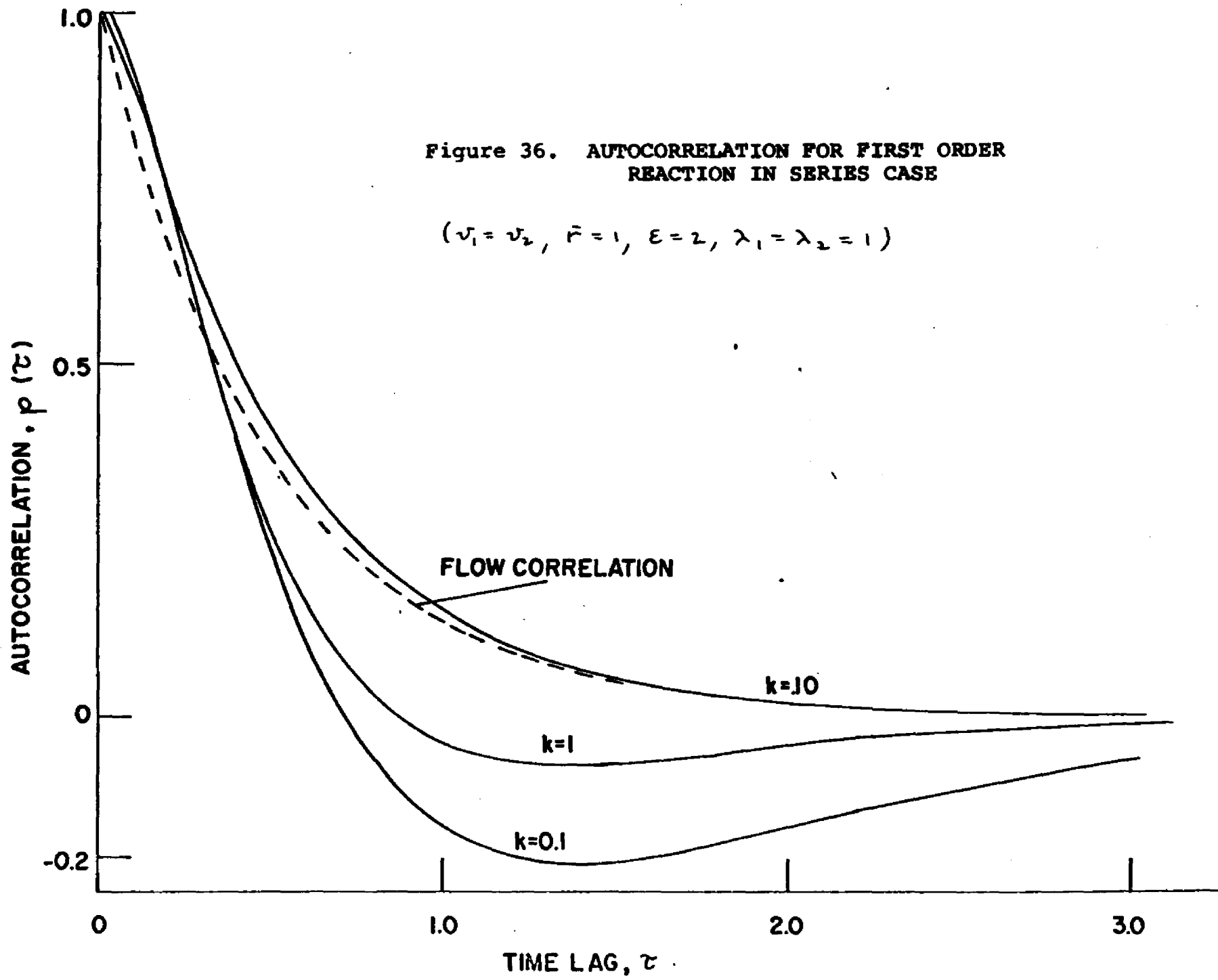


Figure 35. AUTOCORRELATION FOR FIRST ORDER REACTION:
IN PARALLEL CASE
(unsymmetrical)

$$(\nu_1 = 2\nu_2, \bar{v} = 1/2, \epsilon = 1, \lambda_1 = \lambda_2 = 1)$$





function drops to zero rather rapidly. In the asymmetric case, Figure 35, however, the correlation approaches that of the flow states as k becomes large. The curve for $k=0.1$ is rather similar in both cases, indicating that at low values of k it is the lag time of the system itself that becomes important, rather than the switching rate. The series case is seen in Figure 36, to behave in a manner quite similar to the asymmetric parallel case. At high values of k the curves approach the flow correlation.

When the model is used to predict the reaction behavior of a real system, curves such as those in Figures 31-36 could prove useful in analyzing problems in process elements that are coupled to the reaction system. Knowledge of the correlation structure of the disturbances to the process at the design stage allows one to design optimal controllers at the same time as the processing equipment.

D. Stable Regions in Concentration Space

While the solution of the partial differential equations (VIII-30) or (VIII-31) presents some difficulties, some properties of the solutions may be ascertained without actually carrying out the solution. It was shown

in the previous section on single tank reactors that the stationary probability distribution becomes confined to certain regions of the one-dimensional concentration space. This conclusion could be based on the mathematical properties of equation (VII-78) or, alternatively, on a study of possible trajectories in the concentration space.

The second method can be used in the series and parallel cases, provided the trajectories are fairly simple.

For the series and parallel cases, the concentration space is two-dimensional. At each point in the space there are two possible trajectories passing through it, corresponding to the two possible flow states. The trajectories are just the characteristics of the partial differential equations (VIII-30) or (VIII-31), which are always hyperbolic. These curves are relatively easy to calculate, and a careful study of their nature can show which regions of the concentration space have the property that once the system is in this region there is no chance that it will escape from it. The stationary distribution will be concentrated over such regions. In fact it is known quite generally that the characteristics of hyperbolic partial differential equations form the boundaries of regions where the equations have solutions of different analytic character (see, for example, [29]). Since the

concentrations are always between zero and one it is clear that there is a region of concentration space where the probability density is identically zero. The region or regions where the concentration is non-zero must be separated from the zero region by characteristics (or, in this case, trajectories). The problem then reduces to finding which of the trajectories will form the bounds of the stable region.

The procedure that was followed was to first construct the families of trajectories, to then follow an intuitive line of reasoning involving the possible paths the system might take originating from various points in the space, and finally to reinforce these conclusions with a Monte-Carlo computation.

In studying such trajectories it is useful to first derive some general facts concerning their nature. Regardless of the reaction kinetics, the trajectories for either the series or parallel case satisfy equations of the form.

$$\begin{aligned}\frac{dx_1}{dt} &= a_1(x_1, x_2)r + b_1(x_1, x_2) \\ \frac{dx_2}{dt} &= a_2(x_1, x_2)r + b_2(x_1, x_2)\end{aligned}\quad (\text{VIII-44})$$

That is, the derivative functions, $f_1(\mathbf{x}, r)$ and $f_2(\mathbf{x}, r)$, are linear (but not homogeneous) in the flow parameter r .

For each value of r , points which make the right hand sides of (VIII-44) equal to zero are possible steady-state solutions corresponding to r . If these points are plotted for all possible values of r , a locus of steady state solutions is generated. In complex cases this locus may have more than one branch. Points lying on this locus have a special property. The trajectories passing through such a point for any values of r , other than the one for which the point is a steady state, all have the same slope. To see this let (x_1^0, x_2^0) be the point on the steady state locus for $r=r_0$. Then, at the point (x_1^0, x_2^0) , the trajectory for $r=r'$ satisfies

$$\begin{aligned}\frac{dx_1}{dt} &= a_1(x_1^0, x_2^0)(r' - r_0) \\ \frac{dx_2}{dt} &= a_2(x_1^0, x_2^0)(r' - r_0)\end{aligned}\quad (\text{VIII-45})$$

The slope of the trajectory where it crosses the steady state locus is then given by

$$\frac{dx_2}{dx_1} = \frac{a_2(x_1^0, x_2^0)}{a_1(x_1^0, x_2^0)} \quad (\text{VIII-46})$$

which is clearly independent of r' .

For the parallel case with first order kinetics the trajectories satisfy

$$\begin{aligned}\frac{dx_1}{dt} &= \frac{w}{v_1} r x_0 - \left[\frac{w}{v_1} r + k \right] x_1 \\ \frac{dx_2}{dt} &= \frac{w}{v_2} (1-r) x_0 - \left[\frac{w}{v_2} (1-r) + k \right] x_2\end{aligned}\quad (\text{VIII-47})$$

The locus of steady states is then given by

$$x_1 = \frac{x_0}{1 + \frac{kv_1}{rW}}$$

$$x_2 = \frac{x_0}{1 + \frac{kv_2}{(1-r)W}} \quad (\text{VIII-48})$$

Eliminating r between the two equations gives, for the locus,

$$\left[x_1 - \frac{x_0(1 + \frac{kv_2}{W})}{1 + k(\frac{v_1+v_2}{W})} \right] \left[x_2 - \frac{x_0(1 + \frac{kv_1}{W})}{1 + k(\frac{v_1+v_2}{W})} \right]$$

$$= \frac{x_0^2 k^2 \frac{v_1 v_2}{W^2}}{\left[1 + k(\frac{v_1+v_2}{W}) \right]^2}$$

(VIII-49)

This is a hyperbola with vertical and horizontal asymptotes. Along the steady state locus the trajectories passing through it have slope

$$\frac{dx_2}{dx_1} = - \frac{v_1(x_0 - x_2)}{v_2(x_0 - x_1)} \quad (\text{VIII-50})$$

The locus of steady states itself has the slope

$$\frac{dx_2}{dx_1} = - \frac{v_2 \left[r + k \frac{v_1}{W} \right]^2}{v_1 \left[1 - r + k \frac{v_2}{W} \right]^2}$$

(VIII-51)

It is interesting to note that at the point on the steady locus corresponding to $r = \frac{v_1}{v_1 + v_2}$:

$$x_1 = x_2 = \frac{x_0}{1 + k \frac{v_1 + v_2}{W}} \quad (\text{VIII-52})$$

the trajectories are all tangent to the locus. The trajectories are found by solving equation (VIII-47). This gives

$$x_1 = \frac{x_0}{1 + \frac{k v_1}{r W}} + c_1 e^{-\left[\frac{r W}{v_1} + k\right]t}$$

$$x_2 = \frac{x_0}{1 + \frac{k v_2}{(1-r)W}} + c_2 e^{-\left[\frac{(1-r)W}{v_2} + k\right]t}$$
(VIII-53)

where c_1 and c_2 depend on the starting point. The time, t , may be eliminated from (VIII-53) to give

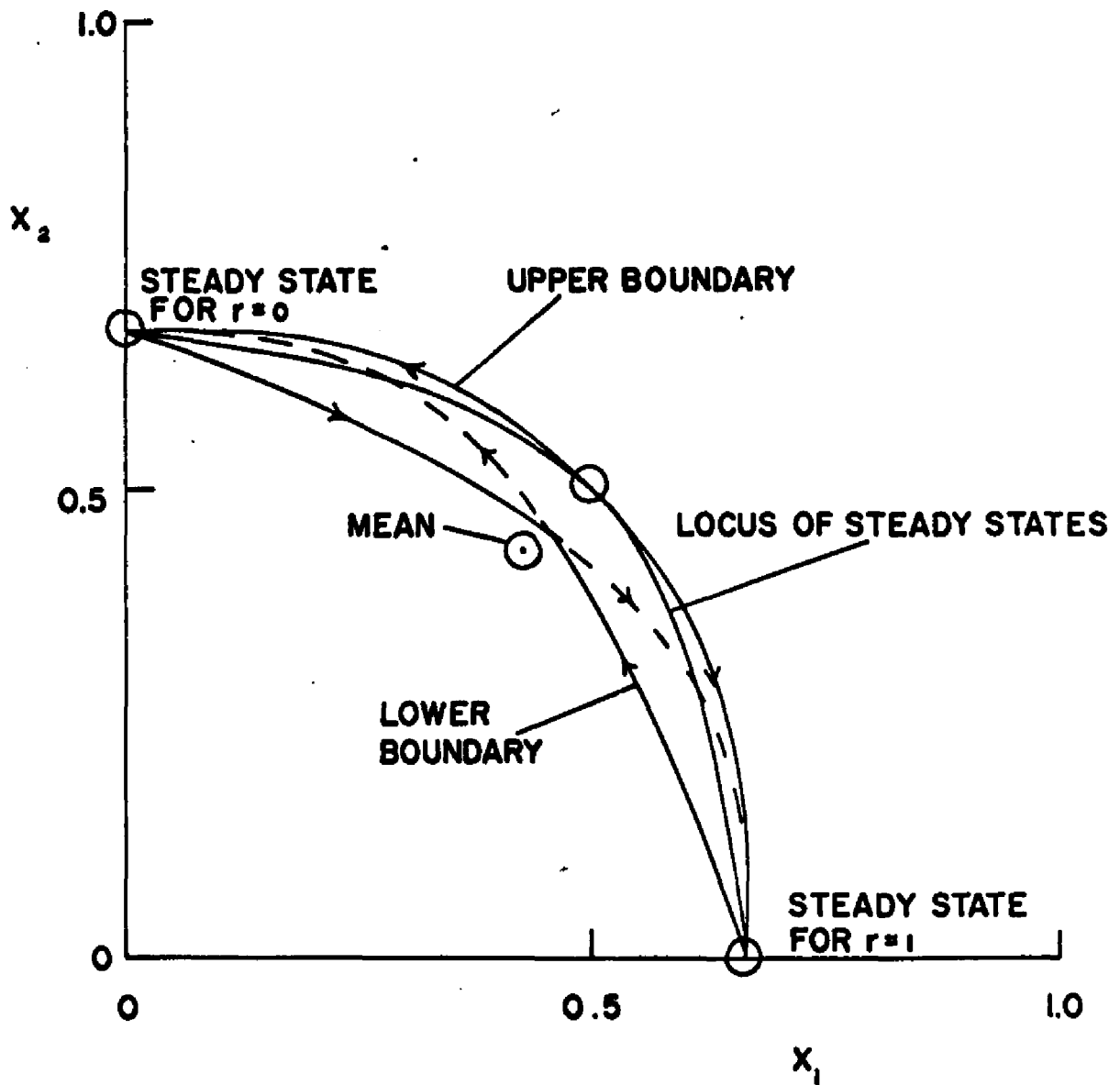
$$\left[x_1 - \frac{x_0}{1 + \frac{k v_1}{r W}} \right]^{\frac{1}{\frac{r W}{v_1} + k}} = c_3 \left[x_2 - \frac{x_0}{1 + \frac{k v_2}{(1-r)W}} \right]^{\frac{1}{\frac{(1-r)W}{v_2} + k}}$$
(VIII-54)

for the trajectories. Equation (VIII-54) defines a one-parameter family of trajectories for any fixed flow state r . Two families of trajectories are of importance in any given case, corresponding to r_1 and r_2 , the two flow states of the system.

In Figure 37, the stable region is shown for the parallel case for typical parameter values. The lower boundary is formed by two trajectories, one of which starts

Figure 37. STABLE REGION FOR PARALLEL CASE

$$(v_1 = v_2, k = 1, r_1 = 0, r_2 = 1)$$



at the steady state corresponding to r_1 and the other of which starts at the steady state corresponding to r_2 .

The upper boundary is formed by two trajectories starting at the point given by equation (VIII-52). The directions of the trajectories are shown by arrows. Note that the mean concentration of the two tanks define a point lying outside of the stable region.

For the series case with first order kinetics, the trajectories satisfy

$$\begin{aligned}\frac{dx_1}{dt} &= \frac{W}{v_1} x_0 - \left[\frac{W}{v_1} (1+r) + k \right] x_1 + \frac{W}{v_1} r x_2 \\ \frac{dx_2}{dt} &= \frac{W}{v_2} (1+r) x_1 - \left[\frac{W}{v_2} (1+r) + k \right] x_2\end{aligned}\quad (\text{VIII-55})$$

The locus of steady states is then given by

$$\begin{aligned}x_1 &= x_0 \frac{\frac{W}{v_1} k + \frac{W^2}{v_1 v_2} (1+r)}{k^2 + (1+r) \left(\frac{W}{v_1} + \frac{W}{v_2} \right) k + \frac{W^2}{v_1 v_2} (1+r)} \\ x_2 &= x_0 \frac{\frac{W^2}{v_1 v_2} (1+r)}{k^2 + (1+r) \left(\frac{W}{v_1} + \frac{W}{v_2} \right) k + \frac{W^2}{v_1 v_2} (1+r)}\end{aligned}\quad (\text{VIII-56})$$

Eliminating r between the two equations gives, for the locus,

$$k \frac{W}{v_2} x_1 + \left[k \frac{W}{v_1} + \frac{W^2}{v_1 v_2} \right] x_2 = \frac{W^2}{v_1 v_2} x_0 \quad (\text{VIII-57})$$

which is a straight line of slope

$$\frac{dx_2}{dx_1} = - \frac{k \frac{w}{v_1}}{1 + k \frac{w}{v_1}} \quad (\text{VIII-58})$$

Along the steady state locus, the trajectories passing through it have slope

$$\frac{dx_2}{dx_1} = - \frac{v_1}{v_2} \quad (\text{VIII-59})$$

which, it is seen, is independent of position on the locus. These slopes can only be equal if $v_1=0$. Otherwise the slope of the trajectories at the steady state locus is always more negative than the slope of the locus. Solving equation (VIII-55) gives, for the trajectories,

$$\begin{aligned} x_1 - x_1^{\infty} &= c_1 \left\{ \frac{b_1 e^{b_1 t} - b_2 e^{b_2 t}}{b_1 - b_2} - \left[\frac{w}{v_1} (1+r) + k \right] \frac{e^{b_1 t} - e^{b_2 t}}{b_1 - b_2} \right\} \\ &\quad + c_2 \frac{w}{v_1} r \frac{e^{b_1 t} - e^{b_2 t}}{b_1 - b_2} \\ x_2 - x_2^{\infty} &= c_1 \frac{w}{v_2} (1+r) \frac{e^{b_1 t} - e^{b_2 t}}{b_1 - b_2} \\ &\quad + c_2 \left\{ \frac{b_1 e^{b_1 t} - b_2 e^{b_2 t}}{b_1 - b_2} - \left[\frac{w}{v_2} (1+r) + k \right] \frac{e^{b_1 t} - e^{b_2 t}}{b_1 - b_2} \right\} \end{aligned} \quad (\text{VIII-60})$$

where b_1 and b_2 are the roots of

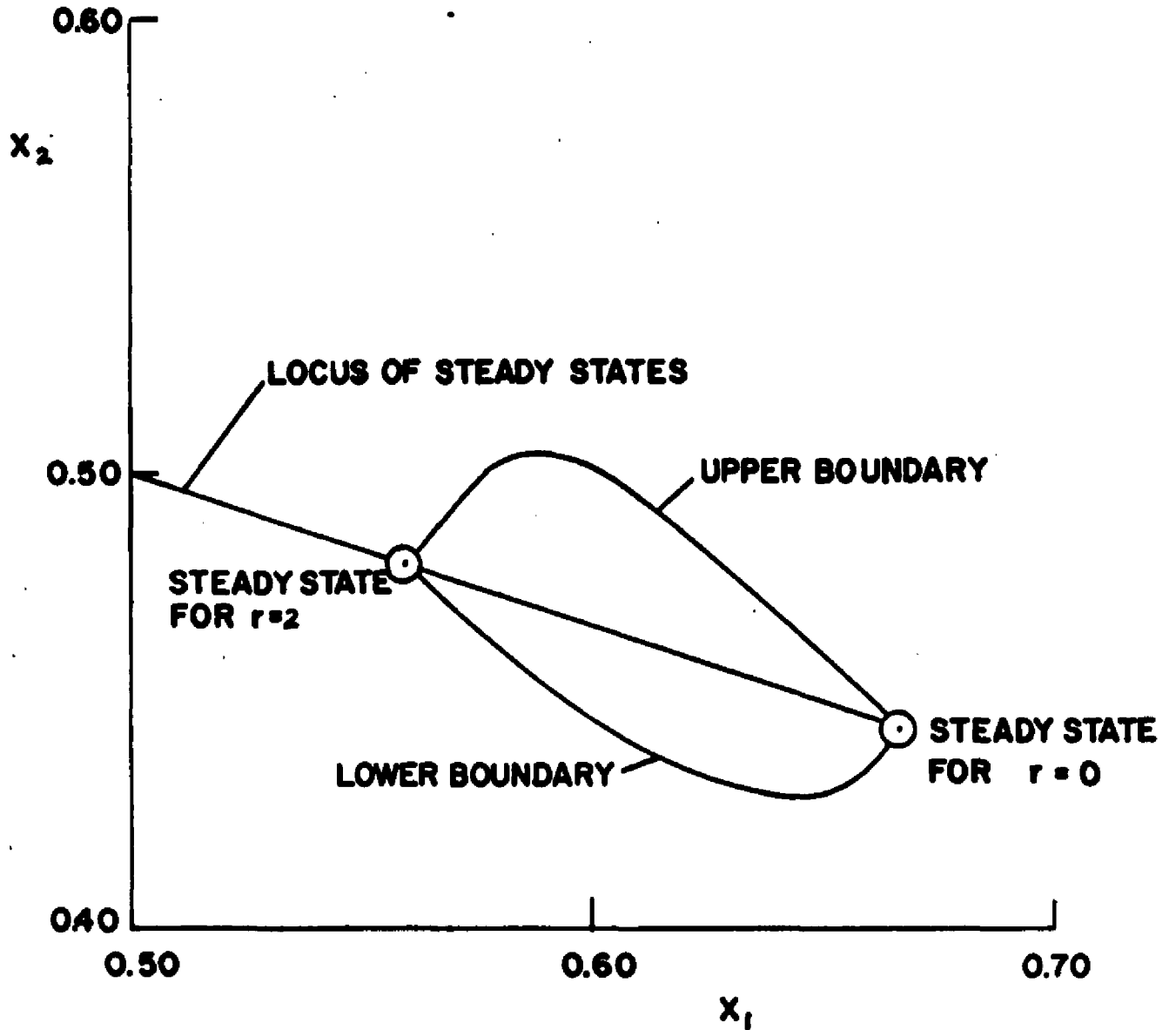
$$b^2 + \left[(1+r) \left(\frac{w}{v_1} + \frac{w}{v_2} \right) + 2k \right] b + k^2 + (1+r) \left(\frac{w}{v_1} + \frac{w}{v_2} \right) k + \frac{w^2}{v_1 v_2} (1+r) = 0$$

(VIII-61)

The quantities x_1^{∞} and x_2^{∞} are the final values, given by (VIII-56).

The stable region for the series case is shown in Figure 38. The situation is somewhat simpler than in the parallel case, only two trajectories being required to define the boundary. Comparison of Figure 38 with Figure 37 shows that the stable region for the series case is much smaller than that for the parallel case (note difference in scale). This is in line with the much smaller variance noted for the series case.

Figure 38. STABLE REGION FOR SERIES CASE
($v_1 = v_2$, $k = 1$, $r_1 = 0$, $r_2 = 2$)



IX. Fluidized Bed Model

A. Formulation

One of the practical cases where the random fluctuations in flow pattern are quite noticeable is the fluidized bed reactor. It is found in practice that a large fraction of the total gas flow passes through the bed in the form of bubbles. When the fluidized particles act as catalyst for the chemical reactions, the mixing between the bubbles and the particulate phase is important. In the absence of such mixing, the gas in the bubbles would bypass the catalyst entirely. It is also observed that such systems exhibit pronounced random fluctuations in their mixing properties due to the randomness of the bubble motion. Thus, the fluidized bed reactor is a good candidate for stochastic modeling.

Various steady state models of fluidized beds have been proposed [2, 26, 27], based on the two-phase picture of such systems. Common to these models is the assumption, based on observation, that the particulate phase behaves as an incompressible fluid whose volume is the same as that of the bed at incipient fluidization, and that the amount of gas passing through the bed in the form of bubbles is just the excess of the total gas flow over that at incipient

fluidization. The models differ in the assumed mixing between and within the phases. For the purposes of this study, the simplified model shown in Figure 39 will be assumed. In this model the particulate phase is assumed to be well-mixed. The quantity v_2 is the interstitial volume of this phase. The total flow rate, w , is constant with time, as is the fraction of the total flow which travels in the form of bubbles, r . The bubble phase is assumed to be of constant volume, v_1 , and is also well-mixed. The mixing flow rate, w_m , is assumed to fluctuate with time, however. It may be noted that while the assumption of perfect mixing in the particulate phase seems reasonable, on the basis of the observed uniformity of temperature in such systems, that of perfect mixing in the bubble phase seems doubtful. In fact it is often assumed that the bubble phase is in a condition of plug flow. It will be shown, however, that many properties of the system are independent of this assumption, so it will be made for convenience. The assumption that the bubble phase is of constant volume results from defining the boundaries of the reactor appropriately.

The equations of change for the system of Figure 39 are

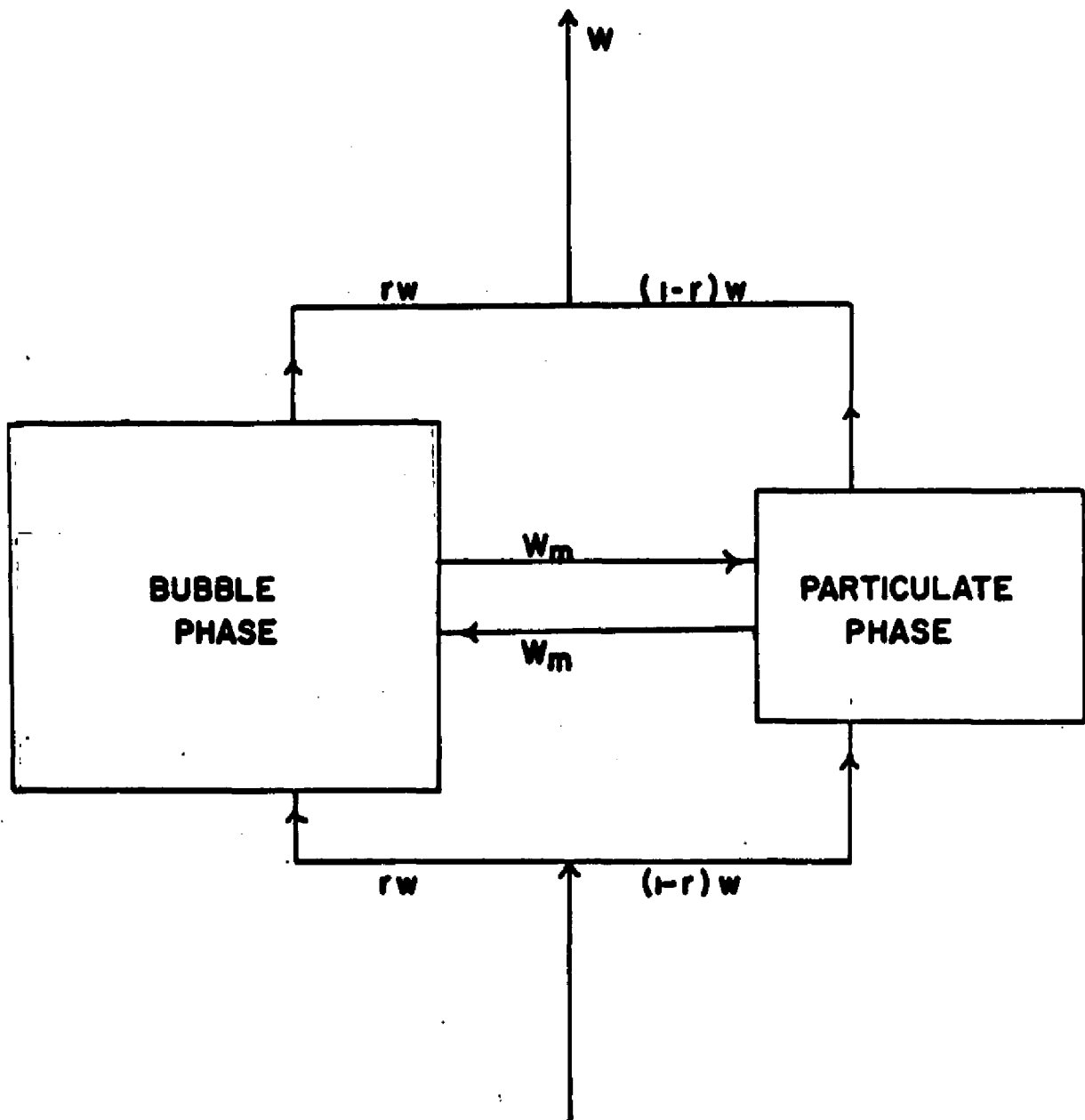


Figure 39. MODEL FOR FLUIDIZED-BED REACTOR

$$v_1 \frac{dx_1}{dt} = rWx_0 - [rW + W_m]x_1 + W_mx_2 \quad (\text{IX-1})$$

$$v_2 \frac{dx_2}{dt} = (1-r)Wx_0 + W_mx_1 - [(1-r)W + W_m]x_2 - v_2 R(x_2)$$

$$z = rx_1 + (1-r)x_2 \quad (\text{IX-2})$$

where $R(x)$ is the reaction rate expression. It is assumed here that only one reaction occurs and that it occurs only in the particulate phase. The concentrations of reactant in the bubble phase and the particulate phase are x_1 and x_2 respectively. For tracer experiments, $R(x)$ is just zero. The quantity z is the outlet concentration.

B. Steady Flow Behavior

Before discussing the effects of fluctuations in W_m on the system behavior, it is useful to first derive some properties of the system with constant w_m . Under this condition the model is just another in the general category previously mentioned, but the effect of fluctuations can only be made clear by comparison with this steady behavior. Also, by analyzing the steady model from the point of view developed for the stochastic models some interesting results are discovered.

Because the reaction takes place, in the model, only in tank 2, the residence time distribution of the system is of minor importance compared to the contact time distribution of gas particles with the particulate phase. Indeed it was for the purpose of analyzing the fluidized bed model that this concept was introduced in section III-D. One of the difficulties with using tracer experiments to study the properties of such systems is the fact that an experiment performed with a tracer that does not interact with the solid particles can furnish information only about the residence time distribution. It is therefore interesting to compare the two distributions.

The residence time distribution is obtained by solving equations (IX-1) with inlet concentration, $x_0(t)$, given by

$$x_0(t) = \delta(t) \quad (\text{IX-3})$$

and with x_1 and x_2 initially zero. The outlet concentration x will then be the residence time density function. This is found to be

$$f(t) = w \left[\frac{r^2}{v_1} + \frac{(1-r)^2}{v_2} \right] \frac{b_1 e^{b_1 t} - b_2 e^{b_2 t}}{b_1 - b_2} - \left\{ w^2 \left[\frac{r^3}{v_1^2} + \frac{(1-r)^3}{v_2^2} \right] + w w_m \left[\frac{r}{v_1} - \frac{(1-r)}{v_2} \right]^2 \right\} \frac{e^{b_1 t} - e^{b_2 t}}{b_1 - b_2} \quad (\text{IX-4})$$

where b_1 and b_2 are the two roots of

$$b^2 + \left[\frac{rw}{v_1} + \frac{(1-r)w}{v_2} + \frac{w_m}{v_1} + \frac{w_m}{v_2} \right] b + \frac{r(1-r)w^2}{v_1 v_2} + \frac{w w_m}{v_1 v_2} = 0 \quad (\text{IX-5})$$

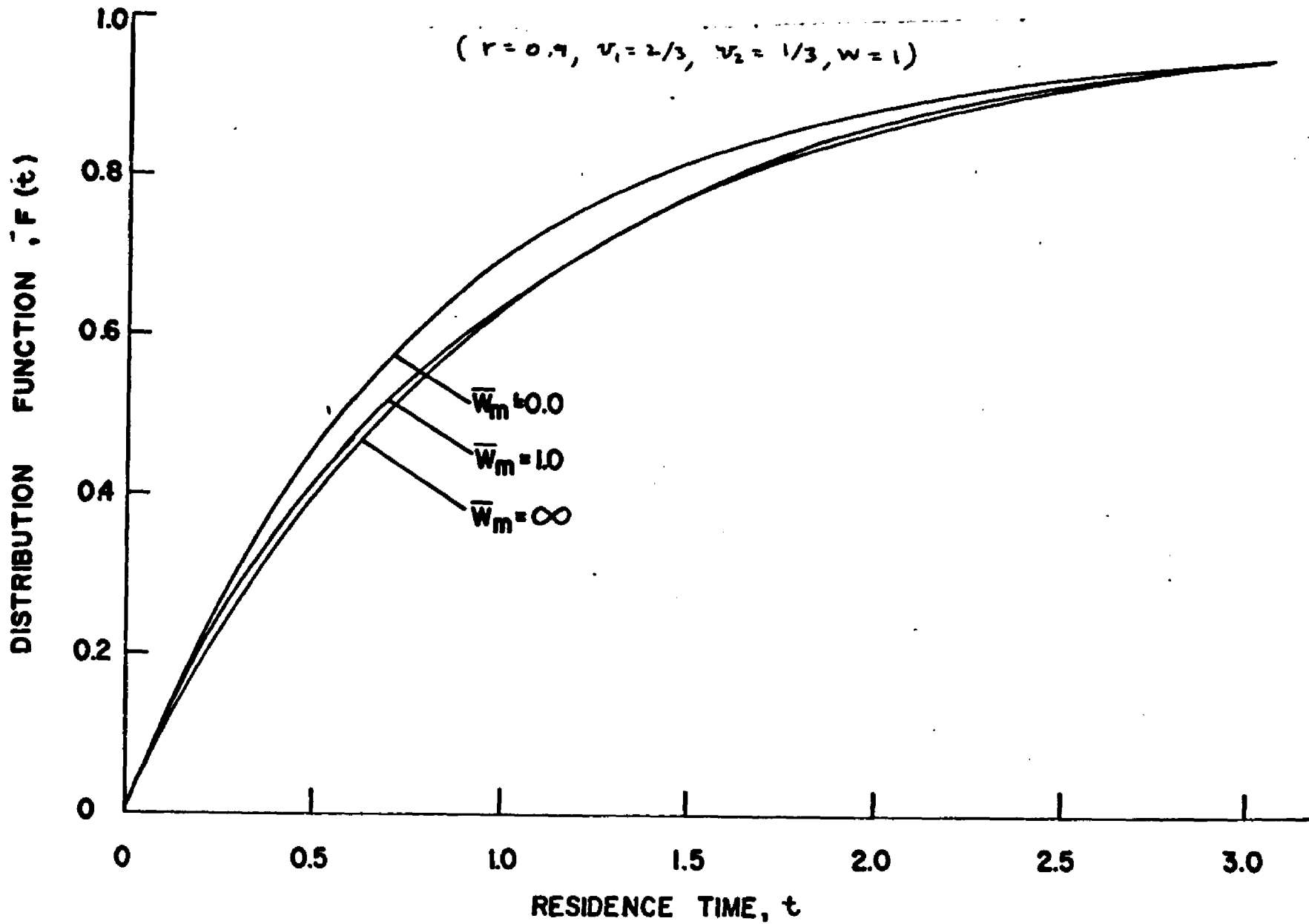
The corresponding distribution function, $F(t)$, is just the integral of equation (IX-4). This is plotted in Figure 40 for typical values of the parameters. The value of $r=0.9$ corresponds to a ratio $\frac{U}{U_0}$ of 10, where U_0 is the superficial gas velocity at incipient fluidization, and U is the superficial gas velocity at the system conditions. The ratio of the two volumes corresponds to a porosity of 0.5 in the particulate phase, and ratio of bed height to bed height at incipient fluidization, $\frac{H}{H_0}$, of 2. These values are thought to be typical of commercial fluidized beds. The values $v_1+v_2=w=1$ are chosen by assuming appropriate scale factors. Under these conditions the mean residence time is equal to one.

The three curves shown are for three values of the mixing flow rate, w_m , covering the range from zero to infinity. It is seen that the residence time distribution is only slightly affected by changes in w_m .

The contact time density function, $f_c(\theta)$, is calculated from equations corresponding to (III-29) and (III-30),

Figure 40. RESIDENCE TIME DISTRIBUTION OF
FLUIDIZED-BED MODEL

($r = 0.9$, $v_1 = 2/3$, $v_2 = 1/3$, $w = 1$)



which become, in this case,

$$f_c(\theta) = \frac{rW}{v_1} g_1(\theta) + \frac{(1-r)W}{v_2} g_2(\theta) \quad (\text{IX-6})$$

and

$$0 = r\delta(\theta) - \left[r\frac{W}{v_1} + \frac{W_m}{v_1} \right] g_1(\theta) + \frac{W_m}{v_2} g_2(\theta) \quad (\text{IX-7})$$

$$\frac{dg_2(\theta)}{d\theta} = (1-r)\delta(\theta) + \frac{W_m}{v_1} g_1(\theta) - \left[\frac{(1-r)W}{v_2} + \frac{W_m}{v_1} \right] g_2(\theta)$$

with $g_2(0)=0$. The solution to these equations is

$$f_c(\theta) = r_b \delta(\theta) + \frac{W}{v_2} (1-r_b)^2 e^{-\frac{W}{v_2} (1-r_b) \theta} \quad (\text{IX-8})$$

where r_b is given by

$$r_b = \frac{r^2 W}{rW + W_m} \quad (\text{IX-9})$$

The quantity r_b above is just the fraction of gas which bypasses the particulate phase entirely, and thus has a zero contact time. When $w_m=0$, it is seen that $r_b=r$, meaning that when there is no mixing between the phases, all the gas that passes through the system in the form of bubbles bypasses the particulate phase completely. The corresponding distribution function, $F_c(t)$, which is just the integral of (IX-8), is plotted in Figure 41 for the same system as was used in Figure 40. For these values,

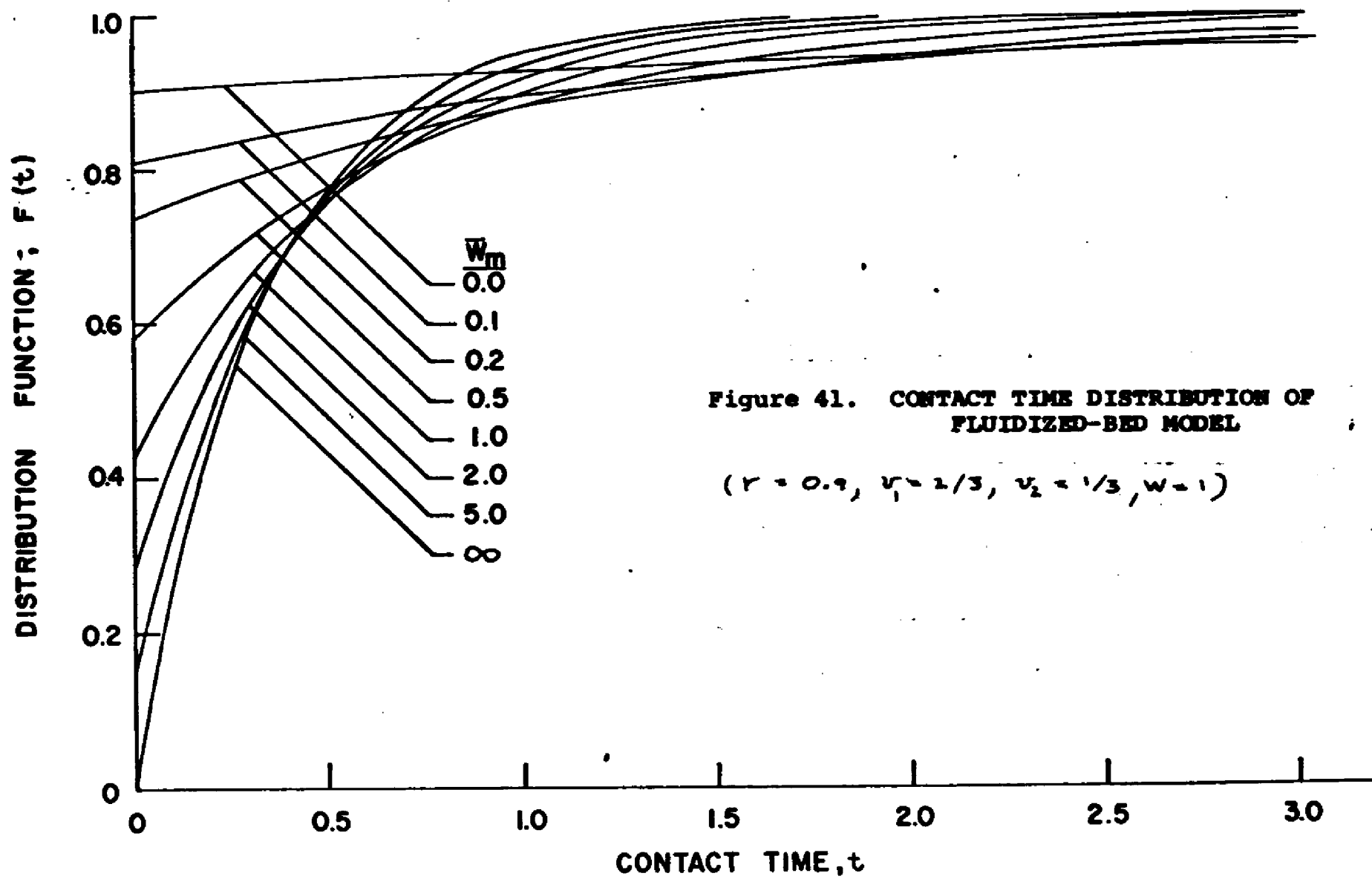


Figure 41. CONTACT TIME DISTRIBUTION OF FLUIDIZED-BED MODEL

$(r = 0.9, v_1 = 2/3, v_2 = 1/3, w = 1)$

the mean contact time, \bar{t}_c/w , is equal to 0.333. Comparison of Figure 40 and 41 shows quite clearly that while the mixing rate, w_m , has only a slight effect on the residence time distribution, it has a pronounced effect on the contact time distribution.

The contact time distribution of this system is closely related to its reaction behavior. Thus the conversion for a single first order reaction is just the Laplace transform of $f_c(\theta)$. The conversion and selectivity of complex first order systems are also determined by this function. Finally, for many reactions, the method of Zwietering [7] can be used to find bounds on conversion on the basis of $f_c(\theta)$. Since such large differences in $f_c(\theta)$, as shown in Figure 41, are consistent with such slight differences in $f(t)$, the residence time distribution, it must be concluded that measurements of $f(t)$, that is tracer experiments performed with non-interacting tracer, where the tracer is introduced in the inlet and is measured in the outlet stream, provide a very poor basis on which to construct a model of the system's reactor performance.

The steady conversion for a first order reaction catalyzed by the solid particles can be calculated from

equations (IX-1) by setting the time derivatives equal to zero and $R(x)=kx$, or by taking the Laplace transform of $f_c(\theta)$. The resulting fraction of unconverted reactant is then given by

$$\frac{M}{X_0} = r_b + \frac{(1-r_b)^2}{1-r_b + k \frac{V_p}{W}} \quad (\text{IX-10})$$

It is interesting to note that this expression is identical to that derived by Davidson and Harrison [26] by assuming plug flow in the bubble phase and complete mixing in the particulate phase. Only the expression for r_b , the bypass fraction, in terms of the system parameters is different, being given in their work by

$$r_b = r e^{-N} \quad (\text{IX-11})$$

where N is the number of transfer units. In fact, as long as the flows are steady, it can be shown that the contact time distribution for the well-mixed particulate phase is given by equation (IX-8) regardless of the nature of the mixing processes in the bubble phase. This is seen by noting that whenever the set of states A consists of only a single state, the system of equations (III-30) reduces to a single linear differential equation. Its solution must then be of the form

$$f_c(\theta) = r_b \delta(\theta) + a e^{b\theta} \quad (\text{IX-12})$$

where a and b are constants. It is known, however, that the integral of $f_c(\theta)$ is one, and that the mean contact time is $\frac{V}{W}$. These two conditions determine a and b .

This fact points up another difficulty in using tracer experiments for studying such systems, namely, that while the reactor performance is relatively insensitive to the nature of the mixing in the bubble phase, the residence-time distribution is just as sensitive to these mixing processes as to those occurring within the particulate phase and between the two phases, so that different assumptions about the mixing in the bubble phase would allow very different conclusions about the particulate phase and the interphase mixing, based on such experiments. On the other hand, for purposes of studying the reaction behavior of such models, the assumption used here, that the bubble phase is well-mixed, is seen to be of minor importance.

The unconverted fraction given by equation (IX-10) is plotted in Figure 42. It is seen there that the mixing rate, w_m , has a very large effect on first order conversion, substantiating the conclusion about the importance of this parameter. At each value of w_m the unconverted fraction approaches an asymptotic value as k , the rate constant,

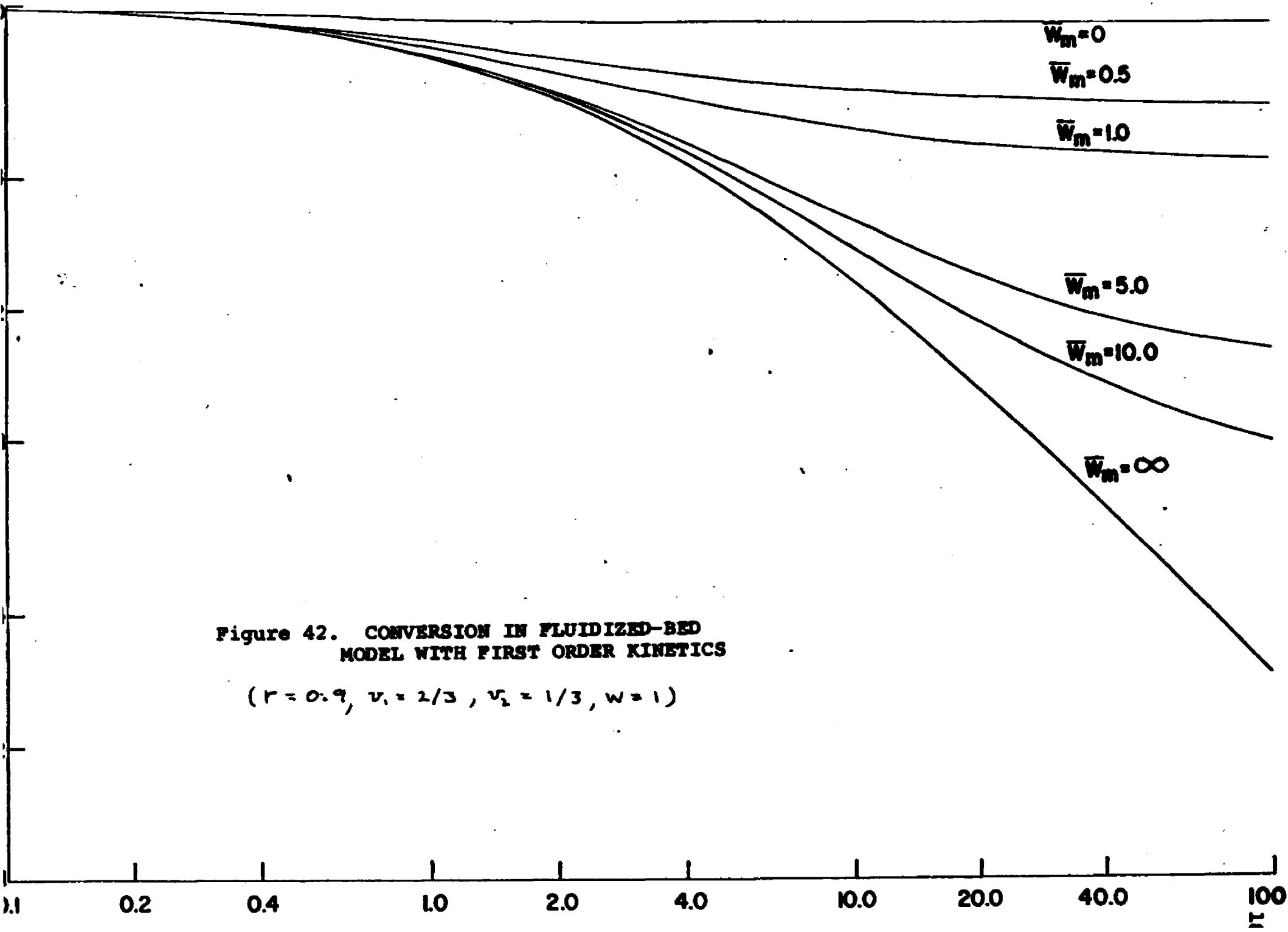


Figure 42. CONVERSION IN FLUIDIZED-BED
MODEL WITH FIRST ORDER KINETICS

$$(r = 0.9, v_1 = 2/3, v_2 = 1/3, w = 1)$$

goes to infinity. This value is just r_b , the bypass fraction.

Another point that emerges in that equation (IX-8) for the contact time distribution contains only one unknown parameter, r_b . In general, w and v_2 will be known in advance. Thus, if one is willing to assume that the particulate phase is well mixed and that the fluctuations in the rate of exchange between the two phases is unimportant, a determination of single quantity r_b can be used to estimate the contact time distribution. This quantity can be measured by carrying out a fast reaction in the system or by using a tracer that is completely absorbed on the solid particles.

C. Behavior with Fluctuating Flow

It will now be assumed that the mixing flow, w_m , fluctuates by switching between two values, w_{m1} and w_{m2} , in the same way as in previous sections. Under these conditions, the equations for the contact time distribution, (III-29) and (III-30), become

$$f_c(\theta) = \frac{rw}{v_1} g_{11}(\theta) + \frac{rw}{v_1} g_{21}(\theta) + \frac{(1-r)w}{v_2} g_{12}(\theta) + \frac{(1-r)w}{v_2} g_{22}(\theta) \quad (\text{IX-13})$$

and

$$0 = r\delta(\theta) - \left[\frac{rw}{v_1} + \frac{w_{m1}}{v_1} + \lambda_1 \right] g_{11}(\theta) + \lambda_2 g_{21}(\theta) + \frac{w_{m1}}{v_2} g_{12}(\theta)$$

$$0 = r\delta(\theta) + \lambda_1 g_{11}(\theta) - \left[\frac{rw}{v_1} + \frac{w_{m2}}{v_1} + \lambda_2 \right] g_{21}(\theta) + \frac{w_{m2}}{v_2} g_{22}(\theta)$$

$$\frac{dg_{12}(\theta)}{d\theta} = (1-r)\delta(\theta) + \frac{w_{m1}}{v_1} g_{11}(\theta) - \left[\frac{(1-r)w}{v_2} + \frac{w_{m1}}{v_2} + \lambda_1 \right] g_{12}(\theta) + \lambda_2 g_{22}(\theta)$$

$$\frac{dg_{22}(\theta)}{d\theta} = (1-r)\delta(\theta) + \frac{w_{m2}}{v_1} g_{21}(\theta) + \lambda_1 g_{12}(\theta) - \left[\frac{(1-r)w}{v_2} + \frac{w_{m2}}{v_2} + \lambda_2 \right] g_{22}(\theta)$$

(IX-14)

with $g_{12}(0) = g_{22}(0) = 0$. To find the residence time distribution the zeros on the left of the first two equations of (IX-14) are replaced by $\frac{dg_{11}}{d\theta}$ and $\frac{dg_{21}}{d\theta}$ respectively.

It is found again that $f_c(\theta)$ contains an atom of probability at zero contact time which is the bypass fraction of the system. For the fluctuating case, this fraction is given by

$$r_b = \frac{r^2 w}{rw + \bar{w}_m} \left\{ \frac{1}{1 - \frac{\bar{p}_1 \bar{p}_2 \epsilon^2}{(rw + \bar{w}_m)[rw + \bar{w}_m + \epsilon(\bar{p}_2 - \bar{p}_1) + v_1(\lambda_1 + \lambda_2)]} \right\}$$

(IX-15)

where $\epsilon = w_{m1} - w_{m2}$ and \bar{w}_m is the mean mixing flow.

Comparison of (IX-15) with (IX-9) shows that the bypass

fraction with fluctuations is always greater than that without for the same mean mixing rate, and that at high switching rates ($\lambda_1 + \lambda_2 \rightarrow \infty$) the two become equal. To illustrate the effect of fluctuations on r_b , this quantity is plotted for some values of the parameters in Figures 43 and 44. In Figure 43, the quantity $\frac{\epsilon}{w_m}$ has been given its maximum allowable value. In general, to keep the flow rates positive,

$$-\frac{1}{\bar{p}_2} \leq \frac{\epsilon}{w_m} \leq \frac{1}{\bar{p}_1} \quad (\text{IX-16})$$

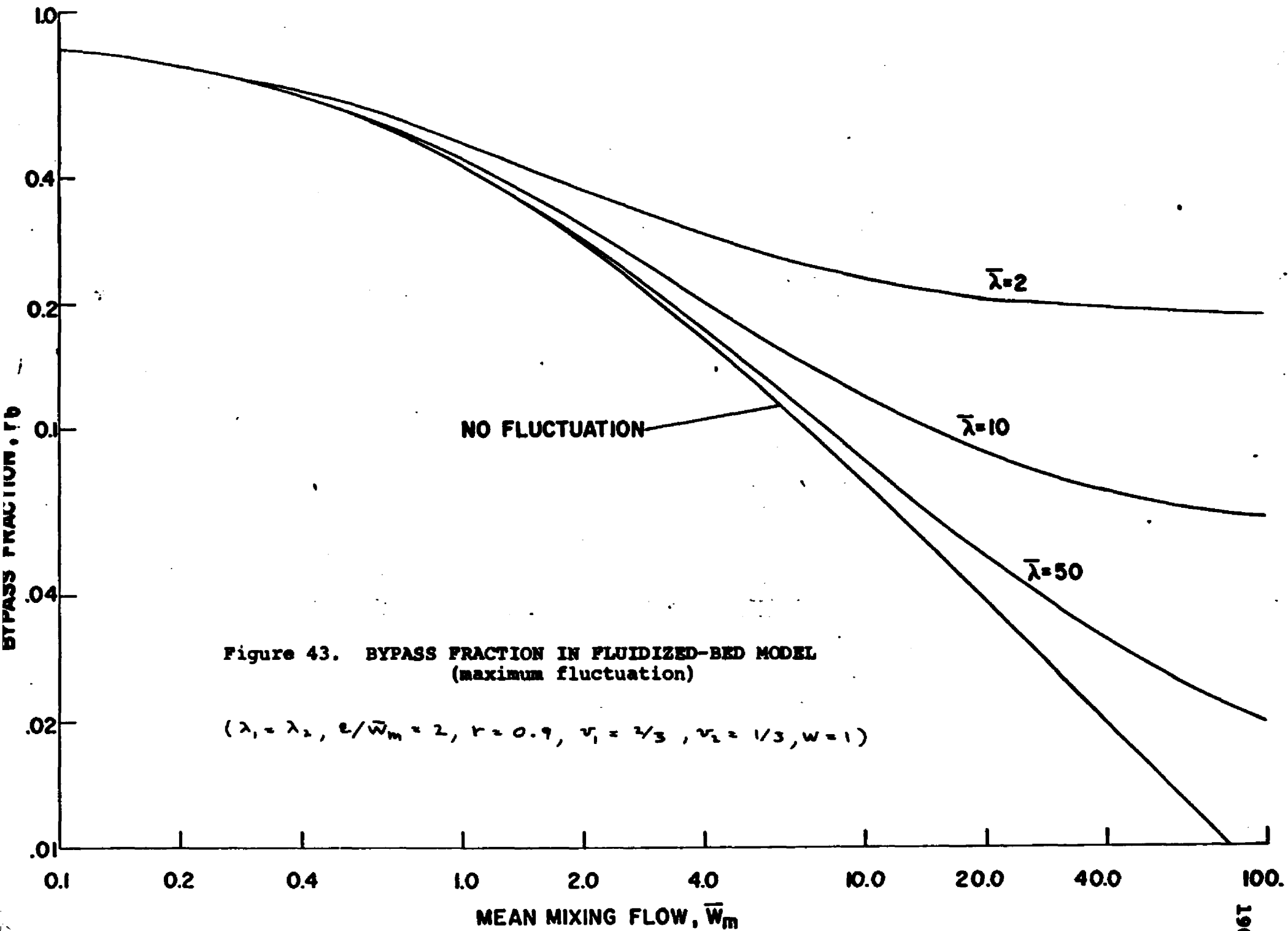
In the case shown, $p_1 = p_2 = \frac{1}{2}$, so $\frac{\epsilon}{w_m}$ has been taken as 2. It is seen that curves of r_b vs. w_m appear to approach asymptotes. Inspection of equation (IX-15) shows that, if $\frac{\epsilon}{w_m}$ is held constant,

$$\lim_{w_m \rightarrow \infty} \{ r_b \} = \begin{cases} \frac{r [1 + \frac{\epsilon}{w_m} (\bar{p}_2 - \bar{p}_1)]}{2 + \frac{\epsilon}{w_m} (\bar{p}_2 - \bar{p}_1) + \frac{r}{r_w} (\lambda_1 + \lambda_2)} ; \frac{\epsilon}{w_m} = \frac{1}{\bar{p}_1} \text{ or } \frac{1}{\bar{p}_2} \\ 0 ; -\frac{1}{\bar{p}_2} < \frac{\epsilon}{w_m} < \frac{1}{\bar{p}_1} \end{cases}$$

(IX-17)

Thus, the fact that the curves in Figure 43 approach asymptotic values depends on the fact that complete cutoff occurs in one of the flow states. Otherwise r_b would approach zero.

When complete cutoff does not occur, it is seen from



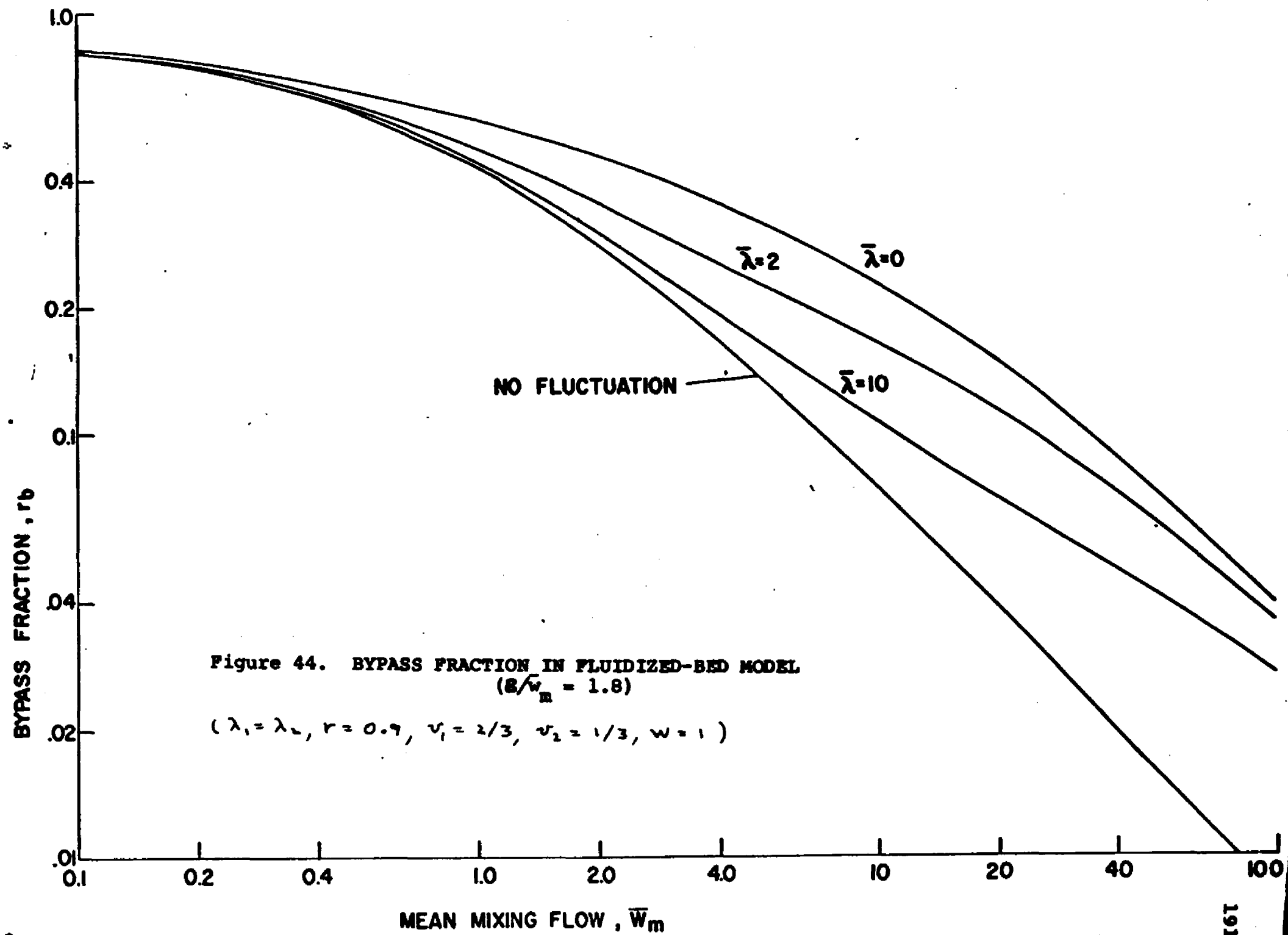


Figure 44. BYPASS FRACTION IN FLUIDIZED-BED MODEL
 $(R/\bar{w}_m = 1.8)$

$(\lambda_1 = \lambda_2, r = 0.9, \nu_1 = 2/3, \nu_2 = 1/3, w = 1)$

equation (IX-15) that the ratio of r_b to the value of r_b with steady flow, as given by equation (IX-9), becomes constant under the above conditions. Thus

$$\lim_{\bar{w}_m \rightarrow \infty} \left\{ \frac{r_b (r_w + \bar{w}_m)}{r^2 w} \right\} = \frac{1 + \frac{\epsilon}{\bar{w}_m} (\bar{\beta}_2 - \bar{\beta}_1)}{1 + \frac{\epsilon}{\bar{w}_m} (\beta_2 - \beta_1) - \bar{\beta}_1 \bar{\beta}_2 \left(\frac{\epsilon}{\bar{w}_m} \right)^2} \quad (\text{IX-18})$$

One notes that, according to (IX-18), the bypass fraction approaches an asymptote that is independent of switching rate. In Figure 44, $\frac{\epsilon}{\bar{w}_m}$ has been taken as 1.8, with the rest of the parameters the same as those in Figure 43.

Again the effect of the fluctuations on r_b is appreciable. For smaller values of $\frac{\epsilon}{\bar{w}_m}$, the effect of fluctuations on r_b is much smaller. Thus, if $\frac{\epsilon}{\bar{w}_m} \approx 10\%$, the ratio given by (IX-18) will be $\approx 1\%$.

From the discussion in the previous section about the behavior of the system with steady flow, it is clear that changes in r_b have a large effect on the reactor performance. Thus, the fluctuations will have an effect on the reactor performance by changing r_b . However, when a model is set up for a particular unit, the parameter r_b will be fixed by experimental means, since it is so important. One would then be interested in how the fluctuations would affect reactor performance once r_b is fixed.

Figures 45 and 46 illustrate the effect of fluctuations on the contact time distribution once r_b is fixed. The distribution has been plotted in the form of $h_c(\theta)$, the contact time intensity function, where

$$h_c(\theta) = \frac{f_c(\theta)}{1 - F_c(\theta)} \quad (\text{IX-19})$$

In Figure 45 the parameters were chosen to keep $r_b=0.5$, while in Figure 46, $r_b=.05$. In both cases ϵ/\bar{w}_m was given its maximum value. It is seen that for $r_b=0.5$ the effect of fluctuations on the contact time distribution is larger than for $r_b=.05$. In both cases, the effect is to decrease the value of $h(\theta)$ for large θ , which means that within the particulate phase itself there is a bypassing due to the bubbles. It is interesting to note that the effect of fluctuations on the fluid bed model contact time distribution is very similar to the effect of fluctuations on the single tank model residence time distribution.

The behavior of the fluctuating system with first order reaction is analyzed in terms of first and second moments by applying equations (V-10) and (V-20) to the fluid bed model. Thus the first moments, $m_{\beta j}$, are found to satisfy

Figure 45

Figure 45. EFFECT OF FLUCTUATING FLOW ON CONTACT TIME DISTRIBUTION ($x_b = 0.5$)

($w = 1$, $v_1 = 2/3$, $v_2 = 1/3$, $\epsilon/\bar{w}_m = 2$)

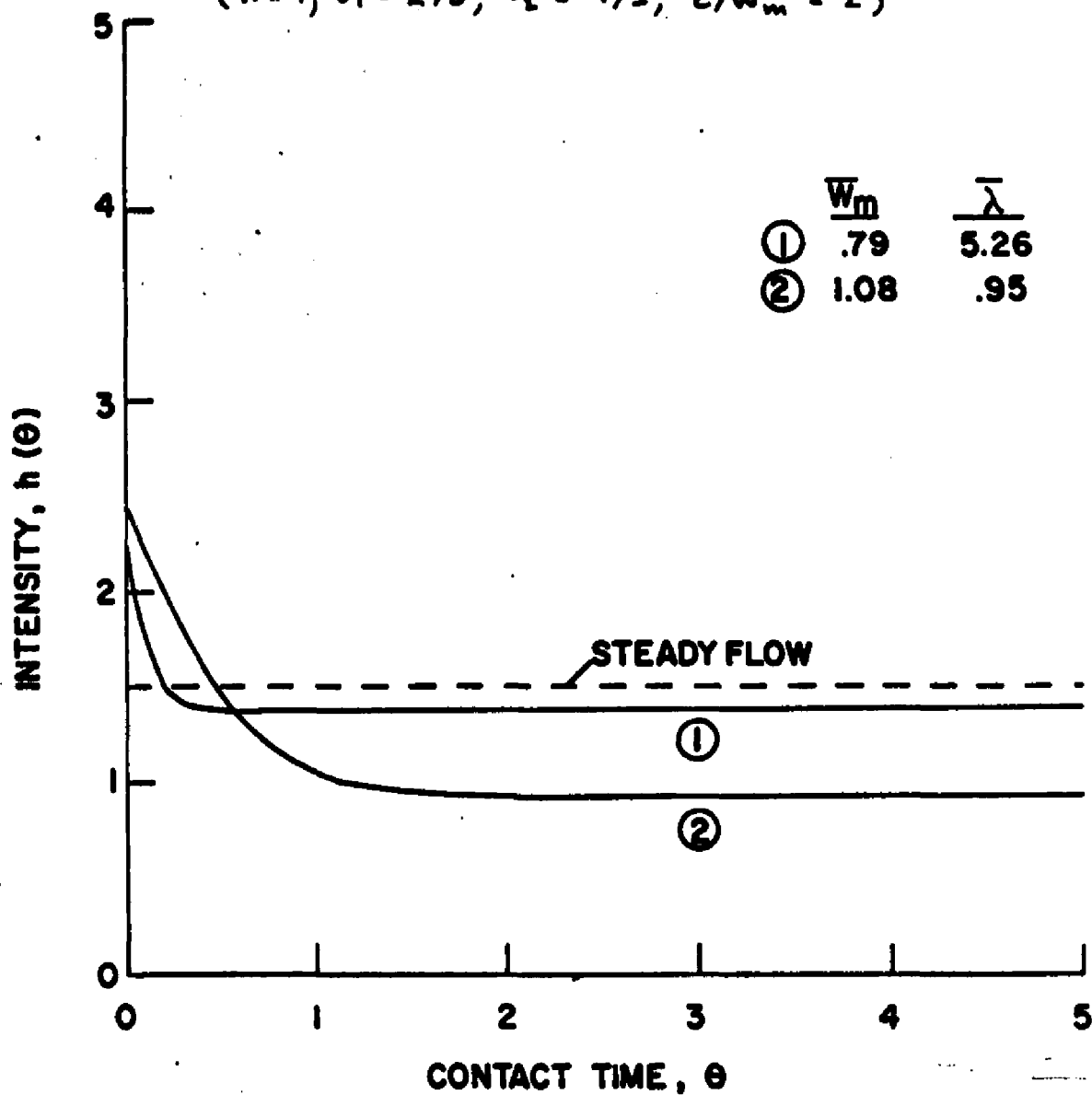
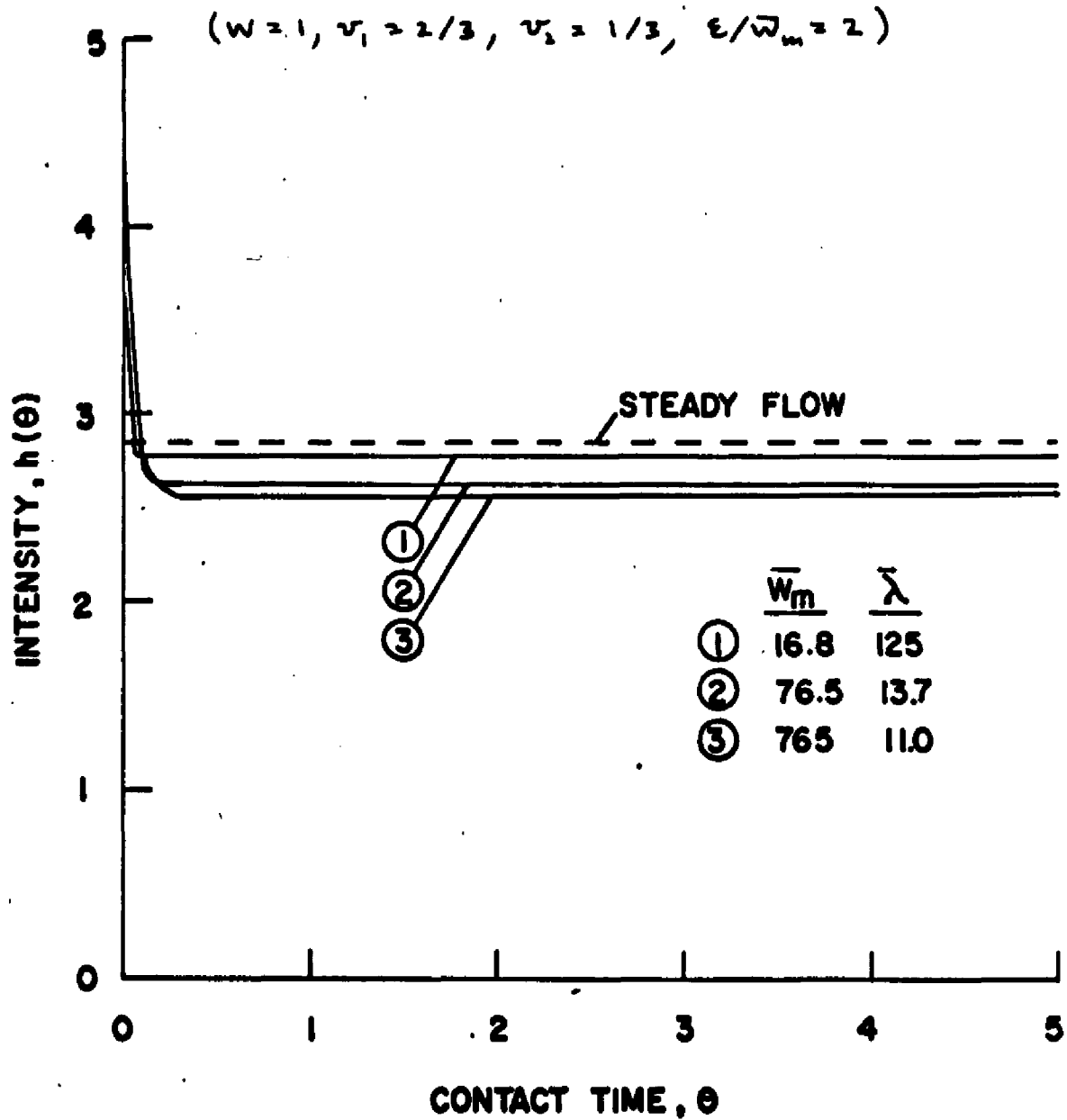


Figure 46. EFFECT OF FLUCTUATING FLOW ON CONTACT TIME DISTRIBUTION ($r_b = 0.05$)



$$\begin{aligned}
\left[\frac{rW}{v_1} + \frac{W_{m1}}{v_1} + \lambda_1 \right] m_{11} - \lambda_2 m_{21} - \frac{W_{m1}}{v_1} m_{12} &= \bar{p}_1 \frac{rW}{v_1} \\
-\lambda_1 m_{11} + \left[\frac{rW}{v_1} + \frac{W_{m2}}{v_1} + \lambda_2 \right] m_{21} - \frac{W_{m2}}{v_1} m_{22} &= \bar{p}_2 \frac{rW}{v_1} \\
-\frac{W_{m1}}{v_2} m_{11} + \left[\frac{(1-r)W}{v_2} + \frac{W_{m1}}{v_2} + k + \lambda_1 \right] m_{12} - \lambda_2 m_{22} &= \bar{p}_1 \frac{(1-r)W}{v_2} \\
-\frac{W_{m2}}{v_2} m_{21} - \lambda_1 m_{12} + \left[\frac{(1-r)W}{v_2} + \frac{W_{m2}}{v_2} + k + \lambda_2 \right] m_{22} &= \bar{p}_2 \frac{(1-r)W}{v_2}
\end{aligned}
\tag{IX-20}$$

Then the expected outlet concentration, $\langle \mathbf{x} \rangle$, is given by

$$\langle \mathbf{x} \rangle = r(m_{11} + m_{21}) + (1-r)(m_{12} + m_{22}) \tag{IX-21}$$

The second moments, $S_{\rho jk}$, satisfy

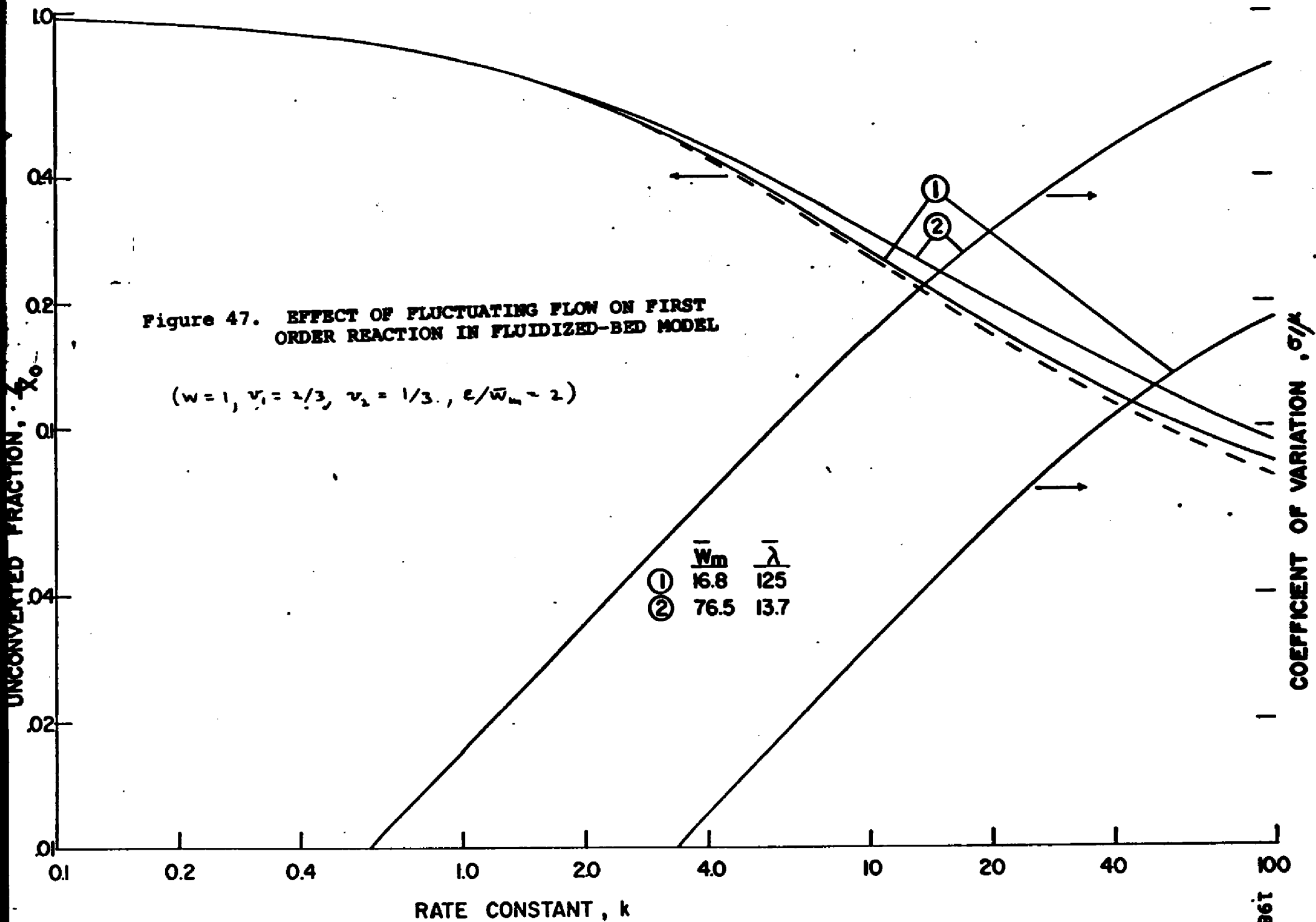
$$\begin{aligned}
\left[2 \left(\frac{rW}{v_1} + \frac{W_{m1}}{v_1} \right) + \lambda_1 \right] S_{111} - \lambda_2 S_{211} - 2 \frac{W_{m1}}{v_1} S_{112} &= 2 \frac{rW}{v_1} m_{11} \\
-\lambda_1 S_{111} + \left[2 \left(\frac{rW}{v_1} + \frac{W_{m2}}{v_1} \right) + \lambda_2 \right] S_{211} - 2 \frac{W_{m2}}{v_1} S_{212} &= 2 \frac{rW}{v_1} m_{21} \\
\left[2 \left(\frac{(1-r)W}{v_2} + \frac{W_{m1}}{v_2} + k \right) + \lambda_1 \right] S_{122} - \lambda_2 S_{222} - 2 \frac{W_{m1}}{v_2} S_{112} &= 2 \frac{(1-r)W}{v_2} m_{12} \\
-\lambda_1 S_{122} + \left[2 \left(\frac{(1-r)W}{v_2} + \frac{W_{m2}}{v_2} + k \right) + \lambda_2 \right] S_{222} - 2 \frac{W_{m2}}{v_2} S_{212} &= 2 \frac{(1-r)W}{v_2} m_{22} \\
-\frac{W_{m1}}{v_2} S_{111} - \frac{W_{m1}}{v_1} S_{122} + \left[\frac{rW}{v_1} + \frac{W_{m1}}{v_1} + \frac{(1-r)W}{v_2} + \frac{W_{m1}}{v_2} + k + \lambda_1 \right] S_{112} \\
-\lambda_2 S_{212} &= \frac{rW}{v_1} m_{12} + \frac{(1-r)W}{v_2} m_{21}
\end{aligned}
\tag{IX-22}$$

$$\begin{aligned}
& - \frac{W_{m2}}{V_2} S_{211} - \frac{W_{m2}}{V_1} S_{222} - \lambda_1 S_{112} + \left[\frac{rW}{V_1} + \frac{W_{m2}}{V_1} + \frac{(1-r)W}{V_2} + \frac{W_{m2}}{V_2} + k + \lambda_2 \right] \\
& \cdot S_{212} = \frac{rW}{V_1} m_{22} + \frac{(1-r)W}{V_2} m_{21}
\end{aligned}
\tag{IX-22}$$

The mean-square outlet concentration, $\langle \bar{x}^2 \rangle$, is then given by

$$\begin{aligned}
\langle \bar{x}^2 \rangle = & r^2 (S_{111} + S_{211}) + (1-r)^2 (S_{122} + S_{222}) \\
& + 2r(1-r) (S_{112} + S_{212})
\end{aligned}
\tag{IX-23}$$

The mean outlet concentration and the coefficient of variation, $\gamma = \sigma/\mu$, calculated from (IX-20)-(IX-23) are shown in Figure 47 for the same parameter values as used in Figure 46. It is seen that the fluctuations have the effect of decreasing mean conversion, and that the coefficient of variation of the output can be quite large, especially for high reaction rates. Since the determination of the mean bypass involves an experiment with high reaction rates ($k \rightarrow \infty$), whatever fluctuations there are would make themselves quite noticeable in the course of this experiment.



X. Conclusions

In studying the mathematical structure of the most general stochastic mixing model, with the number and arrangement of the tanks left unspecified, it was found that the expected response to a tracer input can be related to the distribution of passage times for certain random walks, even when the inlet and outlet flow rates fluctuate. Under the latter condition, however, the situation is more complicated than when the inlet and outlet flows are constant. An estimate of the true residence time distribution, that of the whole population of particles that passes through the system, requires measurement of the mean tracer flow rate response to an impulse or a step in tracer concentration. Other methods of carrying out the experiment result in biased estimates of this distribution. Some of these can be interpreted in terms of the residence time distribution for particles chosen in certain ways from the total population, however. Thus, the mean flow rate response to an impulse or step in flow rate gives the residence time distribution for particles chosen at random times in the inlet stream of the system, and the mean concentration response to an impulse or step in concentration gives the residence time distribution

for particles chosen at random times in the outlet stream of the system. Only the true residence time distribution has a mean value equal to the total system volume divided by the mean volumetric throughput, however.

The relationship between tracer response experiments and first order reaction behavior is somewhat more straightforward. When reactant is fed at constant concentration, the expected outlet concentration and outlet flow rate of unconverted reactant are given by the Laplace transforms of the mean concentration and flow rate response, respectively, to an impulse in concentration. When reactant is fed at constant inlet flow rate, the corresponding responses to impulses in tracer flow rate are used.

If the model is to be applied to heterogeneous systems, the property of a particle's random walk through the system that becomes important is the distribution of its contact times with a given area of the system. It was found in this case that the mean contact time, based on the entire particle population, is just the volume of the active portion of the system divided by the mean volumetric throughput.

The detailed calculations presented for special cases of the model cannot, of course, be the basis of such

far-reaching generalizations. They do, however, exhibit many interesting properties and suggest the kind of effects that stochastic models can be used to explain. One notes, for example, that the effect of fluctuations on the residence time distributions of the single tank model and the parallel model and on the contact time distribution of the fluid bed model is, in each case, very similar to that of bypassing or stagnancy. Such effects produce a characteristic change in the shape of the intensity function and lower the conversion of a first order reaction. It is remarkable that even a system which is perfectly mixed, like the single tank model is, can exhibit bypassing and stagnancy effects due to the presence of fluctuations. The data given by Orcutt, Davidson, and Pigford [28], show clearly that the contact time distribution in a fluidized bed exhibits these effects. While this may be due to the existence of relatively stagnant regions in the particulate phase, they can also be accounted for by stochastic mixing. It may also turn out that a simple stochastic model exhibiting these effects is easier to analyze than an adequate steady model.

In the series case, it was found that the above effect was negligible. In fact it was found that the presence of fluctuations produced a very slight increase

in first order conversion. Intuitively, one would suspect that the three-dimensional nature of turbulent mixing flows would produce effects like those of models with some parallel flow. The very different behavior of the series model from the parallel model suggests that the series model would make a poor representation of turbulent mixing processes.

One interesting result for the single tank model is that while fluctuations in flow rate will make conversion worse when reactant is fed at constant concentration, they will make it better when reactant is fed at constant rate. This does not conflict with the previous statements about stagnancy; the increased conversion results from an increase in mean residence time for particles injected uniformly, which counteracts the stagnancy effect. It is conceivable, however, that such a result could be of value in reactor design.

In all the cases studied, it was found that in the limit of high switching rates the mean behavior approached that for a steady flow system. Moreover, the variances of the tank concentrations went to zero, except for certain impulse responses that become more difficult to realize as the switching rate increases. For any pulse of finite

duration the variances would go to zero. Thus, when the time scale of the flow fluctuations is much smaller than the relaxation time of the system it is unlikely that any stochastic effects will be important.

The calculated coefficients of variation for the various tracer response of a single tank show that the experimental estimation of the true residence time distribution to a given accuracy requires more replications than the determination of the other residence time distributions, due to the greater variability of the corresponding tracer response. In all the cases the magnitude of the coefficient of variation of the impulse response becomes quite large after a time, so that the "tail" of the distribution would be difficult to determine accurately.

The autocorrelation functions calculated for the non-stationary tracer responses show a strong dependence on the starting instant. This makes their interpretation along the lines used for the autocorrelations of stationary processes rather difficult. The autocorrelation functions calculated for stationary outputs in the presence of first-order reactions indicate, in general, somewhat shorter memory times than do the autocorrelations of the underlying Markov processes. As the rate constant

becomes large, the former (almost always) approach the latter. Thus outlet fluctuations at high reaction rates would be rather sensitive to the nature of the flow fluctuations.

In the case of the fluidized bed model, experiments at high reaction rates take on additional importance due to the close connection between the limiting conversion and the structure of the contact time distribution. Under the assumption of perfect mixing in the particulate phase the limiting conversion determines the contact time distribution completely. On the other hand, it was found that the important parameters of the fluid-bed model affected the residence time distribution only slightly, so that experiments designed to measure this property provide a very poor means of characterizing such systems.

Some interesting properties came to light in calculating the probability distribution of concentration for the single tank model. It emerged that the distribution becomes concentrated over certain stable regions of the concentration space. For reactions that give unique steady solutions under constant flow conditions, a single region results. For reactions that give multiple steady states, however, several disjoint regions can develop.

Direct calculation showed that this occurs in the case of an exothermic reaction under adiabatic conditions, for example. These regions merged into one in certain cases, and the resulting probability distribution was very sensitive to changes in the reaction parameters as well as to changes in the switching rate. This situation was rather unusual, though, and it was more likely that one of the stable regions would simply disappear as the parameters were changed.

The disjoint stable regions that occur in this case are characteristic of a kind of ignition phenomenon. Once the system attains a state in one of the stable regions it never leaves the region. When these regions merge into one, the result is a sputtering system with widely fluctuating temperature. When the unignited (low-temperature) stable region disappears, the result is a system that will always ignite eventually and stay ignited. When the ignited stable region disappears, the result is a system which will eventually be extinguished and stay extinguished. One can see in this work the beginnings of a primitive probabilistic combustion stability analysis. It might be interesting to see how the mean extinction time depends on the various parameters.

The calculation of the complete probability distribution is more difficult for the two-tank models than for the single tank model because of the higher dimensionality of the state space. It was possible, however, to find the stable regions in the state space by a relatively simple procedure. The results for first-order reactions in the series and parallel model were shown for illustration, but the method could readily be extended to more complicated chemical kinetics. The partial differential equations describing the evolution of the probability density for models of two or more tanks are of the linear hyperbolic type whose characteristics are simply the steady-flow trajectories of the system. Following the time behavior of an initially uniform distribution numerically, through the method of characteristics, might be a reasonable way to compute the complete probability distributions in such cases.

Finally, it should be pointed out that once a system is successfully represented by such a model, questions of analytical difficulty do not really arise, as any desired statistic can be calculated by a straight forward Monte-Carlo computation. Thus, the proposed model satisfies the requirements of wide applicability, sufficient

analytical structure to allow meaningful conclusions in the general case, and simplicity enough to allow straightforward computation of properties in specific cases. The mathematical methods for treating such models have been systematically developed, and these have been used to calculate both general properties and the properties of some specific examples.

References

1. Kramers, H., and Westerterp, K.R., "Elements of Chemical Reactor Design and Operation", Academic Press Inc., New York (1963)
2. Van Deemter, J.J., "Mixing and Contacting in Gas-Solid Fluidized Beds", Chem. Eng. Sci. 13, 143-154 (1961)
3. Naor, P., and Shinnar, R., "Representations and Evaluations of Residence Time Distributions", I.E.C. Fundamentals 2, 278-286 (1963)
4. Beer, J.M., and Lee, K.B., "The Effect of the Residence Time Distribution on the Performance and Efficiency of Combustors", Tenth Symposium (International) on Combustion, 1187-1202 (1965)
5. Gillespie, B., and Carberry, J.J., "Influence of Mixing on Isothermal Reactor Yield and Adiabatic Reactor Conversion", I.E.C. Fundamentals 5, 164-171 (1966)
6. Danckwerts, P.V., "The Effect of Incomplete Mixing on Homogeneous Reactions", Chem. Eng. Sci. 8, 93-102 (1958)

7. Zwietering, Th.N., "The Degree of Mixing in Continuous Flow Systems", Chem. Eng. Sci. 11, 1-5 (1959)
8. Rietema, K., "Segregation in Liquid-Liquid Dispersions and its Effect on Chemical Reactions", Advances in Chemical Engineering 5, 237-302, Academic Press, New York (1964)
9. Weinstein, H., Adler, R.J., "Micromixing Effects in Continuous Chemical Reactors", Chem. Eng. Sci. 22, 65-75 (1967)
10. Rippin, D.W.T., "Segregation in a Two-Environment Model of a Partially Mixed Chemical Reactor", Chem. Eng. Sci. 22, 247-251 (1967)
11. Winterfeld, G., "On Processes of Turbulent Exchange Behind Flame Holders", Tenth Symposium (International) on Combustion, 1265-1275 (1965)
12. Kristmanson, D., and Danckwerts, P.V., "Studies in Turbulent Mixing - Part I, Dilution of a Jet", Chem. Eng. Sci. 16, 267 (1961)

13. Hinze, J.O., "Turbulence; An Introduction to its Mechanism and Theory", McGraw-Hill, New York (1959)
14. Batchelor, G.K., "Small Scale Variation of Convected Quantities in Turbulent Fluid", J. Fluid Mech. 5, 113-139 (1959)
15. Wilson, R.A.M., and Danckwerts, P.V., "Studies in Turbulent Mixing - II, A Hot Air Jet", Chem. Eng. Sci. 19, 885-895 (1964)
16. Corrsin, S., "The Isotropic Turbulent Mixer: Part II, Arbitrary Schmidt Numbers", A.I. Ch.E. Jour. 10, 870-877 (1964)
17. Corrsin, S., "Statistical Behavior of a Reacting Mixture in Isotropic Turbulence", Phys. of Fluids 1, 42-47 (1958)
18. Gibson, W.E., "Stochastic Model for Turbulent, Reacting Wakes", AIAA Jour. 4, 2001-2008 (1966)

19. Curl, R.L., "Dispersed Phase Mixing I. Theory and Effects in Simple Reactors", A.I.Chem.E. Jour. 9, 175-181 (1963)
20. Spielman, L.A., and Levenspiel, O., "A Monte-Carlo Method for Reacting and Coalescing Dispersed Phase Systems", Chem. Eng. Sci. 20, 247-254 (1965)
21. Kattan, A., and Adler, R.J., "A Stochastic Mixing Model for Homogeneous, Turbulent, Tubular Reactors", 16th Canadian Chemical Engineering Conference, Windsor, Ontario (October, 1966)
22. Feller, W., "An Introduction to Probability Theory and its Applications", John Wiley, New York (1966)
23. Wei, J., and Prater, C.D., "The Structure and Analysis of Complex Reaction Systems", Advances in Catalysis and Related Subjects, vol 13, pp. 203-392, Academic Press, New York (1962)
24. Wei, J., "On Reactor Design for Complex Systems of

- First-Order Chemical Reactions", Canadian Jour. of Chem. Eng. 44, 31-37 (1966)
25. Kats, I. Ia., and Krasovskii, N.N., "On the Stability of Systems with Random Parameters", PMM 24, 809-823 (1960)
26. Davidson, J.F., and Harrison, D., "Fluidised Particles", Cambridge University Press, New York (1963)
27. Gilliland, E.R., and Mason, E.A., Ind. and Eng. Chem. 44, 218 (1952)
28. Orcutt, J.C., Davidson, J.F., and Pigford, R.L., "Reaction Time Distributions in Fluidized Catalytic Reactors", C.E.P. Symposium Series 58 (No. 38), 1-15 (1962)
29. Courant, R., and Friedrichs, K.O., "Supersonic Flow and Shock Waves", Interscience Publishers, Inc., New York (1948)

Nomenclature

A	set of states counted toward contact time distribution
b_1, b_2	constants
c_1, c_2	constants
$f(t)$	residence time density function
$f(\theta), f_c(\theta)$	contact time density function
$f_o(t)$	residence time density function for particles chosen at random times in the outlet
$f_x(t)$	true residence time density function
$f_p(t)$	residence time density function for particles chosen at random times in the inlet
$f_{j\alpha}(x)$	time rate of change of x_j when flow state is α
$f_1(x), f_2(x)$	$f_{j\alpha}(x)$ for the single tank
$F(t)$	residence time distribution function
$F(\theta), F_c(\theta)$	contact time distribution function
$F_o(t)$	residence time distribution for particles chosen at random times in the outlet
$F_x(t)$	true residence time distribution function
$F_p(t)$	residence time distribution function for particles chosen at random times in the inlet
$g(x)$	$ f_1(x)p_1(x) - f_2(x)p_2(x) $
$g_{\alpha i}(\theta)$	$\int_0^{\infty} p_{\alpha i}(t, \theta) dt$
$\hat{g}_{\alpha i}(\theta)$	Laplace transform of $g_{\alpha i}(\theta)$
$G_{\alpha i}(\theta)$	$\int_0^{\theta} g_{\alpha i}(\theta') d\theta'$
$h(t)$	escape intensity; see (VII-33)

$h_c(\theta)$	intensity function for contact time distribution
$h_o(t)$	intensity function for $f_o(t)$
$h_x(t)$	intensity function for $f_x(t)$
$h_\psi(t)$	intensity function for $f_\psi(t)$
k	first order rate constant
k_{∞}	see (VII-100)
$m_{\alpha i}$	$\langle x_i \rangle_\alpha = \int x_i \bar{p}_\alpha(x) dx$ with first order reaction
m_1, m_2	$m_{\alpha i}$ for single tank
n	number of tanks in model
n	reaction order (section VII)
N	number of transfer units
$p_\alpha(t)$	probability of flow state α at time t
$p_{\alpha i}(t)$	probability that the particle is in tank i and the flow state is α at time t
$p_{\alpha i}(t, \theta)$	joint probability distribution of particle state, (α, i) , and accumulated contact time, θ , at time t
$p_a(t, \theta)$	$\sum_\alpha p_{\alpha, n+1}(t, \theta)$
$p_\alpha(t, x)$	joint probability distribution of flow state and tank concentration, $x = \{x_1, x_2, \dots, x_n\}$, at time t
\bar{p}_α	asymptotic stationary value of $p_\alpha(t)$
$\bar{p}_\alpha(x)$	stationary density function of reactant concentrations
p_α^o	initial probability of flow state α (random particle)
p_α^e	probability of flow state α at the instant a random particle leaves the system

$p_{\alpha, n+1}^*(t)$	probability that a particle chosen in the exit stream at a random time was in the system a time less than t and left when the flow state was α
$p_1(x), p_2(x)$	$p_{\alpha j}(x)$ for single tank
$p_1(y), p_2(y)$	probability density for y ; see (VII-79)
$q_{\alpha i}$	see equation (IV-43)
q_1, q_2	$q_{\alpha i}$ for single tank
r	constant (section VII)
r_b	bypass function
r_{α}	fraction of flow entering tank number one when flow state is α (sections VIII and IX)
r_{α}	see equation (IV-42)
$R(x)$	reaction rate
$R(x, T)$	reaction rate
s	constant (section VII)
$s_{\alpha ij}$	$\langle x_i x_j \rangle_{\alpha} = \int x_i x_j p_{\alpha}(t, x) dx$
s_1, s_2	$s_{\alpha ij}$ for single tank
t	time
T	temperature
T_o	inlet temperature
ΔT^*	adiabatic temperature rise for complete reaction
v_i	volume of tank i
w	inlet flow rate (=outlet flow rate)
w_{ij}	flow rate from tank i to tank j ($i \neq j$)

w_{ii}	negative of total flow rate to tank i ; see equation (II-3)
w_m	mixing flow rate
w_α	value of w when flow state is α
$w_{ij\alpha}$	value of w_{ij} when flow state is α
$w_{m\alpha}$	value of w_m when flow state is α
\bar{w}	mean inlet or outlet flow rate
x_j	concentration of tracer or reactant in tank j
$x_o(t)$	inlet concentration of tracer or reactant
$x_1^{\infty}, x_2^{\infty}$	final values of x_1, x_2
y_i	concentration of tracer or reactant in tank i
$y(x)$	see (VII-79)
z	outlet concentration
z_x	outlet reactant concentration for constant inlet reactant concentration
$z_x(t)$	concentration response to an impulse in tracer concentration
z_ψ	outlet reactant concentration for constant inlet reactant flow rate
$z_\psi(t)$	concentration response to an impulse in tracer flow rate

Greek Letters

α	flow state index
α	dimensionless activation energy; see equation (VII-101)
β	flow state index

B	beta function
γ	flow state index
γ	coefficient of variation
$\delta(x)$	Dirac delta function
δ_{ij}	Kronecker delta
ε	$w_1 - w_2$
θ	mean residence time
θ	dimensionless heat release; see equation (VII-10)
θ	contact time
θ_c	mean contact time
θ_φ	mean residence time for particles chosen at random times in the inlet stream j ; see equation (VII-23)
$\theta_{\alpha i}$	$\int_0^\infty p_{\alpha i}(t) dt$
$\lambda_{\alpha\beta}$	switching rate
λ_1	$\lambda_{12} = -\lambda_{11}$ for two flow states
λ_2	$\lambda_{21} = -\lambda_{22}$ for two flow states
$\bar{\lambda}$	mean switching rate, $\frac{1}{2}(\lambda_1 + \lambda_2)$
μ	mean
$\mu_{\alpha i}(t)$	partial first moment, $\langle x_i \rangle_\alpha = \int x_i p_\alpha(t, x) dx$
$\hat{\mu}_{\alpha i}(k)$	Laplace transform of $\mu_{\alpha i}(t)$
μ_1, μ_2	$\mu_{\alpha i}$ for single tank
$\pi(\alpha \rightarrow \beta; \tau)$	probability of transition from state α to state β in time τ

$\pi_t(\alpha, x \rightarrow \beta, y; \tau)$	conditional joint probability distribution of β and y at time $t + \tau$, given that state was (α, x) at time t
$\rho_t(\tau)$	autocorrelation function; see equations (IV-34) and (IV-35)
$\rho(\tau)$	autocorrelation function for stationary process; see equation (VII-8)
σ	standard deviation
σ/μ	coefficient of variation
σ_w	standard deviation of flow rate
σ_z	standard deviation of outlet concentration
σ_v	standard deviation of outlet reactant or tracer flow rate
τ	time interval
$\varphi(t)$	inlet reactant or tracer flow rate
$\varphi_{\alpha i}(t)$	rate at which tracer or reactant is fed into tank i when flow state is α at time t
φ_1, φ_2	$\varphi_{\alpha i}$ for single tank
$\chi_A(\alpha, i)$	characteristic function of the set A , =1 if $(\alpha, i) \in A$ and =0 if $(\alpha, i) \notin A$
ψ	outlet flow rate of tracer or reactant
ψ_x	outlet reactant flow rate for constant inlet reactant concentration
$\psi_r(t)$	flow rate response to an impulse in tracer concentration
ψ_φ	outlet reactant flow rate for constant inlet reactant flow rate
$\psi_\varphi(t)$	flow rate response to an impulse in tracer flow rate

Vita

Frederick J. Krambeck was born March 18, 1941, in New York City. After graduating from Brooklyn Technical High School in June 1958, he entered the City College of New York, receiving the Bachelor of Chemical Engineering degree in January 1963. After graduation, he moved to Pittsburgh, Pennsylvania, where he was employed by Westinghouse Electric Corporation in their Atomic Power Division. He worked in the area of nuclear reactor design, specializing in thermal and hydraulic analysis. At the time, he attended evening graduate courses at the Carnegie Institute of Technology in Chemical Engineering and Applied Mathematics. In September 1964, he returned to New York City to study at the City University, receiving the M.E. degree in June 1966, and successfully defending his Ph.D. dissertation on December 13, 1967. After completing the requirements, he became a research engineer at Mobil Research and Development Corporation in Princeton, New Jersey.